ION ADSORPTION ON OXIDES

Surface charge formation and cadmium binding on rutile and hematite

Promotor: dr. J. Lyklema, hoogleraar in de Fysische en Kolloïdchemie

Co-promotor: dr. A. de Keizer, universitair docent

L.G.J. Fokkink

ION ADSORPTION ON OXIDES

Surface charge formation and cadmium binding on rutile and hematite

Proefschrift
ter verkrijging van de graad van
doctor in de landbouwwetenschappen,
op gezag van de rector magnificus,
dr. C.C. Oosterlee,
in het openbaar te verdedigen
op vrijdag 22 mei 1987
des namiddags te vier uur in de aula
van de Landbouwuniversiteit te Wageningen

CONTENTS

1. INTRODUCTION 1

1.1 General 1

1.1.1 Insoluble oxides 1

1.1.2 Heavy metals 1

1.2 Physico chemical aspects 2

1.2.1 Insoluble oxides 2

1.2.2 Hydrolyzable metal ions 3

1.2.3 Ion adsorption on insoluble oxides 3

1.3 The present study 4

1.3.1 General 4

1.3.2 Outline of this thesis 5

1.4 References 7

2. MATERIALS AND EXPERIMENTAL METHODS 10

2.1 Introduction 10

2.2 pH measurements 10

2.3 Electrochemical cell 11

2.4 Potentiometric titrations 13

2.5 Materials 14

2.5.1 General 14

2.5.2 Oxides 14

2.6 References 16

3. TEMPERATURE DEPENDENCE OF SURFACE CHARGE ON INSOLUBLE OXIDES 17

3.1 Introduction 17

3.2 Experimental 17

3.3 Results 18

3.4 Discussion 22

3.5 Conclusions 37

3.6 References 38

Appendix 39

STELLINGEN

I

Interpretatie van meetgegevens uitsluitend op basis van 'site-binding'-principes leidt tot een vastgeroest beeld van het oxide-oplossingsgrensvlak.

II

Veel oxiden gedragen zich 'klassieker' dan de klassieke modelsystemen voor geladen grensvlakken.

Dit proefschrift, hoofdstuk 3

III

De adsorptie van cadmiumionen op rutiel is entropisch gedreven.

Dit proefschrift, hoofdstukken 6 en 8

IV

Het experiment waarmee Ghiradella, Radigan en Frisch de aanwezigheid van precursor films zeggen aan te tonen, druist zodanig in tegen elementaire chemische beginselen, dat het bij voorkeur niet geciteerd dient te worden.

Ghiradella, H., Radigan, W., en Frisch, H.L., Ref. bij auteur bekend.

Joanny, J.F., proefschrift Université Pierre et Marie Curie, Parijs, 1985.

V

Het 'surface precipitation' model van Farley et al. reikt een oplossing aan voor door het model zelf veroorzaakte problemen.

Farley, K.J., Dzombak, D.A., en Morel, F.M.M., J. Colloid Interface Sci. 106, 226, 1985.

VI

Dubbellaagmetingen aan rutiel en hematiet suggeren dat temperatuurscongruentie algemeen is voor oxiden.

Dit proefschrift, hoofdstukken 3 en 4

VII

Dubbellaagmetingen aan kwik, zilverjodide en oxiden duiden op een universeel karakter van temperatuurscongruentie.

Dit proefschrift, stelling VI

S. Trasatti, in "Modern Aspects of Electrochemistry" (B.E. Conway en J.O'M Bockris, Eds), Vol. 13. Plenum Press, Londen, 1979.

Bijsterbosch, B.H., en Lyklema, J., Adv. Colloid Interface Sci 9, 147, 1978.

VIII

Zonder model vaart niemand wel.

IX

De gebruikelijke opbouw van publikaties in kolloidchemische tijdschriften suggereert ten onrechte een ondergeschikt belang van het experiment.

Xa

Gelet op de uiteenlopende belangen dient de amateur-groenteteler zich niet als 'mini-boer' te gedragen.

Xb

Schrijnende vormen van overdosering van meststoffen ('overbemesting') vinden plaats in partikuliere moestuinen.

XI

Als de herziening van het stelsel sociale zekerheid als voorbeeld moet dienen voor wat het kabinet Lubbers-de Korte verstaat onder 'versimpelen' dient ernstig te worden overwogen om eveneens de betekenis van het begrip 'versimpelen' te herzien.

Regeerakkoord tweede kabinet-Lubbers

XII

Grensvlak-chemisch bezien ligt Australië vlakbij.

Proefschrift L.G.J. Fokkink
Ion adsorption on oxides
Wageningen, 22 mei 1987.

4. THERMODYNAMICS OF CHARGE FORMATION ON OXIDES. MICROCALORIMETRY 41
4.1 Introduction 41
4.2 Experimental 42
4.3 Experimental results 44
4.4 Discussion 47
4.5 Conclusions 55
4.6 Acknowledgements 56
4.7 References 56

5. SOLUTION CHEMISTRY OF CADMIUM 57
5.1 Introduction 57
5.2 Experimental 57
5.3 Results 58
5.4 Discussion 60
5.5 Conclusions 65
5.6 References 65

6. TEMPERATURE DEPENDENCE OF CADMIUM ION ADSORPTION ON RUTILE AND HEMATITE 67
6.1 Introduction 67
6.2 Experimental 69
6.2.1 Adsorption experiments 69
6.2.2 Microelectrophoresis 70
6.3 Results and discussion 71
6.4 Model analysis 75
6.5 Conclusions 83
6.6 References 83

7. SPECIFIC ION ADSORPTION ON OXIDES. SURFACE CHARGE ADJUSTMENT AND PROTON STOICHIOMETRY 85
7.1 Introduction 85
7.1.1 General observations with respect to r_{OH} 85
7.2 Surface charge adjustment 87
7.2.1 Theoretical considerations 87
7.2.2 Model calculations 89

7.3 Comparison with experimental observations 95
7.4 Conclusions 99
7.5 References 100

8. MICROCALORIMETRY OF ION ADSORPTION.
ADSORPTION ENTHALPY OF CADMIUM IN THE RUTILE - KNO_3 SYSTEM 101
8.1 Introduction 101
8.2 Experimental 102
8.3 Results 103
8.4 Discussion 107
8.5 Conclusions 110
8.6 Acknowledgements 110
8.7 References 110

9. CONCLUDING REMARKS AND SUGGESTIONS FOR FURTHER RESEARCH 112
9.1 General picture of surfaces properties of insoluble oxides 112
9.2 Cadmium adsorption on oxides 113
9.3 Applications 117
9.4 Suggestions for further research 118
9.5 References 119

SUMMARY 120

SAMENVATTING 122

LEVENSLOOP 127

NAWOORD 128

1. INTRODUCTION

1.1 General

1.1.1 Insoluble oxides

The adsorption of small ions from aqueous solution onto solid particles has drawn the attention of a large group of scientists stemming from a variety of disciplines. Apart from the mere academic aspects covering the fundamentals of ion binding onto several substrates, the subject is of great importance in applied sciences concerned with the natural environment. Slightly soluble inorganic oxide-solution interfaces play a basic role in regulating the chemical composition of the natural environment, both in the aquatic and in the soil biotope (1).

In natural soils, a large part of the mineral fraction may consist of oxides of Si, Al and Fe. Together with clay minerals and the humic substances they play a role in the availability and transport properties of ionic compounds in the soil environment. Most, if not all, of the inorganic oxides exhibit pH-dependent surface charge densities. Over the pH range normally found in soils (pH 4-8), their amphoteric character makes that they can exist as positive, neutral or negative particles. In contradistinction with the other main soil constituents that bear a net negative charge under the natural conditions, oxides supply a pH-dependent sink and source for ionic species in the soil.

It has been frequently stressed that in natural waters a variety of colloidal inorganic oxides help to regulate the concentrations of ionic species (2). For instance, the concentration of free metal cations in the aquatic environment is amongst others determined by precipitation - dissolution and adsorption - desorption equilibria.

1.1.2 Heavy metals

The term 'heavy metal' is used to indicate a number of metals which are mostly of high density and their ions, usually belonging to the group of transition elements. A quite common characteristic of these metals is that already at low concentrations they are harmful to living organisms, though part of them are essential in very low amount as so-called trace-elements.

Due to a strongly increased industrial activity, the problem of more or less diffuse emission of heavy metals in the environment has become a well-known problem. Examples of heavy metal emitting sources are e.g. industry (ore melters), trafic (lead compounds in gasoline), intensive cattle breeding (Cu and Zn in animal manure) and waste disposal (sanitary landfills).

As an example, cadmium can be mentioned. This element is widely used, e.g. in coating materials and in pigments. It is also applied in batteries (Ni-Cd cells) and in motor oil and car tires (3). Mainly due to the way in which cadmium is applied, most of the industrially processed Cd is bound to end up in the natural environment, where its fate is to a large extent determined by adsorption-desorption equilibria. An extensive study of the adsorption behavior of Cd in different natural soils as a function of electrolyte composition and some other parameters has recently been published by Chardon (4).

1.2 Physico chemical aspects

1.2.1 Insoluble oxides

During the past decades a vast number of physico chemical studies has been devoted to insoluble inorganic oxides. After the classical model systems in colloid and interface science, mercury and silver halides (mainly AgI), the pioneering research on the oxide-solution interface in the late fifties and sixties by a.o. Bolt (5), de Bruyn et al. (6,7) and Lyklema et al. (8,9), revealed the interesting typical surface properties of these materials. Most of the original work on oxides was concerned with the measurement and interpretation of the surface charge development. Dislike the -also reversible- AgI-solution interface, the surface charge density on oxides originates from the adsorption of the non-lattice ions H^+ and OH^-. Therefore, pH is the controlling parameter governing the surface charge on oxides. Another striking difference between AgI and Hg at one hand and insoluble oxides at the other, are the shapes of the surface charge-potential relations. Where on AgI and Hg these curves are concave towards the potential axes, for all oxides hitherto studied they are convex. For most oxides, the surface charge strongly resembles that predicted by diffuse double layer theory (Gouy-Chapman model). The distinction between the charge characteristics of oxides and those of the more classical model systems, initiated

the development of specific models for the oxide-solution interface: the 'surface gel' model by Bérubé and de Bruyn (10) and the porous double layer model by Lyklema (11). Both approaches account for the extremely effective screening of the surface charge by counter ions.

An alternative approach to adsorption phenomena in general at oxide-solution interfaces, based on essentially different principles is the site-binding or surface complexation theory, developed by Healy and coworkers (12-15), Schindler et al. (16,17) and Stumm et al. (18-20). This school of thought considers a special type of surface species to be present in the solid-solution interface, which is able to form surface complexes with ions or molecules from the solution. An overview and discussion of this type of models can be found in a series of recent reviews (e.g. 21-24).

1.2.2 Hydrolyzable metal ions

Apart from the physical characteristic that heavy metals usually are of high density, these compounds show some interesting common chemical features. The multivalent cations are classified as hydrolyzable, implying that they tend to react with water in order to form hydroxo complexes. Normally, aqueous solutions of heavy metal salts are acidic due to this hydrolysis reaction. The degree of hydrolysis strongly depends on the pH of the solution; the concentration of hydroxo complexes increases strongly with increasing pH, where subsequently monohydroxo-, dihydroxo- (multihydroxo-) complexes and eventually metalhydroxide or metaloxide precipitates are formed (25).

Due to their relatively small size and high charge, the free cations of these compounds are strongly hydrated. From literature data on hydrolyzability of heavy metal ions it can be concluded that changes in hydration entropy are important factors determining the solution chemistry of the metal salts.

1.2.3 Ion adsorption on insoluble oxides

The adsorption of both cations and anions onto oxides has been studied extensively. As far as the cationic adsorption is concerned, it is usually observed that hydrolyzable metal ions are strongly bound at the oxide-solution interface (cf. 26). As a rule, however, monovalent cations usually do

not show pronounced specific affinities for oxides. In most cases they can be classified as 'indifferent', i.e. they merely adsorb due to coulombic interaction (27,9).

In heavy metal adsorption studies in oxide systems, historically much has been speculated about the relation between hydrolyzability of cations and their adsorbability onto oxides. A current approach is that, more or less ad hoc, different adsorbabilities are ascribed to the different metal species in solution, thus stressing the importance of knowing the actual solution composition (speciation) as a function of the experimental parameters, such as pH, salt concentration, temperature etc.

Anions, in particular the so-called oxyanions like PO_4^{2-} and SeO_4^{2-}, usually show high affinity adsorption behavior on oxides. Especially phosphate adsorption is a 'hot topic' in soil science literature (cf. 28-36). From the viewpoint of plant nutrition and also of soil hygiene the interest in the subject is quite understandable. A representative example of what can be achieved in this field by essentially physico chemical means is provided by the work of van Riemsdijk and co-workers (32-38).

1.3 The present study

1.3.1 General

This study was undertaken in order to obtain a broader insight into the mechanisms and the thermodynamics of the adsorption of heavy metals onto inorganic oxides. Some of the questions that had to be answered are:

(i) What is so special about multivalent hydrolyzable cations that makes them to adsorb so strongly on oxidic substrates?

(ii) Why is the adsorption always accompanied by the uptake of hydroxyl ions from solution?

In order to answer these and other intriguing questions, we decided to measure the adsorption of a common heavy metal ion (Cd^{2+}) onto representative crystalline inorganic oxides (α-Fe_2O_3, TiO_2) as a function of temperature. This type of measurements supply information on the driving force

in the adsorption process: whether the adsorption is mainly entropy or enthalpy driven. From the change in adsorbed amount of cadmium with temperature, insight into the adsorption entropy can be obtained using classical thermodynamic procedures (39,40).

1.3.2 Outline of this thesis

The subject of this thesis is the thermodynamics of cadmium adsorption onto inorganic oxides. Special attention is paid to the temperature dependence of the adsorption. The influence of temperature on the surface charge of oxides, on the behavior of the adsorptive in solution and on the over-all adsorption process are studied. The contents of this thesis can be subdivided into three main parts.

(i) Thermodynamics and temperature dependence of the process of surface charge formation on inorganic oxides.

(ii) Properties of Cd^{2+} ions in aqueous solutions, in particular the formation of hydroxo complexes.

(iii) Adsorption of cadmium ions onto oxides, with special attention for the concomitant co-adsorption phenomena.

The experimental set-up, which allows accurate measurements of the surface charge density over a relatively wide temperature range, is briefly discussed in **chapter 2**. Some attention is also paid to the potentiometric determination of pH at temperatures other than room temperature. The synthesis and characterization of the hematite and rutile used in this study are described.

Chapter 3 is devoted to the mechanism of surface charge formation on hematite (α-Fe_2O_3) and rutile (TiO_2). The temperature dependence of surface charge - pH relations is experimentally investigated. Thermodynamic properties of the charge formation process are derived and discussed in terms of possible mechanisms. A generalized picture of the double layer on inorganic oxides is presented on the basis of our results and those taken from literature.

In **chapter 4**, direct calorimetric measurements of the surface charge formation on rutile and hematite are presented. Directly measured enthalpies of charge formation are compared to those resulting from the thermodynamic analysis of the temperature dependence of surface charge - pH relations. A

theoretical discussion of the thermodynamics of double layer formation is given, with special emphasis on typical oxide characteristics.

Chapter 5 deals with the solution chemistry of Cd^{2+} ions. The formation of hydroxo complexes as a function of temperature is experimentally determined, using a potentiometric titration procedure. Equilibrium constants for the formation of monohydroxo complexes are derived at 20 and 60 ^{o}C, and from those values enthalpic and entropic contributions are obtained. It is shown that the association of hydrated Cd^{2+} ions with OH^{-} in solution is essentially an entropy driven process.

The experimental adsorption results are treated in **chapter 6.** For several temperatures in the range 5 - 60 ^{o}C the adsorption of cadmium species onto rutile and hematite is measured using a pH-static titration technique, yielding also information on the co-adsorption of OH^{-} ions. Adsorption results are compared to electrophoretic mobility data for the Cd-rutile system. Experimental adsorption data are discussed in terms of a model accounting for electrical and lateral interactions in the adsorbed phase. It is shown that the chemical interaction between adsorbate and surface only slightly depends on temperature. Also the influence of other experimental parameters is relatively small. The nature of the oxide, however, plays a crucial role in determining the chemical affinity of Cd^{2+} ions for the surface phase. Evidence is presented for a relation between the point of zero charge of the oxides and the affinity for Cd^{2+} ions.

The co-adsorption phenomena accompanying Cd^{2+} adsorption are discussed in **chapter** 7. It is shown that apparent OH^{-} co-adsorptions can be understood in terms of surface charge adjustment. Experimental results from literature for the adsorption of divalent ions on several oxides and our results for the adsorption of Cd^{2+} ions onto rutile and hematite are compared to theoretical calculations according to our surface charge adjustment theory. It is shown that there is no need to invoke specific adsorption of hydroxo complexes to explain experimental co-adsorption data.

In **chapter** 8 directly determined cadmium adsorption enthalpies in the rutile-KNO_3 system are discussed. It is shown that direct microcalorimetry offers a good means to obtain thermodynamic data for the heavy metal adsorption process. Adsorption of the Cd^{2+} ions as such, is an energetically unfavourable process, and, therefore, the affinity of the ions for the oxide-solution interface stems from an increase in entropy. It is shown

that adsorbing Cd^{2+} ions lose about half of their hydration shell. A close analogy between Cd^{2+} adsorption and the formation of monohydroxo complexes is observed, stressing the similarity between surface groups of the oxide and OH^- ions in solution. Several arguments for this similarity are given.

Chapter 9 summarizes the main conclusions on the adsorption phenomena in insoluble oxide systems. A picture of the oxide-solution interface, consistent with all observations made in this study, is given. The practical consequences of this study and its applications are discussed. Some recommendations for further research in this field are put forward.

1.4 References

1. Kinniburgh, D.G., and Jackson, M.L., in "Adsorption of Inorganics at Solid-Liquid Interfaces" (M.A. Anderson and A.J. Rubin, Eds), Ann Arbor Science, Ann Arbor, 1981.
2. Stumm, W., and Morgan, J.J, "Aquatic Chemistry", Wiley-Interscience, New York-London-Sydney-Toronto, 1970.
3. de Haan, F.A.M., and Zwerman, P.J., in "Soil Chemistry. A." (G.H. Bolt and M.G.M. Bruggenwert, Eds), Elsevier Scientific Publishing Company, Amsterdam-Oxford-New York, 1978.
4. Chardon, W.H., "Mobiliteit van Cadmium in de Bodem", serie Bodembescherming 37, Staatsuitgeverij, The Hague, 1984.
5. Bolt, G.H., J. Phys. Chem. 61, 1166, 1957.
6. Onada, G.Y., and de Bruyn, P.L., Surface Sci. 4, 48, 1966.
7. Bérubé, Y.G., Onada, G.Y., and de Bruyn, P.L., Surface Sci. 8, 448, 1967.
8. Tadros, Th.F., and Lyklema, J., J. Electroanal. Chem. 17, 267, 1968.
9. Breeuwsma, A., and Lyklema, J., Disc. Faraday Soc. 52, 324, 1971.
10. Bérubé, Y.G., and de Bruyn, P.L., J. Colloid Interface Sci. 28, 92, 1968.
11. Lyklema, J., J. Electroanal. Chem. 18, 341, 1968.
12. James, R.O., and Healy, T.W., J. Colloid Interface Sci. 40, 42, 1972.
13. James, R.O., and Healy, T.W., J. Colloid Interface Sci. 40, 53, 1972.
14. James, R.O., and Healy, T.W., J. Colloid Interface Sci. 40, 65, 1972.
15. Yates, D.E., Levine, S., and Healy, T.W., Chem. Soc. Faraday Trans. I 70, 1807, 1974.

16. Schindler, P.W., Fuerst, B., Dick, B., and Wolf, P.W., J. Colloid Interface Sci. 55, 469, 1976.
17. Schindler, P.W., Waelti, E., and Fuerst, B., Chimia 30, 107, 1976.
18. Stumm, W., Huang, C.P., and Jenkins, S.R., Croat. Chem. Acta 42, 223, 1970.
19. Huang, C.P., and Stumm, W., J. Colloid Interface Sci. 43, 409, 1973.
20. Stumm, W., Hohl, H., and Dalang, F., Croat. Chem. Acta 48, 469, 1976.
21. Westall, J., and Hohl, H., Advan. Colloid Interface Sci. 12, 265, 1980.
22. Sposito, G.J., J. Colloid Interface Sci. 91, 329, 1983.
23. James, R.O., and Parks, G.A., in "Surface and Colloid Science", Vol. 12 (E. Matijević, Ed.), Plenum Press, New York-London, 119, 1982.
24. Healy, T.W., and White, L.R., Adv. Colloid Interface Sci. 9, 303, 1978.
25. Hunt, J.P., "Metal Ions in Aqueous Solution", W.A. Benjamin, Inc., New York-Amsterdam, 1963.
26. Corey, R.B., in "Adsorption of Inorganics at Solid-Liquid Interfaces" (M.A. Anderson and A.J. Rubin, Eds.), Ann Arbor Science, Ann Arbor, 1981.
27. Breeuwsma, A., thesis, Wageningen, 1973.
28. Goldberg, S., and Sposito, G., Colloids Surf. 2, 101, 1981.
29. Bowden, J.W., Nagarijah, S., Barrow, N.J., Posner, A.M., and Quirk, J.P., Aust. J. Soil Res. 18, 49, 1980.
30. Barrow, N.J., J. Soil Sci. 34, 733, 1983.
31. Barrow, N.J., Bowden, J.W., Posner, A.M., and Quirk, J.P., Aust. J. Soil Res. 18, 395, 1980.
32. van Riemsdijk, W.H. and de Haan, F.A.M., Soil Sci. Soc. Amer. J. 45, 261, 1981.
33. van Riemsdijk, W.H., Boumans, L.J.M., and de Haan, F.A.M., Soil Sci. Soc. Amer. J. 48, 541, 1984.
34. van der Zee, S.E.A.T.M., and van Riemsdijk, W.H., Geoderma 38, 293, 1986.
35. van der Zee, S.E.A.T.M., van Riemsdijk, W.H., and de Haan , F.A.M., in "Contaminated Soil" (J.W. Assink and W.J. van den Brink, Eds). Martinus Nijhoff Publ., Dordrecht.
36. van der Zee, S.E.A.T.M., Fokkink, L.G.J., and van Riemsdijk, W.H., Accepted for publication in Soil Sci. Soc. Amer. J., 1987.

37. van Riemsdijk, W.H., and Lyklema, J., Colloids Surf. 1, 33, 1980.

38. van Riemsdijk, W.H., and Lyklema, J., J. Colloid Interface Sci. 76, 55, 1980.

39. Blaakmeer, J., M.Sci thesis, Wageningen, 1983.

40. Lyklema, J., in "Interactions Solide-Liquide dans les Milieux Poreux" (J.M. Cases, Ed.), Editions Technip, Paris, 1985.

2. MATERIALS AND EXPERIMENTAL METHODS

2.1 Introduction

In the limited number of papers dealing with adsorption of H^+/OH^- at the oxide-solution interface as a function of temperature (1-4) only a minute amount of experimental detail on the actual pH measurements can be found. Therefore it became necessary to develop our own experimental procedure to obtain accurate pH measurements in oxide suspensions over a relatively wide temperature range. In this chapter the basic potentiometric titration procedure and the experimental set-up are described. Furthermore, we will shortly discuss the synthesis and characterization of the hematite and rutile used throughout this study.

2.2 pH measurements

Strictly speaking it is impossible to measure the activity of H^+ in solution at any temperature because individual ionic activities (and individual activity coefficients) cannot be uniquely and rigorously defined by thermodynamics (5). Instead, an operational definition of the pH is to be formulated (6)

$$pH = pH_s + \frac{(E - E_s)F}{2.303RT} \qquad [2.1]$$

Besides R,T and F which have their usual meaning, the subscript s refers to some standard solution and E is the electromotive force of the cell used to measure the pH of the standard and unknown solution. Eq.[2.1] yields correct values for pH only if the measurements are carried out in a cell without liquid junctions or if the liquid junction potentials are independent of the composition of the solution to be measured. The cell used in the present investigation, however, has several phase boundaries, but the variation of the diffusion potentials at the bridge-solution interfaces is minimized by using a special bridge construction. In order to avoid problems concerning the stability of the reference electrode at elevated temperatures, a saturated calomel electrode was placed in a thermostatted

vessel and kept at 20.0 °C, regardless of the actual working temperature in the titration vessel. It was connected to the vessel by an electrolyte bridge, so that there was a variable temperature gradient over the salt bridge.

In general the electromotive force, E, of a cell used in acid - base titration experiments may be expressed as

$$E_{cell} = E^{o'} - (2.303RT/F)pH \qquad [2.2]$$

where $E^{o'} = E^{o}_{glass} - E_j - E_{ref}$.

E^{o}_{glass} is the standard potential of the glass electrode, E_j is the (sum of) liquid junction potential(s) and E_{ref} is the potential of the reference electrode. The value of $E^{o'}$ can be determined at any temperature using calibration standards. In the present study we calibrated the cell against four Merck Titrisol standard buffer solutions of pH 4.00, 7.00, 9.00 and 11.00 (values at 20.0 °C). The pH values of these buffer solutions as a function of temperature are available from the manufacturer (7). From these calibration measurements $E^{o'}$ and (RT/F) in Eq.[2.2] are obtained at the desired temperatures. Detailed measurements in our cell over a temperature range of 5 - 85 °C, Nernst' factors were obtained that coincided within 1 % with the theoretical value.

2.3 Electrochemical cell

All titration experiments were carried out in the experimental set-up as represented in Fig.2.1. It contains a 600 ml double-walled pyrex glass titration vessel connected to a 100 ml thermostatted reference vessel by means of a salt bridge. Thermostatted water of the desired temperature was pumped continuously round the titration vessel, whilst the temperature of the reference vessel was kept constant at 20.0 °C using a second thermostat.

The salt bridge used was of the van Laar type (8), as modified by Bijsterbosch (9). This bridge consists of two capillaries having an electrical resistance of ca. 0.3 MΩ each. It is filled with a van Laar solution (1.75 M KNO_3 and 0.25 M $NaNO_3$) which minimizes liquid junction potentials

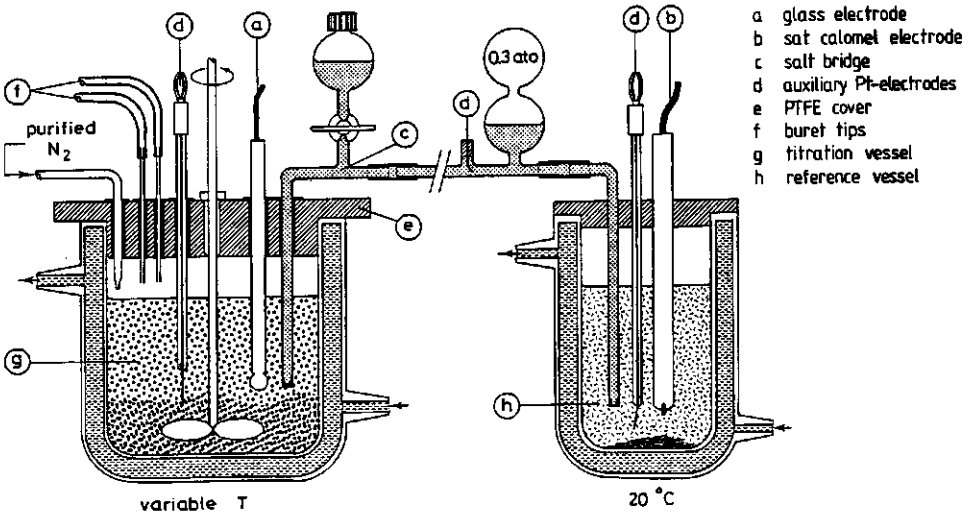

Fig. 2.1 Experimental set-up for potentiometric titrations at variable temperatures.

because in this mixture the transport of charge by cations and anions is equal. A small over-pressure is applied to obtain a constant, but very small stream of solution through the capillaries. The electrical resistance of the bridge and of the individual capillaries were checked from time to time by connecting a resistance bridge to the platinum electrodes (d) in the set-up.

In most of the experiments a temperature gradient had to develop. The stability of the potential readings was not markedly affected by increasing the temperature difference, therefore it was concluded that the gradient settles at a fixed place in the bridge (presumably the 'hot' side of the capillary) and therefore the thermo-electrical contribution to the potential can be calibrated out conveniently.

The measuring electrode was a Schott N1180 glass electrode with a temperature working range of 5 - 80 °C. As reference electrode a saturated calomel electrode (Schott, B291) was used.

Purified nitrogen was used to create a CO_2-free atmosphere in the titration cell. Technical N_2 (Hoek-Loos) was purified by passing it over a series of wash bottles, containing concentrated sulfuric acid, dry $CaCl_2$, 20 % (w/w) sodium hydroxide, water and 0.1 M NaOH respectively. After saturating it at ambient temperature by bubbling it through two wash bottles with water, the

N_2 was led into the titration vessel at such a rate that a small overpressure of nitrogen was maintained continuously in the cell. The whole set-up was placed in a closed metal box which acts as a Faraday cage.

2.4 Potentiometric titrations

The surface charge, σ_o, defined by

$$\sigma_o \equiv F(\Gamma_{H+} - \Gamma_{OH-}) = F(\Gamma_{HNO_3} - \Gamma_{KOH}) \qquad [2.3]$$

was determined using a potentiometric titration technique developed by the Dutch school of colloid scientists (8,10) and first applied to inorganic oxide systems by Bolt (11). In principle this technique is rather simple: a suspension of the colloid under study is titrated with electrolytes containing surface ions, in the case of inorganic oxides H^+ and OH^-. The change in the charge adsorbed at the oxide-solution interface, $\Delta\sigma_o$, is calculated from the difference in volumes of titrant needed to establish a certain pH (E) in the oxide suspension as compared to a blank (same solution but without the oxide).

$$\sigma_o^* = \frac{[(V.t)_{susp} - (V.t)_{blank}]F}{g} \qquad [2.4]$$

where V is the volume of titrant added, t is its concentration and g denotes the mass of oxide in the suspension.
The relative values for the surface charge density expressed per gram of oxide, σ_o^*, obtained in this way are made absolute by referring them to the point of zero charge (pH^o, p.z.c.) of the oxide. The point of zero charge can be identified with the common intersection point (c.i.p.) of a family of $\sigma_o(pH)$ curves at different concentrations of indifferent electrolyte.

A volume of concentrated stock suspension, containing 5 to 10 grams of the oxide was washed into the titration vessel with water, dry KNO_3 was added and the vessel made up to volume with water. The suspension was stirred and equilibrated at the desired temperature at low pH. After this equilibration, at least three to four titration curves were obtained by adding small aliquots of 0.2 M KOH or HNO_3, from automatic burets (Metrohm 655 Dosimat). Thereafter the electrolyte level was raised by the addition of dry KNO_3, and the procedure repeated. The whole titration procedure was controlled by

a microcomputer (Hewlett-Packard HP 86B) with data acquisition system (HP 3488A) and multimeter (HP 4378A). The computer program was designed such that titrations could be performed under variable equilibration conditions, regarding such parameters as the maximum drift in electromotive force per unit of time, the maximum time interval between subsequent additions, etc. During a titration experiment, at intervals of one to two minutes, the electromotive force of the cell was measured. Measurements were performed under non-stirred conditions, because stirring appeared to slightly interfere with the electromotive force readings. Thirty seconds before a reading the stirrer was stopped. Then E was sampled ten times over a period of ten milliseconds. The mean out of these readings was taken as 'the' electromotive force of the cell. Standard deviations of E obtained in this way mostly were below 0.01 mV and never exceeded 0.05 mV. In most titrations the system was taken to be at equilibrium when the drift was less than 0.02 mV/min, whereas the maximum time interval per addition was usually set at 60 minutes. Normally 30 to 40 experimental points per titration were obtained. Typically, titration curves were recorded as a function of E. By means of calibration before and after the measurement of a whole set of curves these were converted to the sought $\sigma_o(pH)$ curves.

2.5 Materials

2.5.1 General

All chemicals used in this study were of pro-analysi quality, and used without further purification. Water was pre-purified by reversed osmosis and subsequently passed through a Millipore Super-Q system. Prior to use the water was degassed in vacuo for ca. 20 minutes to avoid CO_2 contamination of the solutions. Titrants used were 0.2 M HNO_3 and KOH prepared from Merck Titrisol standard solutions. All glassware used was made of borosilicate glass and cleaned with concentrated nitric acid and extensively rinsed with water prior to use.

2.5.2 Oxides

The hematite (α-Fe_2O_3) used in this study was prepared according to Breeuwsma (12). In this procedure an acidic $FeCl_3$ solution is slowly hydrolyzed by the addition of base to yield an amorphous precipitate of iron oxides. We used Merck $Fe(NO_3)_3$ (lot no. 2521026) as the starting material.

Ageing of the precipitate in an autoclave at 140 - 150 °C yields pure hematite. The autoclaved samples were washed carefully with water at pH 7 to 8, where the material did coagulate readily, untill the conductivity of the supernatant did not exceed 1 μS/cm. Following Penners (13), the final washing steps were performed at pH < p.z.c. The stock sample hematite was stored in conductivity water and diluted as far as necessary prior to the adsorption experiments.

The BET surface area (N_2, a_o=16 nm^2) of the hematite sol was 29 m^2/g, whereas X-ray analysis showed no detectable impurities of the oxide.
Rutile (TiO_2) was prepared by hydrolysis of liquid $TiCl_4$ (Fluka, lot no. 34807 686) as described by Bérubé and de Bruyn (1). After ageing for three weeks by boiling the suspension, the resulting product proved to be X-ray pure rutile with a BET surface area of 51 m^2/gram.
Electron micrographs of the hematite and rutile standard sols are given in Fig.2.2. The hematite particles are more or less regular spheres, with a mean particle diameter of about 65 nm. The rutile suspension consists of very thin platelets, that show a strong tendency to form side-by-side agglomerates. The average dimensions are about 130 x 15 nm.

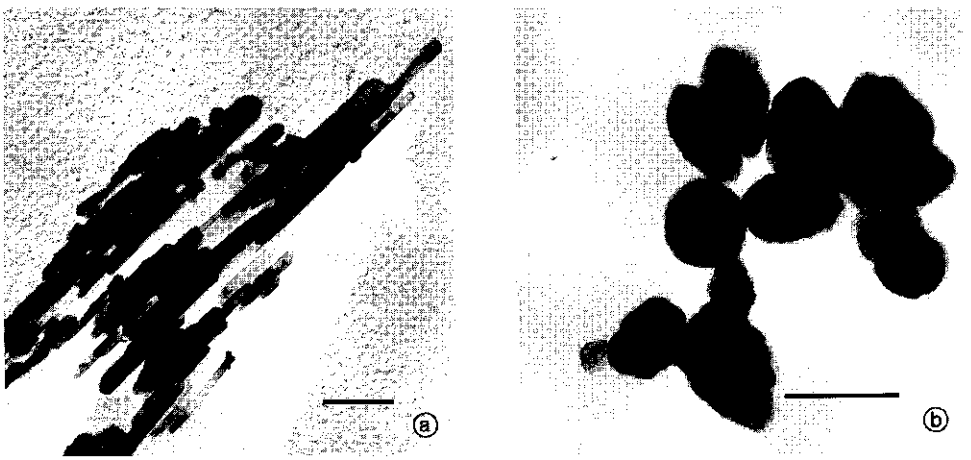

Fig.2.2 Electron micrographs of the rutile and hematite samples.
The bar indicates 100 nm.
a. Rutile (shaded specimen). b. Hematite.

2.6 References

1. Bérubé, Y.G., and de Bruyn, P.L., J. Colloid Interface Sci. 27, 305, 1968.
2. Tewari, P.H., and McLean, A.W., J. Colloid Interface Sci. 40, 267, 1972.
3. Tewari, P.H., and Campbell, A.B., J. Colloid Interface Sci. 55, 531, 1976.
4. Blesa, M.A., Figliolia, N.M., Maroto, A.J.G., and Regazzoni, A.E., J. Colloid Interface Sci. 101, 410, 1986.
5. Bates, R.G., "Electrometric pH Determinations", John Wiley & Sons, Inc., New York. Chapman & Hall, Ltd., London, 1954.
6. NBS Letter Circular LC933, National Bureau of Standards, Washington, D.C., 1950.
7. Anonymous, "Puffersubstanzen-Pufferloesungen-Puffer Titrisol Konzentrate", E. Merck, Darmstadt, undated.
8. van Laar, J.A.W., thesis, Utrecht, 1952.
9. Bijsterbosch, B.H., thesis, Utrecht, 1965.
10. Mackor,E.L., thesis, Utrecht, 1951.
11. Bolt, G.H., J. Phys. Chem. 61, 1166, 1957.
12. Breeuwsma, A., thesis, Wageningen, 1973.
13. Penners, N.H.G., thesis, Wageningen, 1985.

3. TEMPERATURE DEPENDENCE OF SURFACE CHARGE ON INSOLUBLE OXIDES

3.1 Introduction

Insoluble inorganic oxides derive their surface charge in aqueous suspensions from adsorption of protons and hydroxyl ions from the bulk solution. The generally accepted mechanism of charge formation is reaction of hydrolyzed surface species with H^+ or OH^-, which thermodynamically is equivalent to adsorption onto or desorption of protons from the surface.

One of the obvious ways to study basic properties of charge formation and related phenomena taking place in the interfacial region is to investigate the charge as a function of temperature. Comparison of experimental observations at different temperatures leads towards important thermodynamic parameters characterizing the adsorption equilibria.

Only little attention has been paid to the temperature dependence of the surface charge of oxides. This may be partly due to experimental and interpretational problems encountered in the potentiometric titrations that are commonly used to measure $\sigma_0(pH)$ curves. Until now investigations on the temperature dependence of the surface charge on oxide-solution interfaces (1-4) were mainly restricted to the position of the point of zero charge as a function of temperature.

From the group of inorganic insoluble oxides two representatives were selected for the investigations. Hematite (α-Fe_2O_3) was chosen as a 'basic' oxide and rutile (TiO_2) as an example of more 'acid' materials. Both oxides have been studied extensively during the past decades.

3.2 Experimental

Hematite and rutile suspensions and the potentiometric acid/base titration technique were described in chapter 2.

Obtaining detailed and accurate $pH^o(T)$ data is obviously one of the most important objects of this study. In principle, the previously described potentiometric titration technique offers a good means to do so, albeit that the measurement of a complete set of sufficiently accurate (pH^o,T) data would be an extremely time consuming matter. Moreover, in general practice, the fact that intersection points in potentiometric titration

curves at different salt concentrations are not always exactly sharp detracts from the possibility to treat the data thermodynamically. To overcome these problems we adopted the following experimental procedure, shortly called 'ΔT titration', yielding information on the relative position of σ_o(pH) at any temperature with respect to pH^o at 20 °C. The method is simple: after some acid/base titration cycles, a suspension of the oxide is equilibrated at its pH^o at 20 °C in 0.02 M KNO_3. Then, without addition of any chemicals, the temperature of the suspension is changed and, at equilibrium, the accompanying change in electromotive force, ΔE, is registered. From ΔE the shift in pH is calculated and from this, using proper activity corrections (5) the shift in surface charge, $\Delta\sigma_o$, follows. Experiments performed on batches of ca. 10 grams of the oxides in 500 ml suspension showed that $\Delta\sigma_o$, on changing the temperature never exceeded a few hundreths of a C/g, resulting in the fact that the new pH may be identified as the sought pH^o at the new temperature.

3.3 Results

The charge at the solid-solution interface has been measured for rutile and hematite as a function of KNO_3 concentration and temperature.

In Fig.3.1 the surface charge on rutile as a function of pH is given for some consecutive runs at different concentrations of KNO_3 at 20 °C. Al-

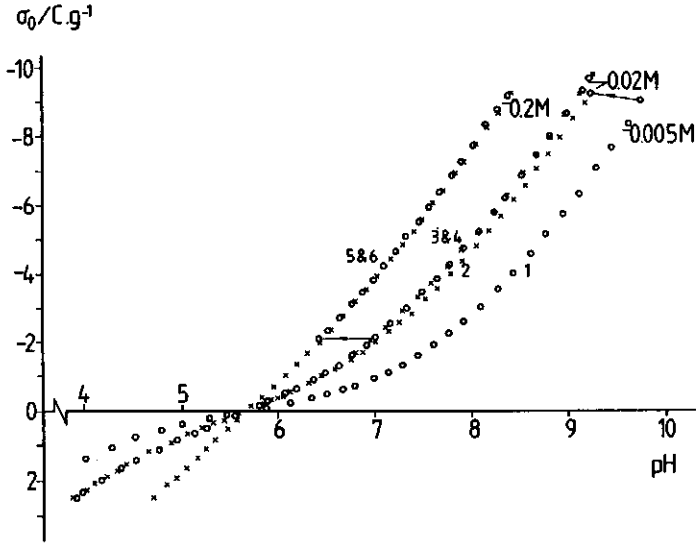

Fig.3.1 Surface charge density on rutile as a function of pH. Electrolyte: KNO_3, concentration indicated. Temperature: 20 °C. Specific surface area (BET): 51 m^2/g. Number of titration run is indicated.

though titrations were performed at the rather strict equilibrium criterion of a shift in E of less than 0.02 mV/min., the first titration at a new salt concentration is usually not a true equilibrium one. The second and further runs at the same, fixed salt concentration do not show detectable 'hysteresis' any more. The reversible curve obtained after the first up and down titrations is taken as 'the' equilibrium curve. While several titration cycles are needed per electrolyte concentration in order to obtain the real equilibrium titration curve and as these repeated titrations lead to an increase of the background electrolyte concentration, it was impossible to work at very low salt concentrations. Therefore, definitive titrations were performed in solutions containing at least 0.005 M KNO_3. Fig.3.2 shows σ_o(pH) curves for rutile at 5 and 50 °C, respectively. Here also good reproducible curves were obtained after the first run.

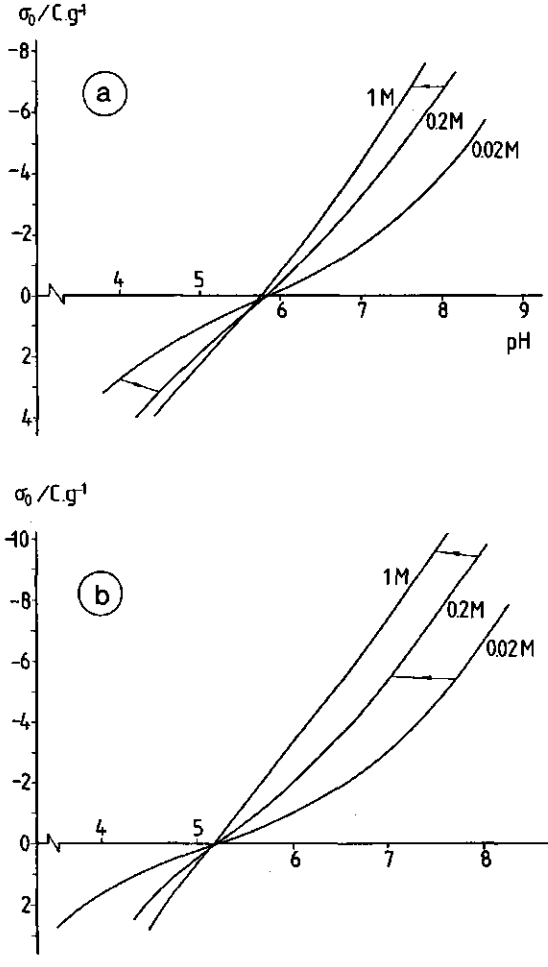

Fig.3.2 Surface charge density on rutile as a function of pH.
Electrolyte: KNO_3, concentration indicated. Specific surface area (BET): 51 m^2/g.
2a. Temperature: 5 °C.
2b. Temperature: 50 °C.

For hematite, titration results at 20 °C are given in Fig.3.3. Typically, the reproducibility for this material is somewhat less than for rutile. Usually, equilibration is much slower and some acid-base hysteresis seems to be omnipresent.

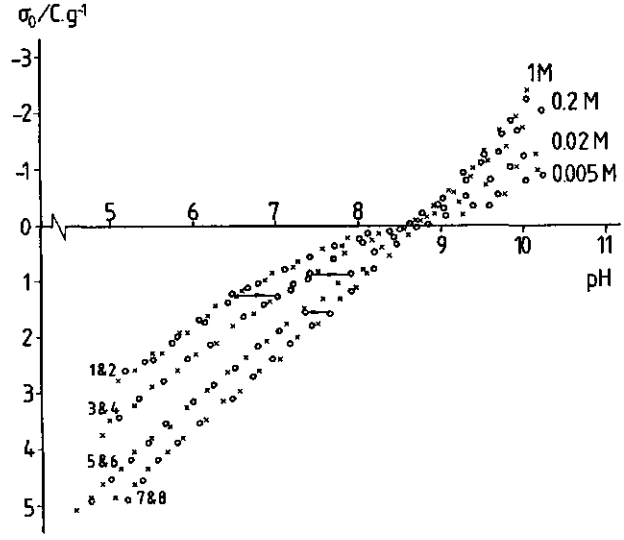

Fig.3.3 Surface charge density on hematite as a function of pH. Electrolyte: KNO_3, concentration indicated. Temperature: 20 °C. Specific surface area (BET): 29 m^2/g. Number of titration run is indicated.

By way of examples, σ_0(pH) relations for hematite at 5 and 60 °C are shown in Fig.3.4. As was the case for rutile, measuring at temperatures other than room temperature did not markedly affect experimental accuracy.

On inspection of Figs 3.1 through 3.4 some general trends become clear. At any temperature, surface charge–pH curves tend to become parallel lines at sufficient distance from pH^o. This would imply that $\partial\sigma_0/\partial pH$ is then constant at given surface charge density and independent of the electrolyte concentration. Furthermore, a downward shift of pH^o with increasing temperature is observed, for rutile from ca. 5.8 at 5 °C to ca. 5.1 at 50 °C and for hematite from 9.3 (5 °C) to 7.8 (60 °C).

ΔT titrations in the range 10 - 70 °C were performed on both oxides in order to check and supply pH^o data from potentiometric titrations. On both oxides several experimental runs in 0.02 M KNO_3 were performed (20 → 70, 70 → 10 °C, etc.), resulting in very reproducible relative pH^o(T) relations.

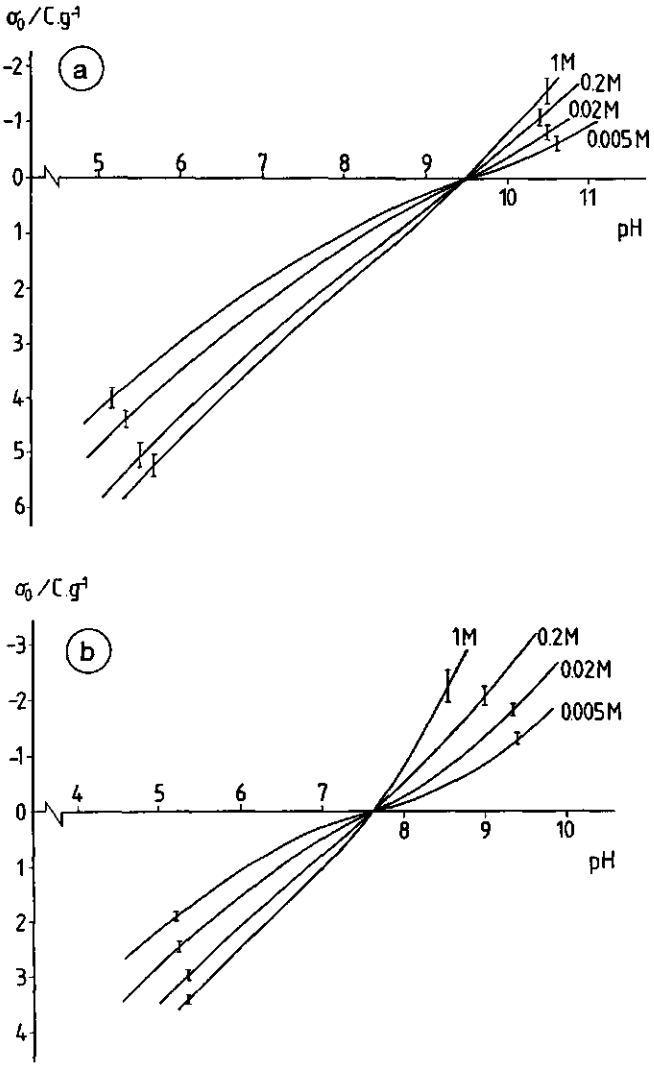

Fig.3.4 Surface charge density on hematite as a function of pH.
Electrolyte: KNO_3, concentration indicated. Specific surface area (BET): 29 m^2/g.
4a. T=5 °C.
4b. T=60 °C.

The values obtained for $pH^o(T)$ with both techniques are presented in Fig.3.5 for rutile and hematite.

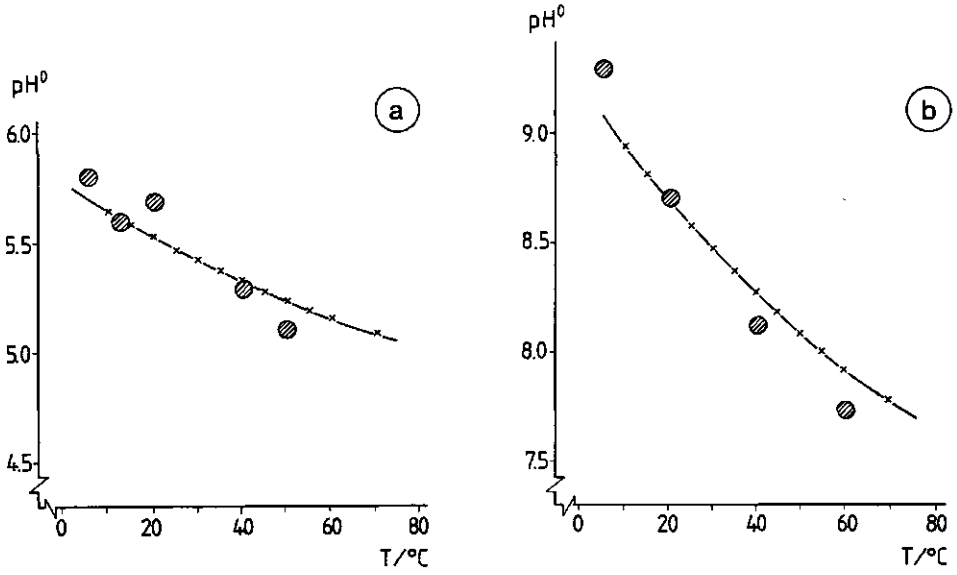

Fig.3.5 Point of zero charge of rutile and hematite as a function of temperature. O: determined by potentiometric acid/base titration, x: from 'ΔT titration' (see text).
5a. Rutile. 5b. Hematite.

3.4 Discussion

Figs 3.2 - 3.5 in principle contain three types of information. First, the shapes of the titration curves as a function of temperature are important features furnishing insight into the charge-determining processes. Second, comparison of results obtained for the two different oxides helps to distinguish between oxide-specific and general double layer properties. Finally, the dependence of pH^0 upon temperature is related to the nature of the chemical interactions between the interfaces and the adsorbing ions (H^+ and OH^-). We shall now elaborate these aspects.

Charge - pH behavior

To determine the influence of temperature on the charge - potential behavior of both oxides, $\sigma_0(pH)$ curves were normalized by replotting them with respect to their own pH^0 at every temperature. Results are given in Fig.3.6 for rutile and in Fig.3.7 for hematite. In the case of rutile an almost

perfect temperature congruence of the curves is observed. Also for hematite temperature congruence is observed, though within an admittedly larger experimental error. Accepting temperature congruence as a fact for both oxides, we will in the following focus our discussion on the 'mastercurves' (Figs 3.6 and 3.7) at any electrolyte level for both rutile and hematite.

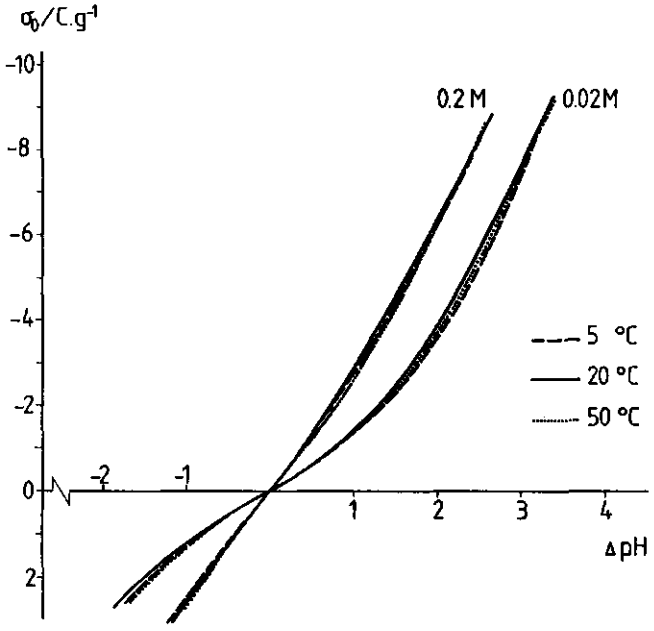

Fig.3.6 Temperature congruence of the surface charge density on rutile as a function of pH relative to pH^o. Electrolyte: KNO_3, concentration indicated.

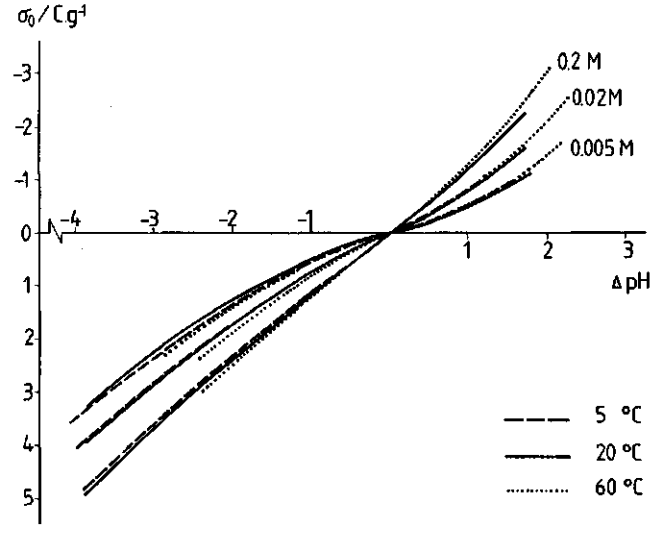

Fig.3.7 Temperature congruence of the surface charge density on hematite as a function of pH relative to pH^o. Electrolyte: KNO_3, concentration indicated.

Surface charge - pH curves for the oxides at 0.02 and 0.2 M KNO_3 with respect to their own pH^o are compared in Fig.3.8. It is clear that the shape of the curves is very similar. In the diagram charge densities are recorded on a mass basis. As has already been noted in a previous paper (6), for three oxides an identical charge(pH) relation is observed for different salt concentrations at 20 °C, when the BET surface area is used to calculate charge densities. For both oxides under study here, this too applies for other temperatures in the range investigated, as can be judged from the calculated ratio $r_{\sigma_o} = \sigma_{o,rutile}/\sigma_{o,hematite}$, at constant pH of 1.8 ± 0.1.

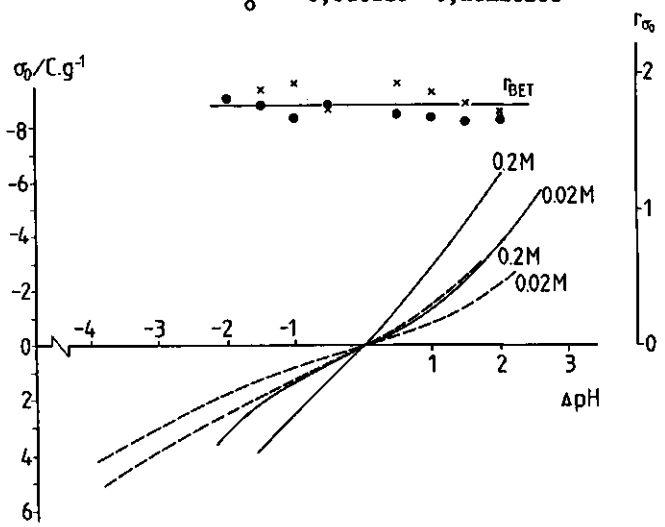

Fig.3.8 Surface charge-($pH-pH^o$) mastercurves for rutile and hematite at arbitrary temperature. Solid lines refer to rutile, dashed to hematite. Points refer to r_{σ_o}, ●: 0.02 M, x: 0.2 M KNO_3.

This value compares well with the ratio in BET surface areas for the oxides, $r_{BET} = 51/29 = 1.76$. This result leads to the conclusion that when charge densities are calculated on the basis of the (BET) surface area, $\sigma_o(pH-pH^o)$ curves are identical within experimental error for all temperatures investigated. From this finding two important conclusions can be drawn:

(i) The BET surface area for rutile and hematite seems to be a reliable measure for the 'electrochemical' surface area at any temperature, and

(ii) Charge formation at the oxide-solution interface starting from pH^o seems to be a rather aspecific process. The mechanisms determining the double-layer properties must therefore be governed mainly by the solution side.

For the description of the σ_o-pH curves finding (ii) made us wonder to which extent a simple Gouy-Stern approach is able to account for experi-

mental observations. To that end we used the Poisson-Boltzmann equation for a flat diffuse double layer, extended with a charge-free Stern layer. At a given ψ_o the matching values of σ_o were calculated. In these calculations the only adjustable parameter is the value of the Stern layer capacitance

$$C_s = \varepsilon_s \varepsilon_o / \delta \qquad [3.1]$$

with δ being the thickness and ε_s the relative dielectric constant of that layer.

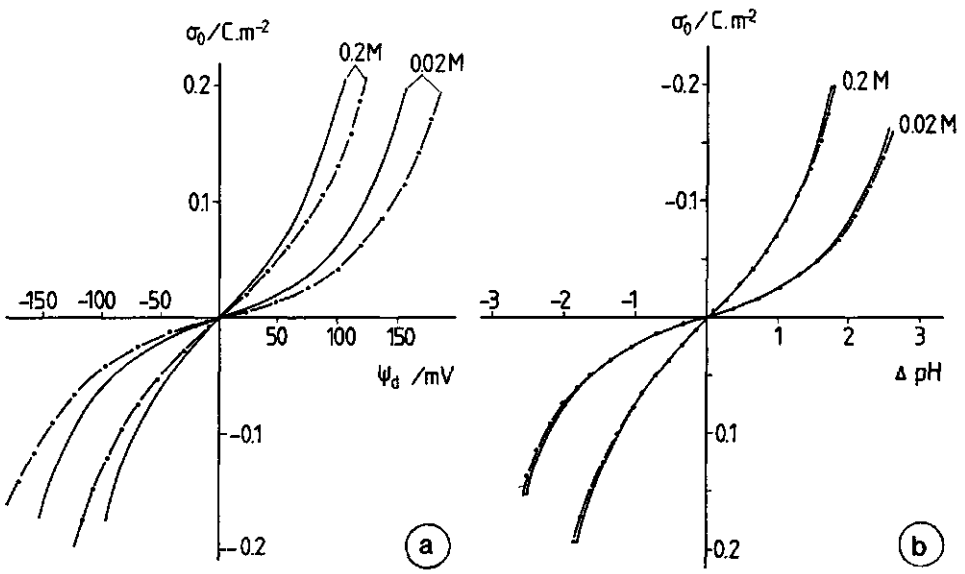

Fig.3.9 Theoretical surface charge density of a purely diffuse flat double layer in different concentrations KNO_3 at 20 and 70 °C.
9a. as a function of diffuse potential
9b. as a function of ΔpH

As is seen from Fig.3.9, the influence of temperature on the diffuse part of the double layer becomes negligibly small if the surface potential depends on solution pH according to Nernst's law

$$\psi_o = -2.303 \frac{RT}{F} (pH - pH^o) \qquad [3.2]$$

The high extent of T-congruence in the diffuse σ_o-pH relation is due to an

almost exact compensation of 'RT-effects' by the temperature dependence of ε^L (7). As has been demonstrated elsewhere (8) (pseudo-) Nernstian behavior of the oxide surface with respect to solution pH is obtained when only a small fraction of the available surface groups is (de)protonated in the charging process (or in other terms: when the μ's of the surface groups are not significantly altered on adsorption or desorption of H^+). In the charge density interval that is presently under consideration this is the case. Only small Stern corrections have to be made (i.e. high values for C_s are needed) to provide a reasonable fit with experimental results. If, for sake of convenience, the Stern layer capacitance is thought to be invariant with T a value for C_s of ca. 450 $\mu F/cm^2$ follows from the fitting procedure (Fig.3.10). The exact value of C_s in this order of magnitude is no longer critical.

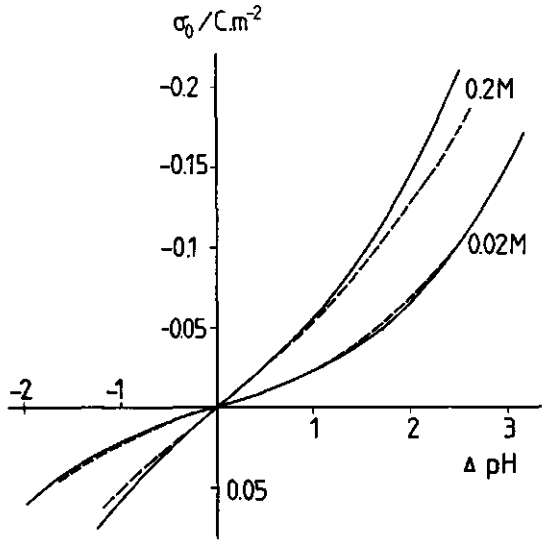

Fig.3.10 Surface charge-ΔpH behavior of rutile and hematite at 5-70 °C. Dashed curves: experimental observations, solid: theoretical according to Gouy-Stern with $C_s \sim 450$ $\mu F/cm^2$.

The adsorption of protons (and hydroxyl ions) as a function of proton activity can always be written as a general mathematical function

$$f(\sigma_o, c_{salt}, T) = 10^{-pH} \qquad [3.3]$$

The proton adsorption isotherm is classified as congruent in temperature,

provided the function f is separable into a product of two functions, as follows

$$f'(\sigma_o, c_{salt}) \cdot f''(T) = 10^{-pH} \qquad [3.4]$$

or

$$- {}^{10}\log f'(\sigma_o, c_{salt}) - {}^{10}\log f''(T) = pH \qquad [3.5]$$

where f' is independent of T.
The temperature congruence can be experimentally verified if shifting along the pH axis leads to merging of the (σ_o,pH) curves. From the analysis above it follows that

$${}^{10}\log f''(T) = pH^o \qquad [3.6a]$$

and

$${}^{10}\log f'(\sigma_o, c_{salt}) = pH - pH^o \qquad [3.6b]$$

If the double layer were purely diffuse, f' is hardly a function of temperature. The function f'' yields information on the enthalpy of proton adsorption as will be demonstrated below.

A value of a few hundred $\mu F/cm^2$ for the Stern layer capacitance is considerably higher than the one found for Hg and AgI (ca 30 $\mu F/cm^2$) (9). In comparing the Stern layer capacitances of simple inorganic oxides on one hand with the more 'classical' model systems Hg and AgI on the other, one has to consider a pronounced difference in hydrophobicity between the two groups of systems. Water molecules at the rather hydrophobic surface of Hg and AgI will be strongly oriented by hydrophobic hydration (10,11). The interface of usual inorganic oxides, however, after chemi- and physisorption of water will show a 'bulk water-like' structure, because only the first, dissociatively adsorbed water layer shows strong interactions with the oxide surface (12). Beyond any doubt the charge-free space, whenever existent in oxide systems, will be located in this 'watery' region. It is not unlikely that ε_s does not differ too much from the value for bulk solu-

tions and therefore high Stern layer capacitances are to be expected for oxides.

Point of zero charge

Analysis of the temperature dependence of the point of zero charge leads us to important thermodynamic parameters of the process of charge formation. In principle, there are two possible ways of facing the problem; a strictly thermodynamic approach and a model-bound ('site-binding') way of reasoning. Both methods will be discussed in this section.
The thermodynamic approach starts from the Gibbs equation

$$d\gamma = -S^{\sigma}dT - \Gamma_{w}^{\sigma}d\mu_{w} - \Gamma_{HNO_3}^{\sigma}d\mu_{HNO_3} - \Gamma_{KOH}^{\sigma}d\mu_{KOH} - \Gamma_{s}^{\sigma}d\mu_{s} - \Gamma_{ox}^{\sigma}d\mu_{ox} \qquad [3.7]$$

where γ is the interfacial tension, S^{σ} is the surface excess entropy per unit area, Γ_i^{σ} is the surface excess concentration of component i per unit area and μ_i is its chemical potential. The subscripts w, s and ox refer to water, KNO_3 and oxide, respectively.
The chemical potentials of the components in the system are not independent. The changes in chemical potentials of HNO_3, KOH, KNO_3 and H_2O are related as follows

$$d\mu_{KOH} = d\mu_{s} + d\mu_{w} - d\mu_{HNO_3} \qquad [3.8]$$

Furthermore, the Gibbs-Duhem relation can be applied to both the solution and the oxide phase.
For the solution the following relation is obtained

$$d\mu_{w} = -S^{w}dT - \frac{x_{HNO_3}}{x_{w}}d\mu_{HNO_3} - \frac{x_{KOH}}{x_{w}}d\mu_{KOH} - \frac{x_{s}}{x_{w}}d\mu_{s} \qquad [3.9]$$

where x_i is the mole fraction of component i in solution and S^{w} is the molar entropy of the solution.

For the oxide phase the Gibbs-Duhem relation assumes the following form

$$S^{ox}dT + d\mu_{ox} = 0 \qquad [3.10]$$

where S^{ox} is the molar entropy of the solid.
Using relations [3.8] to [3.10], the Gibbs equation can be written as

$$d\gamma = -(S^{\sigma} - (\Gamma_w^{\sigma} + \Gamma_{KOH}^{\sigma})\, S^{w} - \Gamma_{ox}^{\sigma}\, S^{ox})dT$$

$$- [\Gamma_{HNO_3}^{\sigma} - \Gamma_{KOH}^{\sigma} + (\frac{x_{KOH} - x_{HNO_3}}{x_{KOH} + x_w})\,(\Gamma_w^{\sigma} + \Gamma_{KOH}^{\sigma})]d\mu_{HNO_3} \qquad [3.11]$$

$$- [\Gamma_s^{\sigma} + \Gamma_{KOH}^{\sigma} - (\frac{x_{KOH} + x_s}{x_{KOH} + x_w})\,(\Gamma_w^{\sigma} + \Gamma_{KOH}^{\sigma})]d\mu_s$$

Eq.[3.11] is reformulated as follows

$$d\gamma = -S^{(s)}dT - (\frac{\sigma_o}{F})\, d\mu_{HNO_3} - \Gamma_{K^+}^{(s)} d\mu_s \qquad [3.12]$$

In Eq.[3.12] $S^{(s)}$ is the relative surface excess entropy, defined as

$$S^{(s)} = S^{\sigma} - \Gamma_w^{\sigma}\, S^{w} - \Gamma_{KOH}^{\sigma} S^{w} - \Gamma_{ox}^{\sigma} S^{ox} \qquad [3.13]$$

The symbol $\Gamma_i^{(s)}$ is used to indicate the relative surface excess concentration of component i, according to

$$\Gamma_i^{(s)} = \Gamma_i^{\sigma} - \frac{x_i}{x_w + x_{KOH}}\,(\Gamma_w^{\sigma} + \Gamma_{KOH}^{\sigma}) \qquad [3.14]$$

The symbol σ_o denotes the surface charge density,

$$\sigma_o = F[\Gamma_{HNO_3}^{\sigma} - \Gamma_{KOH}^{\sigma} + (\frac{x_{KOH} - x_{HNO_3}}{x_{KOH} + x_w})\,(\Gamma_w^{\sigma} + \Gamma_{KOH}^{\sigma})] =$$

$$= F(\Gamma_{HNO_3}^{(s)} - \Gamma_{KOH}^{(s)}) \qquad [3.15]$$

and $\Gamma^{(s)}_{K^+}$ is the total relative surface excess of K^+, given by

$$\Gamma^{(s)}_{K^+} = (\Gamma^{(s)}_{s} + \Gamma^{(s)}_{KOH}) \qquad [3.16]$$

A prove that the relative excess quantities $S^{(s)}$ and $\Gamma^{(s)}_{i}$ are independent of the choice of the Gibbs dividing plane is given in the appendix.
By introduction of an alternative function of state ξ, defined by

$$\xi = \gamma + \frac{\sigma_o}{F} \mu_{HNO_3} \qquad [3.17]$$

Eq.[3.12] can be rewritten to yield

$$d\xi = -S^{(s)}dT - \Gamma^{(s)}_{K^+} d\mu_s + \frac{\mu_{HNO_3}}{F} d\sigma_o \qquad [3.18]$$

By cross differentiation in Eq.[3.18] we obtain

$$\frac{1}{F} \left(\frac{\partial \mu_{HNO_3}}{\partial T}\right)_{\sigma_o,\mu_s} = - \left(\frac{\partial S^{(s)}}{\partial \sigma_o}\right)_{T,\mu_s} \qquad [3.19]$$

Considering that in experimental situations usually $c_s >> c_{HNO_3}$, it follows that for constant μ_s, $d\mu_{HNO_3} \sim d\tilde{\mu}_{H+}$, and Eq.[3.19] yields

$$\frac{1}{F} \left(\frac{\partial \tilde{\mu}_{H+}}{\partial T}\right)_{\sigma_o,\mu_s} = - \left(\frac{\partial S^{(s)}}{\partial \sigma_o}\right)_{T,\mu_s} \qquad [3.20]$$

In this equation $\tilde{\mu}_{H^+}$ is the electrochemical potential of the proton.

Stated otherwise,

$$\left(\frac{\partial \tilde{\mu}_{H+}}{\partial T}\right)_{\sigma_o,\mu_s} = - \left(\frac{\partial S^{(s)}}{\partial (\sigma_o/F)}\right)_{T,\mu_s} \equiv - S^{(s)}_{H^+} \qquad [3.21]$$

where $S^{(s)}_{H^+}$ is the relative surface excess entropy of proton adsorption.

Equation [3.21] can be reformulated as

$$\left(\frac{\partial[\tilde{\mu}_{H+}/T]}{\partial T}\right)_{\sigma_o,\mu_s} = -\frac{\tilde{\mu}_{H+}}{T^2} - \frac{1}{T}\left(\frac{\partial\tilde{\mu}_{H+}}{\partial T}\right)_{\sigma_o,\mu_s} = \quad [3.22]$$

$$= -\frac{\tilde{\mu}_{H+}}{T^2} + \frac{S^{(s)}_{H+}}{T} = -\frac{H^{(s)}_{H+}}{T^2}$$

For the standard state in the liquid phase it can be shown that

$$\left(\frac{\partial[\mu^o_{H+}/T]}{\partial T}\right)_{P,n_{H+},n_i} = -\frac{H^L_{H+}}{T^2} \quad [3.23]$$

At equilibrium, the electrochemical potential of the proton in the surface phase equals the chemical potential of the proton in solution, thus

$$\tilde{\mu}_{H+} = \mu_{H+} = \mu^o_{H+} + RT\ln a_{H+} \quad [3.24]$$

Here a_{H+} is the proton activity in the bulk solution.
With help of Eqs [3.23] and [3.24] for the point of zero charge Eq.[3.22] can be rewritten to yield

$$\left(\frac{\partial \ln a_{H+}}{\partial T}\right)_{\mu_s,\sigma_o} = -\frac{\Delta_{ads}H_{H+}}{RT^2} \quad [3.25]$$

where

$$\Delta_{ads}H_{H+} = H^{(s)}_{H+} - H^L_{H+} \quad [3.25a]$$

is the molar enthalpy change of proton adsorption at surface charge σ_o.
In practice, experiments are usually performed at constant electrolyte concentration. In this situation Eq.[3.25] can be rewritten by means of the following relation

$$\left(\frac{\partial \ln a_{H+}}{\partial T}\right)_{\sigma_o,\mu_s} = \left(\frac{\partial \ln a_{H+}}{\partial T}\right)_{\sigma_o,c_s} - \left(\frac{\partial \ln a_{H+}}{\partial \mu_s}\right)_{\sigma_o,T}\left(\frac{\partial \mu_s}{\partial T}\right)_{\sigma_o,c_s} \quad [3.26]$$

In fact all terms in Eq.[3.26] are accessible.

At the point of zero charge the situation simplifies considerably. If there is no specific adsorption of supporting electrolyte ions -as is presumably the case for our oxides in KNO_3- pH^o is obtained as the common intersection point of $(\sigma_o, pH)_T$ curves at different electrolyte concentrations and therefore $(\partial \ln a^o_{H+}/\partial \mu_s)_T$ equals zero. The proton activity at the p.z.c. is indicated as a^o_{H+}. At the p.z.c. the second term at the RHS of Eq.[3.26] vanishes. As a result, in indifferent electrolyte, the isosteric heat of proton adsorption on oxides in the p.z.c. simply follows from the shift in pH^o with temperature, according to

$$\left(\frac{\partial pH^o}{\partial T}\right)_{c_s} = \frac{\Delta_{ads}H_{H+}}{2.303RT^2} \qquad [3.27]$$

In the case of specific adsorption, the p.z.c. varies with the electrolyte concentration, and hence the extra term in Eq.[3.26] is needed in the calculation of $\Delta_{ads}H_{H+}$.

After this thermodynamic elaboration of a relation between the shift in pH^o with T, it could be verified whether or not a site-binding approach leads to the same conclusions. In this approach the oxide surface is visualized by an array of surface sites (we could think of hydrolyzed metal atoms) able to react with, or release protons. We will keep the model as general as possible by considering a series of charge forming reactions. Thus the following general dissociation reaction can be written down:

$$SH_q^{(q-n)+} \overset{}{=} \underset{K_q}{} SH_{(q-1)}^{(q-n-1)+} + H^+ \qquad [3.28]$$

where n+ is the valency of the lattice cation and the q^{th} protonation/dissociation step is considered.

General chemical thermodynamics provides the relation describing the shift in equilibrium with temperature:

$$\frac{d\ln K_q}{dT} = \frac{\Delta H_q}{RT^2} \qquad [3.29]$$

in which ΔH_q is the enthalpy change of the protonation step q, and K_q is its equilibrium constant.

If the equilibrated system is moved away from equilibrium by addition of, say, acid the relative contributions of the individual kinds of sites,

$SH_q^{(q-n)+}$ in equilibration will change accordingly. This difference can be expressed by attributing weight factors w_i to the individual reactions. For the overall series of reactions we thus obtain

$$\sum_i w_i \frac{d\ln K_i}{dT} = \frac{\sum_i w_i \Delta H_i}{RT^2} = \frac{\Delta_{ads} H_{H+}}{RT^2} \qquad [3.30]$$

For the overall reaction constant, K_t, one can write

$$K_t = K_1^{w_1} K_2^{w_2} K_3^{w_3} \ldots K_q^{w_q} \qquad [3.31]$$

Substituting mass law expressions for the individual K_i's in Eq.[3.31] yields

$$K_t = a_{H+} \cdot \left\{ \frac{[S^{n-}]^{w_1}}{[SH^{(n-1)-}]^{w_1}} \cdots\cdots \frac{[SH_{q-1}^{(q-n-1)+}]^{w_q}}{[SH_q^{(q-n)+}]^{w_q}} \right\} \qquad [3.32]$$

'configuration term'

Since the total site concentration in the system will be extremely high and consequently the redistribution of protons is only infinitesimally small, we may, to a good approximation, consider the configuration term in Eq.[3.32] to be constant and absorb it in the equilibrium constant by substituting

$$K_t' = K_t / \text{'configuration term'}$$

At the p.z.c. Eq.[3.32] attains the following form

$$K_t' = a_{H+}^o \qquad [3.33]$$

From this it follows directly that

$$\left(\frac{\partial \ln K'_t}{\partial T}\right)_{c_s} = \left(\frac{\partial \ln a^{o}_{H+}}{\partial T}\right)_{c_s} = 2.303 \left(\frac{\partial pH^{o}}{\partial T}\right)_{c_s} \qquad [3.34]$$

Combination of Eqs [3.30] and [3.34] then yields

$$\left(\frac{\partial pH^{o}}{\partial T}\right)_{c_s} = -\frac{\Delta_{ads}H_{H+}}{2.303RT^2} \qquad [3.35]$$

Comparison of Eqs [3.35] and [3.27] learns that both methods lead to the same conclusion:
The shift in pH^{o} with T is related to the isosteric enthalpy change of proton adsorption at the oxide-solution interface. The minus sign in Eq.[3.35] is due to the fact that all reactions were written as proton dissociations

By using the dissociation equilibrium of water it is possible to write all relations hitherto derived also in terms of a_{OH^-}. By following this procedure, the heat of neutralization is absorbed in $\Delta_{ads}H$.

For analysis of the change in the point of zero charge with temperature of rutile and hematite we use Eq.[3.27]. When pH^{o} data collected in Fig.3.5 are replotted as a function of reciprocal temperature, very good straight lines for both rutile and hematite are obtained ($r>0.999$), indicating, within experimental error, a constant value for $\Delta_{ads}H_{H+}$ for both oxides over the temperature range investigated. From the slopes the enthalpy change of proton adsorption at the point of zero charge is found. Standard Gibbs energy changes for proton transfer to the surface in the point of zero charge are obtained as a function of T from the absolute values of pH^{o} in Fig.3.5 using Eq.[3.33]. Thermodynamic parameters at 20 and 60 °C are given in Table 3.1.

To enable comparison of the processes on the oxide's surface with a analogous bulk process, the corresponding parameters for the protonation of bulk hydroxyl ions are included. From the hydrolysis constant of water as a function of temperature (13) we computed the heats of neutralization from the slope of a $\ln K_w$ vs. T plot using Eq.[3.29]. Here ΔH depends on temperature, varying in an almost linear fashion from -62 kJ/mol at 0 °C to - 49 kJ/mol at 60 °C.

Table 3.1. Thermodynamic parameters for H^+ binding onto inorganic oxides and bulk hydroxyl ions as a function of temperature.

'OXIDE'	$\Delta_{ads}H_{H+}$ kJ/mol		$\Delta_{ads}G^{o}_{H+}$ kJ/mol		$\Delta S^{o}_{ads}H^{+}$ $J/mol.K^{-1}$	
	20°C	60°C	20°C	60°C	20°C	60°C
RUTILE	-17.6		-31.0	-32.8	+45.7	+45.6
HEMATITE	-36.3		-48.8	-50.4	+42.7	+42.3
bulk OH^-	-57.5	-49.4	-79.5	-83.0	+75.1	+100.6

In the ΔH values in Table 3.1 a clear trend is observed: ΔH becomes more exothermic in the sequence rutile<hematite<OH^-. As far as both oxides are concerned this trend can be understood by realizing that electronic densities on the metal ions (i.e. Ti(IV) and Fe(III)) will substantially affect the electronegativity of the corresponding OH groups in the surface, thereby influencing the bond strength and hence the affinity for protons. The higher charged titanium ion will more strongly lower the electron density on a neighboring OH group than does Fe(III). This is reflected by the stronger bonding of protons onto hematite compared to rutile. That for the bulk process an even stronger bonding is observed, is due to the fact that here the electrical effects are of an ionic rather than inductive nature. Therefore presumably a better comparable bulk process would be the formation of hydrogen bonds in bulk water. For this process, ΔH is ca. -10.5 kJ/mol as determined by spectroscopic techniques (14). May be the most comparable analogous bulk process is something between proton binding to OH^- and H_2O, with an intermediate value for ΔH (say minus 20 - 30 kJ/mol) , then, realizing that 'pH^o' for water is about 7, the sequence in points of zero charge would be reflected by the ΔH values in Table 3.1.

The entropy data in the table presumably are best interpreted in terms of changes in hydration of the ions and the interface on adsorption. As a first step we compare changes in hydration accompanying proton association with oxide surface groups or bulk hydroxyl ions. In the bulk reaction the total change in hydration entropy amounts to a loss of hydration of the

proton and hydroxyl ion and gain of 'hydration' of the resulting water molecule. From a hydration point of view an OH group in the interface behaves as if it were half a bulk hydroxyl ion, whereas the resulting OH_2^+ group will be roughly half as much 'hydrated' as bulk water. Visualizing the charging process by association of half-way dehydrated protons with half-way hydrated surface OH groups under the formation of 'surface water', which is hydrated by half a 'water hydration shell', one would expect the overall change in hydration at the oxide interface to be roughly half as large as in bulk neutralization. This reasoning is confirmed by the entropy data in Table 3.1. As is obvious from the table, entropies for the protonation of oxides are rather aspecific and are hardly a function of temperature in the range considered.

The treatment of Bérubé and de Bruyn (1) on the temperature dependence of pH^o of rutile yields quantities called ΔH^* and ΔS^*, standing for the differences in enthalpy and entropy of transfering H^+ and OH^- from the bulk solution to the interfacial region at the point of zero charge. These parameters are related to the ones in Table 3.1 by the following equations

$$\Delta H^* = (\Delta_{ads}H_{H+} - \Delta_{ads}H_{OH-})/2, \text{ and } \Delta_{ads}H_{H+} + \Delta_{ads}H_{OH-} = \Delta_{neutr}H_{H_2O} \qquad [3.37]$$

Thus,

$$\Delta H^* = (2\Delta_{ads}H_{H+} - \Delta_{neutr}H_{H_2O})/2$$
$$\Delta S^* = (2\Delta_{ads}S_{H+} - \Delta_{neutr}S_{H_2O})/2 \qquad [3.38]$$

From the values for ΔH^* and ΔS^* (1), the following values for the enthalpy and entropy of adsorption of protons at the rutile - solution interface are derived:

$\Delta_{ads}H_{H+} = -14.9$ kJ/mol and

$\Delta_{ads}S^o_{H+} = +46.1$ J/mol.K^{-1} (20 °C).

These results agree reasonably well with ours. One must be aware, however, that the value of ΔH^* is only indirectly related to the measurable heat of proton adsorption.

Microcalorimetric measurements of the enthalpy of charge formation on rutile and hematite grossly confirm the results in this study. In a forth-

coming chapter, microcalorimetric experiments will be discussed in detail, thereby paying special attention to the relation between microcalorimetry and titration experiments of oxides outside the point of zero charge (chapter 4).

3.5 Conclusions

From σ_o-pH relations on rutile and hematite it follows that the point of zero charge, pH^o, is determined by specific interactions of the surface with protons in solution: whether an oxide behaves 'acidic' ($pH^o < \frac{1}{2}pK_w$) or 'basic' ($pH^o > \frac{1}{2}pK_w$) is governed by the relative affinity of the surface for protons as compared to bulk OH^- ions. This is a specific oxide property. However, the build-up of charge on the surface starting from the point of zero charge is rather aspecific. At constant electrolyte concentration, σ_o-(pH-pH^o) curves are within experimental error identical for rutile and hematite if the BET(N_2) surface area is used for the calculation of charge densities. Changes in temperature only affect the position of titration curves, but do not influence their shape: both oxides show temperature congruence of σ_o(pH) curves. This leads to the practical conclusion that per electrolyte concentration, given the BET surface area and pH^o, one 'mastercurve' suffices to describe σ_o(pH) for both rutile and hematite (and presumably other simple oxides of the type) at any temperature in the range studied.

From our thermodynamic analysis of the temperature dependence of the p.z.c., heats of surface charge formation at that point were obtained. It was shown that charge formation by adsorption of protons or hydroxyl ions thermodynamically can not be distinguished. By using properly defined excess quantities, this problem could be solved satisfactorily. It is shown that the position of pH^o is rather determined by enthalpic interactions than by entropic ones.

Presupposing the applicability of Nernst's law to both oxides, the double layer structure on these materials is satisfactorily modeled using the simple Gouy - Stern approach with high values for the Stern layer capacitance (~400-500 $\mu F/cm^2$).

3.6 References

1. Bérubé, Y.G., and de Bruyn, P.L., J. Colloid Interface Sci. 27, 305, 1968.
2. Tewari, P.H., and McLean, A.W., J. Colloid Interface Sci. 40, 267, 1972.
3. Tewari, P.H., and Campbell, A.B., J. Colloid Interface Sci. 55, 531, 1976.
4. Blesa, M.A., Figliolia, N.M., Maroto, A.J.G., and Regazzoni, A.E., J. Colloid Interface Sci. 101, 410, 1984.
5. Davies, "Ion Association", Butterworths, London, 1962.
6. Fokkink, L.G.J., de Keizer, A., Kleijn, J.M., and Lyklema, J., J. Electroanal. Chem. 208, 401, 1986.
7. CRC Handbook of Physics and Chemistry (R.C. Weast and M.J. Astle, Eds), 62nd Edition, E-58, 1981.
8. Healy, T.W., and White, L.R., Adv. Colloid Interface Sci. 9, 303, 1978.
9. Bijsterbosch, B.H., and Lyklema, J., Adv. Colloid Interface Sci. 7, 147, 1978.
10. Vincent, B., Bijsterbosch, B.H., and Lyklema, J., J. Colloid Interface Sci. 37, 171, 1971.
11. Billett, D.F., and Ottewill, R.H., S.C.I. Monograph 25 (Wetting), 253, 1967.
12. Hendewerk, M., Salmeron, M., and Somorjai, G.A., Surface Sci. 172, 544, 1986.
13. CRC Handbook of Physics and Chemistry (R.C. Weast and M.J. Astle, Eds), 62nd Edition, D-145, 1981
14. Lilley, T.H., in "Water", Vol.3 (F. Franks, Ed.), Plenum Press, New York-London, 277, 1973.

APPENDIX

In the main text, the relative surface excess entropy and the relative surface excess concentration are defined by the following equations

$$S^{(s)} \equiv S^{\sigma} - (\Gamma_w^{\sigma} - \Gamma_{KOH}^{\sigma})\, S^{w} - \Gamma_{ox}^{\sigma} S^{ox} \qquad [A]$$

and

$$\Gamma_i^{(s)} \equiv \Gamma_i^{\sigma} - \frac{x_i}{x_w + x_{KOH}} (\Gamma_w^{\sigma} + \Gamma_{KOH}^{\sigma}) \qquad [B]$$

It can be proven that $S^{(s)}$ and $\Gamma_i^{(s)}$ are independent of the choice of the Gibbs dividing plane. To that end we introduce two Gibbs surfaces x and y located a distance λ apart. The surface excess entropies at x and y are called S^x and S^y, and for the surface excess concentrations the symbols Γ_i^x and Γ_i^y are used. The relation between the corresponding excess quantities at x and y follows directly

$$S^y = S^x - [S^{ox} c_{ox}^{ox} - S^w (c_{H_2O}^w + c_{KOH}^w)]\lambda \qquad [C]$$

and

$$\Gamma_i^y = \Gamma_i^x - (c_i^{ox} - c_i^w)\lambda \qquad [D]$$

where c_i^{α} is the concentration of component i in phase α

The identity of $S^{(s)}$ at x and y follows from [A] and [C]

$$S^{(y)} = S^{y} - S^{w}(\Gamma^{y}_{w} + \Gamma^{y}_{KOH}) - \Gamma^{y}_{ox} S^{ox}$$

$$= S^{x} - S^{ox} c^{ox}_{ox} \lambda - S^{w}(c^{w}_{H_2O} + c^{w}_{KOH})\lambda$$

$$- S^{w}[\ \Gamma^{x}_{w} - (c^{ox}_{w} - c^{w}_{w})\lambda + \Gamma^{x}_{KOH} - (c^{ox}_{KOH} - c^{w}_{KOH})\lambda]$$

$$-\Gamma^{x}_{ox} S^{ox} - (c^{ox}_{ox} - c^{w}_{ox})\lambda$$

$$= S^{x} - (\Gamma^{x}_{w} + \Gamma^{x}_{KOH})\ S^{w} - \Gamma^{x}_{ox}\ S^{ox} = S^{(x)}$$

The identity of $\Gamma_i^{(s)}$ at x and y follows analogously from [B] and [D]

$$\Gamma_i^{(y)} = \Gamma_i^{y} - \frac{x_i}{x_w + x_{KOH}} (\ \Gamma^{y}_{w} + \Gamma^{y}_{KOH})$$

$$= \Gamma_i^{x} - (c_i^{ox} - c_i^{w})\lambda - \frac{x_i}{x_w + x_{KOH}} [\Gamma^{x}_{w} - (c^{ox}_{w} - c^{w}_{w})\lambda + \Gamma^{x}_{KOH} - (c^{ox}_{KOH} - c^{w}_{KOH})]$$

$$= \Gamma_i^{x} - \frac{x_i}{x_w + x_{KOH}} (\Gamma^{x}_{w} + \Gamma^{x}_{KOH}) = \Gamma_i^{(x)}$$

It can thus be concluded that $S^{(s)}$ and $\Gamma_i^{(s)}$ are invariant with the choice of the Gibbs dividing plane as is required for a consistent thermodynamic treatment.

4. THERMODYNAMICS OF CHARGE FORMATION ON OXIDES. MICROCALORIMETRY

4.1 Introduction

The fact that insoluble oxides acquire surface charges in electrolyte solutions containing protons or hydroxyl ions is a well-known phenomenon in colloid science. Generally, this surface charge formation is depicted by the following reactions

$$\equiv S\text{-}OH + H^+ \rightleftharpoons \equiv S\text{-}OH_2^+$$

and

$$\equiv S\text{-}OH + OH^- \rightleftharpoons \equiv S\text{-}O^- + H_2O$$

In these equations the symbol ≡S-OH stands for a surface hydroxyl group in the oxide-solution interface.

Taking these reactions as representative for the formation of charged sites in the interfacial region, it follows that from a mechanistic point of view, it suffices to consider only protons as the charge determining species, because a (net) negative interface is formed by dissociation of H^+ from surface groups, forming water in the bulk solution, whereas positive surface charges result from association of neutral surface sites with protons. From a phenomenological viewpoint, however, it cannot be distinguished whether the disappearance of hydroxyl ions from the solution is due to adsorption of these species, or to desorption of protons followed by water formation.

For two insoluble oxides: rutile (TiO_2) and hematite (α-Fe_2O_3), the surface charge (σ_o) - pH behavior has been studied extensively as a function of temperature (1). In this study it was amongst others observed that the point of zero charge (p.z.c., pH^o) of the oxides shifts towards lower pH with increasing temperature. We related the pH^o shifts with temperature to the enthalpy of adsorption of protons at this point. Microcalorimetry of acid/base titrations of oxide suspensions is a direct means to study the thermodynamics of the process of surface charge formation. Direct microcalorimetry of charge formation provides insight into the thermodynamics of

double layer systems. Initiated by Verwey and Overbeek (2) and Overbeek (3), the thermodynamics of double layers still is of great interest (4,5). Since total enthalpies of double layer formation are accessible by means of microcalorimetric methods, it can be verified whether experimental results can be described with the current double layer theories, using the typical characteristics of oxide-solution interfaces. Furthermore, directly measured adsorption enthalpies can then be compared to those inferred from the temperature dependence of the p.z.c.

Independently of our research on the direct microcalorimetry of oxides, Machesky and Anderson (6) recently studied the charge formation processes on rutile and goethite, using an essentially identical calorimetric procedure.

In the present study the enthalpy of surface charge formation on rutile and hematite is determined as a function of surface charge density and discussed in the light of earlier results.

4.2 Experimental

Hematite and rutile were taken from the same batches as used in chapter 3. HNO_3 and KOH titrants used were 0.2 M, diluted from standard solutions (Merck Titrisol). All other chemicals were analytical grade. Water was pretreated as described in chapter 2.

Enthalpy measurements were performed in a Tronac titration microcalorimeter (Model 450). A sketch of the microcalorimetric set-up is given in Fig.4.1. The principle is quite simple. The heat involved in a reaction is measured as the adiabatic temperature change, recorded with a thermistor (a). After equilibration of the measuring device by passing a known current through a heating resistor (b) during a given period of time, the temperature change is converted into a total reaction enthalpy.

For measurements on oxide suspensions some experimental problems did arise. First, attempts were made to directly measure pH in the titration vessel, using a combined micro electrode (Schott N59 A). However, after some preliminary experiments it became clear that this method failed:

i) an extremely unstable and noisy signal was obtained from the electrode, most likely due to electrical problems caused by the fact that the whole titration cell is immersed in a water bath.

ii) thermal equilibration of the calorimeter became slower, possibly caused by the relatively high heat capacity of the electrode.

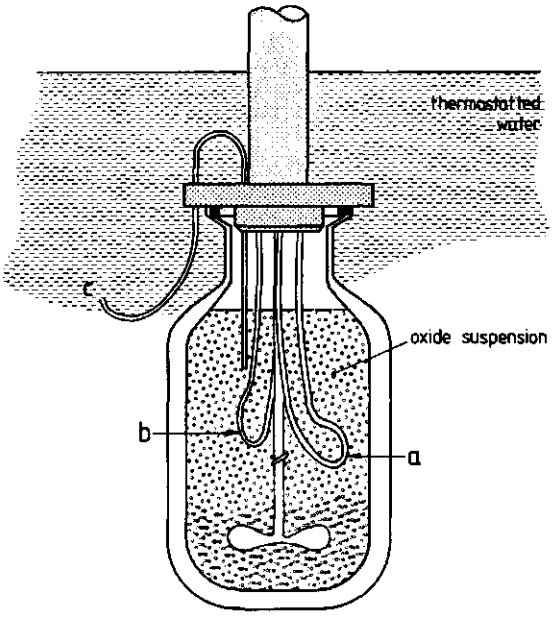

Fig.4.1 Scheme of the titration microcalorimeter.
a. Thermistor
b. Heating resistor
c. Titrant delivery tube.

Finally, the following experimental procedure was adopted and used in all further experiments. In a microcalorimetric measurement, after each addition of titrant and thermal equilibration, the titration vessel was carefully removed from the water bath and the pH measured using a pH meter (Ankersmit) with combined pH electrode (Schott N50 A). Directly thereafter the titration cell was reinstalled in the calorimetric set-up and, after reestablishment of thermal equilibrium, the next addition of titrant was made. Titrants were added from an automatic buret (Metrohm 655 Dosimat), equiped with long delivery tubing immersed in the water bath to ascertain thermal equilibrium between the titrant and the oxide suspension. During an experiment, several calibrations of the calorimeter were performed, enabling proper corrections for the steady increase in total volume during a titration run.

All calorimetric measurements presented in this study were obtained without maintaining an inert atmosphere in the titration vessel, e.g. by flushing with nitrogen. To be able to do so an extremely accurate thermal

equilibrium between gas and sol would have been required, which was a very difficult prerequisite. By not rigorously preventing CO_2 influences in our experiments, data obtained for the basic pH range (pH $\gtrsim$ 9) may possibly suffer from small errors caused by 'CO_2 effects', albeit that during the main part of experimentation the vessel was hermetically closed and immersed in a water bath. However, the main body of our work relates to lower pH values where this problem is absent.

4.3 Experimental results

In order to check the accuracy of the titration procedure in the calorimetric experiments, surface charge - pH relations were also measured directly in the calorimeter. This was accomplished by calculating $\Delta\sigma_0$ from the volume of titrant added and the measured shift in pH, using theoretical blank corrections and scaling of the curves with respect to the known p.z.c.

For four independent base titrations, performed on suspensions containing different amounts of rutile in 0.2 M KNO_3, results are plotted in Fig.4.2 and compared to the corresponding 'standard curve', obtained in an especially designed titration set-up and reported in chapter 3. Even though titration in the micro calorimeter is by no means optimal for the measurement of accurate (σ_0,pH) relations, the agreement between the two methods is satisfactory. A second conclusion that follows from this figure is that there is no significant influence of the solid - solution ratio on the titration behavior of the suspensions. The fact that the surface charge density in the calorimetric measurements is somewhat higher than the corresponding curve from chapter 3, might be due to the use of theoretical blanks and/or activity coefficients in the calculations. This slight deviation could also have an analytical origin (titrant concentration, buret inaccuracy).

The satisfactory agreement between the two sets of data, indicates that this 'standard' curve can be used to convert measured heat effects into molar adsorption enthalpies. By relating experimentally observed pH shifts to changes in surface charge density using the standard curves, adsorption enthalpies can be expressed in terms of kJ/mol H^+/OH^- adsorbed or desorbed.

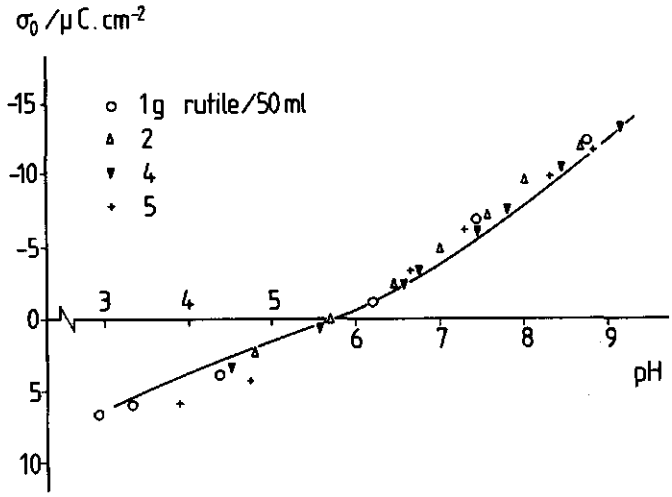

Fig.4.2 Surface charge - pH relation for rutile, determined in the calorimeter. Electrolyte: 0.2 M KNO_3. Temperature: 20 ^oC. Rutile concentration indicated. Solid curve: (σ_o,pH) for rutile in 0.2 M KNO_3 at 20 ^oC in specially designed cell, taken from chapter 3.

Total enthalpies of charge formation were obtained from the measured values by correcting them for the bulk neutralization reaction and heats of dilution. The heat of neutralization has been experimentally determined by means of calorimetric acid - base titration of blank solutions containing the same concentration of electrolyte as the oxide suspensions. No significant influence of salt concentration (corrected for dilution effects) could be observed. For a number of acid and base titrations of electrolyte solutions containing KNO_3 in the concentration range 0.002 - 1 M, the heat of neutralization was found to be -57.5 ± 1.5 kJ/mol. This value agrees well with literature (-56 kJ/mol: (7)).

Typical results of a calorimetric titration experiment are shown in Fig.4.3 for rutile and hematite in KNO_3. In this figure the cumulative enthalpy change (ΔH_{cum}, kJ/mol adsorbed) is plotted against the net surface charge density. As is clear from Fig.4.3, the slope of the lines depends on the direction of the titration. From a phenomenological viewpoint these slopes provide a check on the experimental accuracy attained. In the following titration cycle: acid titration from pH_1 to pH_2 or, for that matter from $\sigma_{o,1}$ to $\sigma_{o,2}$, followed by base titration back to pH_1 ($\sigma_{o,1}$), the net effect is the formation of x moles of water. Therefore the following relation must be always obeyed

$$\Delta_{ads}H_{H^+} + \Delta_{ads}H_{OH^-} = \Delta_{neutr}H_{H_2O} \qquad [4.1]$$

at any value of pH

In Table 4.1, experimentally determined heats of surface charge formation, obtained from both acid and base titration, are given for rutile and hematite as a function of c_{KNO_3}. As it is impossible to distinguish between positive adsorption of protons and desorption of hydroxyl ions and vice versa, all enthalpy values in Table 4.1 are expressed on the basis of the depletion of H^+ or OH^- from solution, respectively.

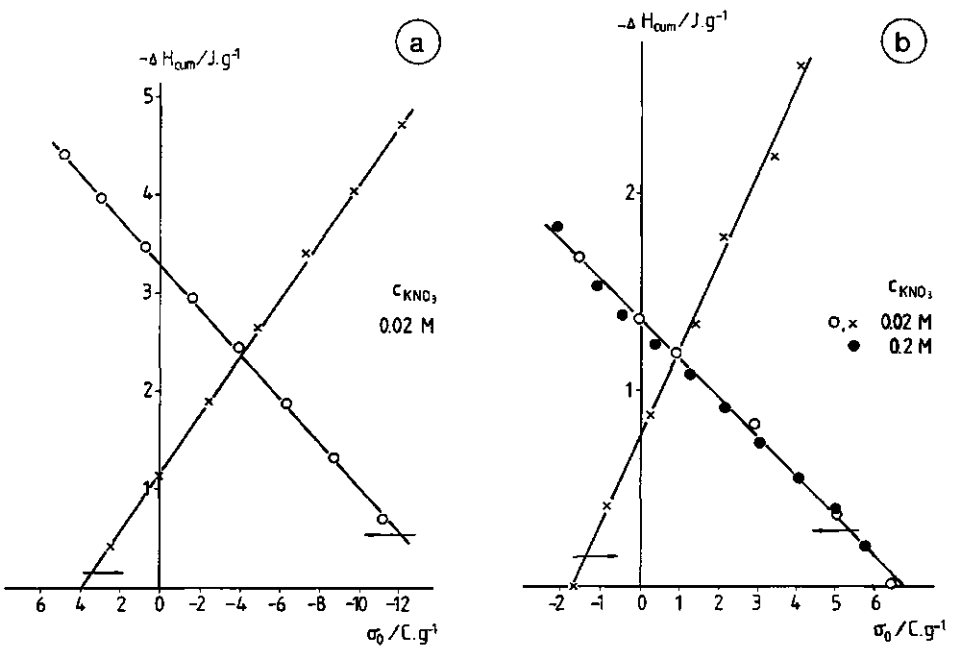

Fig.4.3 Cumulative heat of adsorption as a function of surface charge density for rutile and hematite. Temperature: 20 °C. Electrolyte: KNO_3, concentration indicated. o: acid titration, x: base titration.
4a. rutile. 4b. hematite.

The sum of the adsorption enthalpies in corresponding acid and base titrations in Table 4.1, equals within a few kJ/mol the heat of neutralization (-56 kJ/mol). The actual disagreement reflects the inaccuracy of the calorimetric procedure, most likely caused by a slight acid-base hysteresis, frequently observed in so-called fast potentiometric titrations of oxides (1). The data given by Machesky and Anderson (6) do not allow such a reversibility check, because all their data are presented as proton adsorp-

tion enthalpies. In all cases, within a few kJ/mol, $\Delta_{ads}H$ values were obtained that are independent on the surface charge density, i.e. always linear ($\Delta H_{cum}, \sigma_o$) relations were found. We could not observe a significant effect on the adsorption enthalpy by changing the electrolyte concentration from 0.02 to 0.2 M. For sake of comparison in the table values for the enthalpy of charge formation, derived from our thermodynamic analysis of the shift in pH^o with temperature (chapter 3) are included in the table.

Table 4.1 Enthalpies of adsorption for protons and hydroxyl ions onto rutile and hematite in 0.02 and 0.2 M KNO_3 at 20 °C.

OXIDE	c_{KNO_3} M	$\Delta_{ads}H_{H+}$ kJ/mol H^+	$\Delta_{ads}H_{OH-}$ kJ/mol OH^-	$\Delta_{ads}H_{H+}(pH^o)$ kJ/mol H^+
RUTILE	0.02	-22	-32	-18
	0.2	-21	-29	-18
HEMATITE	0.02	-36	-19	-36
	0.2	-40	-19	-36

4.4 Discussion

Adsorption of charge determining ions in the point of zero charge

In the point of zero charge (pH^o), enthalpy changes reflect the purely chemical interaction between surface ions and the oxide, as at this point electrical contributions are absent. The agreement between $\Delta_{ads}H$ values (in the point of zero charge) obtained from the different methods for rutile and hematite is satisfactory. Therefore our conclusions regarding the differences in $\Delta_{ads}H$ between the two oxides given in chapter 3 are confirmed by the present direct measurements. These differences can be understood in terms of differences in chemical affinity of surface ions for the surface, which may be due to different inductive effects of lattice ions.

Due to the presence of electrical contributions, outside the point of zero charge the situation is much more complicated, as will be discussed in a following section.

Our conclusion that no significant influence of the salt concentration could be observed if $\Delta_{ads}H$ values are expressed per mol H^+ adsorbed, is in agreement with the conclusions of Machesky and Anderson (6), who found the same to apply for the charge formation on goethite and rutile at variable concentrations of $NaNO_3$. Also the magnitudes of the $\Delta_{ads}H$'s at the p.z.c. for rutile (-22 kJ/mol) and goethite (-36 kJ/mol) agree with ours.

A point of interest is that for the two iron oxides, both the total Gibbs energy of adsorption, $\Delta_{ads}G$(p.z.c.) (~pH^o), and $\Delta_{ads}H$(p.z.c.) are similar, and therefore the entropic contributions to the proton/hydroxyl ion adsorption must also be similar. This indicates that the actual morphology of the oxide lattice is not of major importance in the thermodynamics of charge formation. The inductive effects of the lattice (cat)ions on the surface groups, however, in our opinion are a central factor in determining the position of pH^o of inorganic oxides.

Enthalpy of double layer formation

In our study of the temperature dependence of the (σ_o,pH) relation of rutile and hematite (1) we noticed an almost perfect temperature congruence of these curves in the range 5<T<70 °C, meaning that (σ_o,pH-pH^o) curves at different temperatures coincide within experimental error. From the temperature congruence of (σ_o,ΔpH) curves important conclusions can be drawn regarding the several enthalpic contributions involved in the process of charge formation on these materials. In ref.1 it was argued that the shift in pH^o with temperature is related to the enthalpy of proton adsorption at this point according to the following relation

$$\left(\frac{\partial pH^o}{\partial T}\right)_{c_s} = \frac{\Delta_{ads}H_{H^+}}{2.303RT^2} \qquad [4.2]$$

The observed temperature congruence implies that

$$\left(\frac{\partial pH}{\partial T}\right)_{c_s,\sigma_o \neq 0} = \left(\frac{\partial pH^o}{\partial T}\right)_{c_s,\sigma_o=0} \qquad [4.3]$$

and, therefore, $\Delta_{ads}H$ must be independent of σ_o. Within experimental error this is now indeed confirmed by our calorimetric measurements. Outside the point of zero charge, electrical interactions become important. Here, $\Delta_{ads}H$ is of a composite nature and from the observed independence of the molar adsorption enthalpy on σ_o important conclusions can be drawn concerning the process of double layer formation on these materials.

In the following it will be shown how the several enthalpic contributions to the adsorption of charge determining ions onto charged interfaces can be calculated. First the thermodynamics of double layer formation will be discussed in general. Later, we will focus our attention on the specific case of oxide - solution interfaces.

The excess Gibbs energy of a charged interface, ΔG^s, can be derived from the following hypothetical charging process (2). We consider the particles in contact with a solution containing charge determining ions, equilibrium at the interface not yet established. The double layer is formed isothermally and in a reversible way, by bringing charge determining ions by infinitesimally small amounts from the bulk solution to the interface. After each step the formation of countercharge at the solution side of the interface is allowed to occur. Three sub-processes can thus be distinguished.

i) The chemical contribution of the charge determining ions, which obviously have a chemical preference for the surface above the bulk solution.

ii) The transport of charge determining ions against the increasing potential around the particle.

iii) The formation of the countercharge distribution at the solution side of the interface.

Thus, ΔG^s consists of electrical and chemical contributions

$$\Delta G^s = \Delta G^s_{el}(pX) + \Delta G^s_{chem}(pX) \qquad [4.4]$$

In Eq.[4.4], ΔG^s_{el} and ΔG^s_{chem} are the electrical and chemical parts of the Gibbs energy of the interface, respectively. The Gibbs energy contributions are a function of the activity of charge determining ions in solution,

indicated as pX (where pX denotes pAg for silver halides and pH for oxides, respectively). The reversible isothermal electrical work needed to build up the charged layer at the solid phase boundary is given by

$$\Delta G^{s}_{el} = \int_{o}^{\sigma_o} \psi_o d\sigma_o \qquad [4.5]$$

The chemical contribution consists of two parts: a reference contribution at the p.z.c. and an additional term due to charge determining ions.

$$\Delta G^{s}_{chem}(pX) = \Delta G^{s}_{chem}(pX^{o}) - \sum_{i} \Gamma_i \Delta\mu_i \qquad [4.6]$$

In this equation, $\Delta G^{s}_{chem}(pX^{o})$ is the Gibbs energy of the uncharged interface, i.e. that part of the total Gibbs energy that is determined by the chemical (non-electrostatic) contributions which, in turn are related to the position of the point of zero charge (pH^{o} for oxides, pAg^{o} for silver halides).

The last term in Eq.[4.6] opposes the sum of the differences in chemical potential of the charge determining species at pX and pX^{o}. The sum extends over all charge determining ionic species.

For a Nernstian charge - potential relation, at equilibrium it follows that

$$\tilde{\mu}_{X^+} = \mu^{o,s}_{X^+} + F\psi_o$$

$$\tilde{\mu}_{Y^-} = \mu^{o,s}_{Y^-} - F\psi_o$$

where X^+ and Y^- are the charge determining ions. The symbol $\mu^{o,s}$ denotes the standard chemical potential of the ions in the solid phase.

If for species i, $\Delta\mu_i$ is defined as

$$\Delta\mu_i = \tilde{\mu}_{i,pX} - \tilde{\mu}_{i,pX^{o}}$$

for the sum in Eq.[4.6] we can write

$$\sum_{i} \Gamma_i \Delta\mu_i = (\Gamma_{X^+} - \Gamma_{Y^-})F\psi_o \equiv \sigma_o\psi_o$$

Carrying out this substitution, combination of Eqs [4.4] - [4.6] gives

$$\Delta G^{s}_{chem}(pX) = \Delta G^{s}_{chem}(pX^{o}) - \sigma_o\psi_o + \int_{o}^{\sigma_o} \psi_o d\sigma_o \qquad [4.7]$$

or by partial integration

$$\Delta G^{s}_{chem}(pX) = \Delta G^{s}_{chem}(pX^{o}) - \int_{o}^{\psi_o} \sigma_o d\psi_o \qquad [4.8]$$

Often the integral in Eq.[4.8] is called the Gibbs energy of a double layer, but it should be clear, however, that also the constant term, $\Delta G^{s}_{chem}(pX^{o})$ contributes to ΔG^{s}.

It should be realized that in terms of enthalpies a closer inspection of the various contributions to $\Delta G^{s}_{chem}(pX)$ is needed. On adsorption of surface ions, forming a net charged interface, a rearrangement of countercharges occurs at the solution side of the interface. The Gibbs energy of this (diffuse) countercharge formation, ΔG^{s}_{cc}, equals zero because the entropical and enthalpic contributions exactly compensate each other (2). Hence, the corresponding enthalpy change involved is definitely not zero.

In order to find the enthalpy of double layer formation, we reasoned as follows. The chemical affinity part of ΔH^{s} follows directly from the measured heat of adsorption in the p.z.c., or can be assessed from the shift in pH^{o} with temperature (1). As stated before, the chemical term equals $-\sigma_o\psi_o$ and exactly outweighs the configurational entropy change of the charge determining ions in the bulk solution. The electrical part of the Gibbs energy of a double layer is mainly enthalpic. Therefore ΔH^{s}_{el} approximately equals $\int \psi_o d\sigma_o$. As a result, the enthalpy of a double layer is given by the following relation.

$$\Delta H^{s}(pX) = \Delta H^{s}(pX^{o}) + \Delta H^{s}_{el}(pX) + \Delta H^{s}_{cc}(pX) \qquad [4.9]$$

The enthalpy of countercharge rearrangement, ΔH^{s}_{cc} follows from the average positions of the various ions in the double layer and can be computed on the basis of some double layer model. For an ion positioned at a mean

distance x from the surface, the gain in molar enthalpy, Δh_{ion}, is given by the following equation.

$$\Delta h_{ion} = zF\psi(x) \qquad [4.10]$$

where z is the valency of the ion, sign included and $\psi(x)$ is the electrical potential at the position of the ion. For the total countercharge, the enthalpy of formation, ΔH^s_{cc}, follows from the integral from x =0→∞, summed over all ionic species present.

$$\Delta H^s_{cc} = \sum_i \left(\int_o^\infty c_i(x) z_i F\psi(x) dx \right) \qquad [4.11]$$

where $c_i(x)$ is the concentration of ions i and $\psi(x)$ is the electrical potential at a distance x from the surface.

For the computation of ΔH^s_{cc} let us take oxides as the model colloids. For these systems it has been established that (1,8)

1) Inner layer capacitances are in the order of 300 - 500 $\mu F/cm^2$, where exact values are no longer critical.

2) Gouy - Stern theory provides a satisfactory means to describe surface charge - pH relations

3) The surface potential, ψ_o, of oxides seems to obey Nernst's law over a wide range of experimental situations.

The diffuse part of the double layer enthalpy follows from the Gouy model. Using Poisson-Boltzmann statistics for the countercharge, Eq [4.11] can be rewritten as follows.

$$\Delta H^s_{cc} = \sum_i \left[\int_o^\infty c_{i,o} \exp(-z_i F\psi(x)/RT) z_i F\psi(x) dx \right] \qquad [4.12]$$

where $c_{i,o}$ is the bulk concentration of ion i.

Eq.[4.12] was solved numerically using a Fortran '77 computer program based on the non-linear Poisson-Boltzmann equation for a flat surface. Integrations were performed according to the Runge-Kutta method, using IMSL routines. From earlier work (8) we already concluded that any influence of the particle geometry, in the surface area range of interest for our oxides, is practically absent.

The electrical part of the double layer enthalpy, ΔH^s_{el} could be readily obtained by calculating $\int \psi_o d\sigma_o$ from theoretical (σ_o, ψ_o) relations, using essentially the same numerical procedures.

As stated before, in the microcalorimetric determination of adsorption enthalpies on oxides no significant dependence on σ_o could be observed. This leads us to the conclusion that ΔH^s_{cc} and ΔH^s_{el} (Eq.[4.9]) should largely compensate each other.

In Fig.4.4 the enthalpy contributions ΔH^s_{el} and ΔH^s_{cc} are plotted as a function of the inner layer capacitance, C_s, in 0.01 M KNO_3 at room temperature for a (Nernst) surface potential of -200 mV (corresponding to $pH-pH^o = 3.44$), of the same order of magnitude as the highest values for ΔpH reached in our experiments.

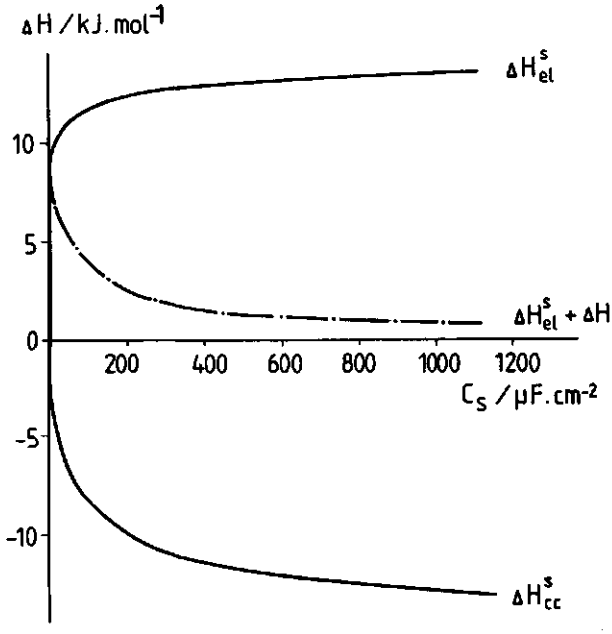

Fig.4.4 Electrical (ΔH^s_{el}) and countercharge part (ΔH^s_{cc}) of the enthalpy of double layer formation as a function of the innerlayer capacitance (C_s). The sum of both contributions (——·——·——) is also indicated. Surface potential: -200 mV. Electrolyte: 0.01 M (1-1). Temperature: 20 °C.

Fig.4.5 illustrates the differences between ΔH^s_{cc} and ΔH^s_{el} as a function of C_s for different concentrations of supporting (1-1) electrolyte. Results are given for a (Nernstian) surface potential of -200 mV. It is clear that at higher values of C_s the terms ΔH^s_{el} and ΔH^s_{cc} almost compensate and the sum is only a few kJ/mol. With decreasing inner layer capacitances (C_s<100 $\mu F/cm^2$), however, this sum increases rapidly. Furthermore it follows that, also in this respect, the exact value for C_s is not very critical, provided

it is high enough ($\gtrsim$ 300 $\mu F/cm^2$). For the most-likely range of inner layer capacitances on our oxides, 300 - 500 $\mu F/cm^2$ (chapter 3), it is clear that the difference of ΔH^s_{cc} and ΔH^s_{el} is only of the order of 1-3 kJ/mol, somewhat dependent on the electrolyte level. Even at these high ΔpH values, the differences are almost within the experimental error of an enthalpy measurement. For 'low capacitance' interfaces like the AgI - solution system (9), much bigger differences (ΔH^s_{el} + ΔH^s_{cc}) are to be expected according to Fig.4.5, and therefore a relatively strong dependence of $\Delta_{ads}H$ on the surface charge density.

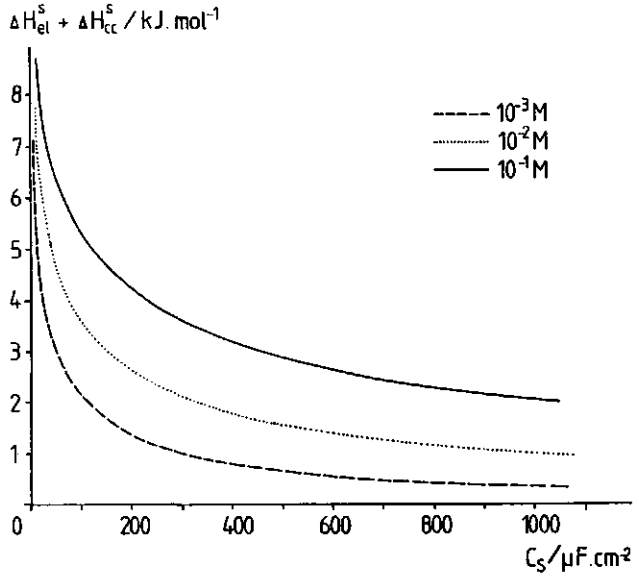

Fig.4.5 Sum of electrical and counter charge contributions to the enthalpy of the double layer as a function of the inner layer capacitance. (1-1) Electrolyte, concentration indicated. Surface potential: -200 mV. Temperature: 20 °C.

The physical explanation of the fact that in those cases where high inner layer capacitances apply, an almost exact compensation of ΔH^s_{el} and ΔH^s_{cc} is observed is as follows. In changing the surface charge by adsorption of charge determining ions from zero to the final value, σ_o, the amount of electrical work to be performed in bringing an ion to the interface steadily increases. In the limiting case of low potentials, where the linear Poisson-Boltzmann equation applies, it can be easily shown that the electrical work amounts to $-1/2\sigma_o\psi_o$. If the inner layer capacitance is very high and therefore, counterions can closely approach the surface, the mean potential in the diffuse layer will approach $\psi_o/2$. In this situation it is to be expected that ΔH^s_{cc} and ΔH^s_{el} almost exactly oppose each other. For lower values of C_s, the effective distance of closest approach of the coun-

ter ions increases, thus lowering the mean potential in the diffuse layer. In those cases, therefore, ΔH^s_{el} in an absolute sense overrules ΔH^s_{cc}.

Notwithstanding the numerical agreement in the point of zero charge between our calorimetric data and those of Machesky and Anderson (6), some important deviations between both studies exist. The fact that Machesky and Anderson report a change of slope of ($\Delta_{ads}H_{H+}$, pH) curves in the p.z.c., has been interpreted in terms of dipolar contributions in the overall process. Spectroscopic evidence, however, indicates that strong oxide-water interactions are extremely short range in character: only the first (dissociatively) adsorbed water layer shows strong interactions with the surface (10), in full agreement with frequently observed high inner layer capacitances on oxides. Apart from the fact that, given the indicated experimental uncertainties, the data of the former authors hardly discriminate between constant $\Delta_{ads}H_{H+}$ and pH- (or σ_o-) dependent adsorption enthalpies, our earlier results on the temperature congruent (σ_o,pH) curves for rutile and hematite confirm that $\Delta_{ads}H_{H+}$ is independent of the surface charge density under the experimental conditions. It follows that dipolar interactions of an enthalpic nature hardly play a role in the process of charge formation on inorganic oxides.

4.5 Conclusions

Directly measured heats of surface charge formation on rutile and hematite agree well with values derived from the shift of pH^o with temperature. Experimentally determined values of $\Delta_{ads}H_{H+}$ are within experimental error independent of the surface charge density on the oxides. This result is consistent with our earlier observation that (σ_o,pH) curves of these oxides are congruent in temperature.

In systems with high inner layer capacitances, an almost constant adsorption enthalpy with σ_o is to be expected, because in this case the electrical contributions practically compensate each other. Therefore, in fact the only contributions to be measured are the chemical interactions between protons (and hydroxyl ions) and surface groups. Thus, a change in $\Delta_{ads}H_{H+}(\sigma_o)$ at the p.z.c. is not very likely. If the charge formation is thought to be due to dissociation of protons from, or association of protons with surface groups, as is a current vision, from a chemical point of view both for $pH<pH^o$ and $pH>pH^o$ making (or breaking) of O-H bonds is con-

cerned, for which chemical bond enthalpies will not differ too much. Enthalpic contributions due to adsorbed water dipole reorientation are of minor importance in the process of double layer formation on rutile and hematite.

4.6 Acknowledgements

The valuable contributions, both in technical as in interpretational matters, of Mr. B.J. Groenenberg, Mrs. A.G. Rhebergen and Mr. A.J. Korteweg are greatfully acknowledged.

4.7 References

1. Fokkink, L.G.J, de Keizer, A., and Lyklema, J., in preparation/ this thesis, chapter 3.
2. Verwey, E.J.W., and Overbeek, J.Th.G., "Theory of the Stability of Lyophobic Colloids", Elsevier, Amsterdam, 1948.
3. Overbeek, J.Th.G., in "Colloid Science I" (H.R. Kruyt, Ed.), Elsevier Publishing Company, Amsterdam-Houston-New York-London, 1952.
4. Chan, D.Y.C., and Mitchell, D.J., J. Colloid Interface Sci. 95, 193, 1983.
5. Hall, D.G., J. Colloid Interface Sci. 108, 411, 1985.
6. Machesky, L.M., and Anderson, M.A., Langmuir 2, 582, 1986.
7. Tyrell, H.J.V., and Beezer, A.E., "Thermometric Titrimetry", Chapman and Hall Ltd, London, 1986.
8. Fokkink, L.G.J., de Keizer, A., and Lyklema, J., submitted to J. Colloid Interface Sci./this thesis, chapter 7.
9. Bijsterbosch, B.H., and Lyklema, J., Adv. Colloid Interface Sci. 9, 147, 1978.
10. Hendewerk, M., Salmeron, M., and Somorjai, G.A., Surface Sci. 172, 544, 1986.

5. SOLUTION CHEMISTRY OF CADMIUM

5.1 Introduction

In line with our attempts to unravel the mechanism of binding of cadmium ions onto insoluble oxides, a study of the behavior of the adsorptive in aqueous solutions may eventually lead to insight into the role of hydroxo complexes in the process. Two main reasons to take a closer look at the Cd-OH chemistry as part of our study are:

(i) The obvious chemical affinity of Cd^{2+} for hydroxyl ions. Cd ions are known to be hydrolyzable in aqueous solutions, where $Cd(OH)^{+}$ and, to a much lesser extent, $Cd(OH)_2$ complexes are formed (cf. (1)).

(ii) The important role of OH^{-} in the adsorption of heavy metal ions onto inorganic oxides. From experiments in literature it appears that in the case of insoluble oxides OH^{-} ions (or experimentally indistinguishable: protons) play a major role (2). Observed changes in pH upon adsorption of Cd ions onto substances like rutile may originate from a change in the cadmium complexation equilibria combined with preferential adsorption of one of the Cd species, co-adsorption of hydroxyl ions or both. From a mechanistic viewpoint, co-adsorption of OH^{-} could be ascribed both to the adsorption of real $Cd(OH)_x$ entities, or to an adjustment of the oxide's surface charge on adsorption.

Study of the speciation of Cd (i.e. its distribution over the several chemical forms) as a function of the parameters in the adsorption experiments, will provide information on the chemical interactions between Cd^{2+} and OH^{-} ions in solution.

As far as we are aware, not much is known about the influence of temperature on the solution chemistry of Cd ions, especially in solutions of compositions like the ones used used in our adsorption experiments.

5.2 Experimental

Speciation of cadmium as a function of pH in KNO_3 solutions was determined experimentally from potentiometric (acid/)base titrations at 20 and 60 °C. The experimental set-up used was essentially the same as described in chapter 2. Under variable solution conditions, amounts of complex-bound OH^{-} were determined by comparing titration curves of $Cd(NO_3)_2$ solutions with a

corresponding blank titration curve (same solution but without the Cd compound) in the pH range 4 - 8. To the initial solution (500 ml), equilibrated at low pH, small aliquots of 0.1 M KOH were added and the equilibrium electromotive force, E, was registered ($\Delta E<0.02$ mV/min). Then the solution was titrated with 0.1 M HNO_3 back to its initial pH, solid $Cd(NO_3)_2$ was added and the procedure was repeated. Measurements were performed at variable concentration of indifferent electrolyte (KNO_3), total Cd concentration, Cd_{tot}, and temperature. Amounts of complex-bound OH^-, OH_{compl}, at any pH (E) were calculated from the differences in volumes of titrant needed to establish this pH in the test solution and the blank.

$$OH_{compl} = [(vt)_{Cd}-(vt)_{bl}]/V \qquad [5.1]$$

where v is the volume of titrant added, t is the concentration of the titrant and V is the total volume of the test solution. The subscripts Cd and bl refer to test solution and blank, respectively.

5.3 Results

By way of example, titration curves of $Cd(NO_3)_2$ in 0.2 M KNO_3 at 20 °C are given in Fig.5.1. In the acid pH region no significant difference can be observed between the blank and the two cadmium levels, indicating that activity effects are within the detection limit of the measurement. The analogous experiment at 60 °C showed a similar result. At a supporting electrolyte concentration of 0.02 M KNO_3, addition of $Cd(NO_3)_2$ usually showed a shift in E, though normally only a few mV. This slight activity change is found in the electromotive force - pH conversion. Given the limited purpose of this part of our research, we reasoned that a few millivolts uncertainty in E (< 0.05 pH) is acceptable, and therefore we henceforth neglected such activity changes in our calculations of OH_{compl}. In all experiments we assumed that at pH=4 still no Cd-OH complex is formed.

One may wonder why addition of salt does not remarkably change the electromotive force of the experimental cell. The activity of protons obviously is unchanged, though their activity coefficient certainly will have decreased. Although the activity of H^+ will be substantially changed upon addition of $Cd(NO_3)_2$, a shift in E is not to be expected however, as long as the activity coefficients of OH^- and H^+ are influenced in the same way: the disso

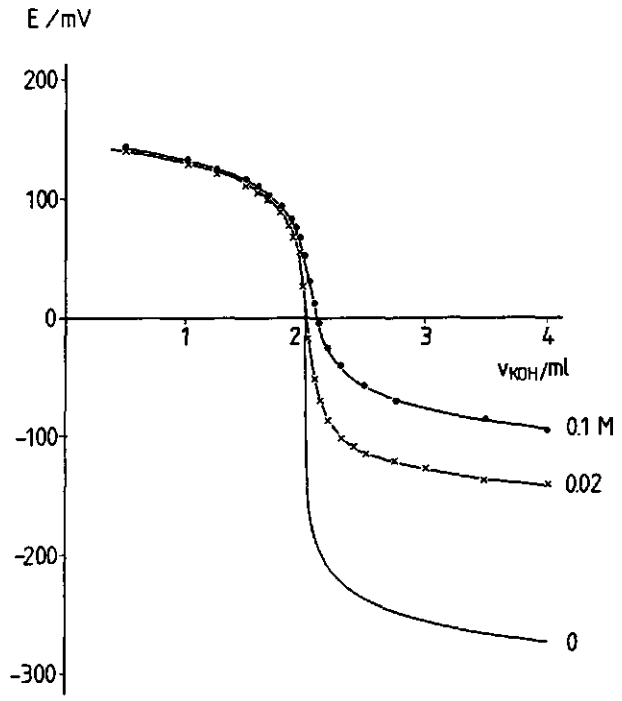

Fig.5.1 Potentiometric titration curves of $Cd(NO_3)_2$ solutions in 0.02 M KNO_3 with 0.1 M KOH. T = 20 °C. Concentration of $Cd(NO_3)_2$ is indicated.

ciation of water is governed by the (activity) dissociation constant, which is independent of the electrolyte level. Therefore addition of salt will change the concentrations of hydroxyl ions and protons, but does not change their activity.

From titration data as given in Fig.5.1 amounts of bound hydroxyl ions as a function of pH could be calculated. Results in 0.02 and 0.2 M KNO_3 at 20 and 60 °C, for a total cadmium level of 0.02 and 0.1 M are given in Fig.5.2. On first inspection of this figure, an interesting temperature effect is observed: curves obtained at identical composition shift towards lower pH when the temperature is raised, but their shapes remain virtually unchanged.

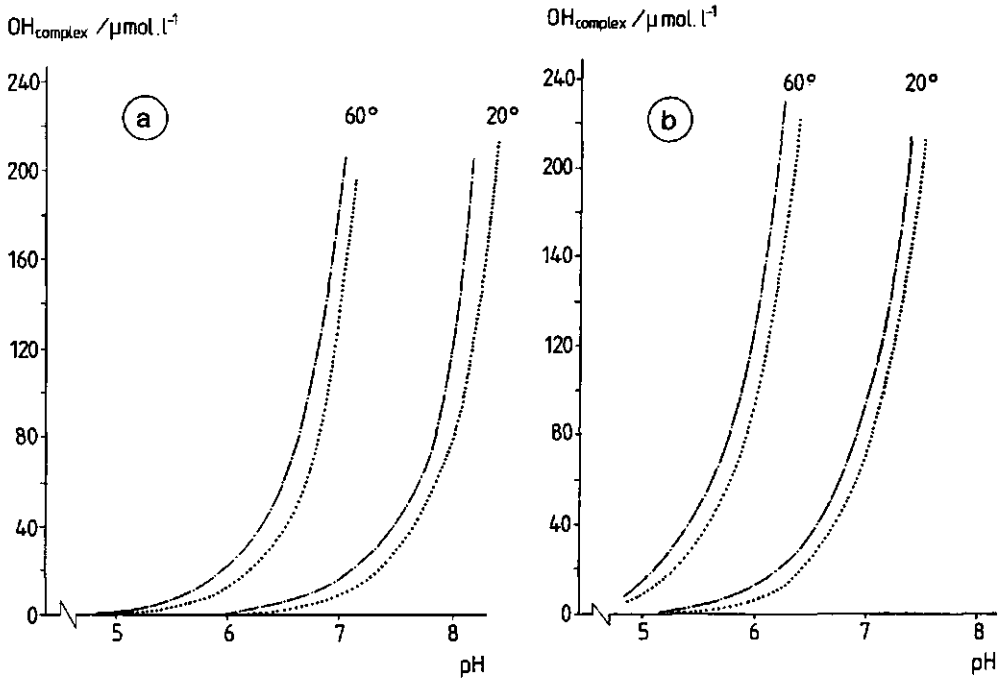

Fig.5.2 Concentration of complex - bound OH^- as a function of pH in solutions of $Cd(NO_3)_2$ in 0.02 and 0.2 M KNO_3 at 20 and 60 °C.
KNO_3 concentration: -·-·-·- 0.02 M, · · · · · 0.2 M.
2a. Cd_{tot} = 0.02 M. 2b. Cd_{tot} = 0.2 M.

5.4 Discussion

Assuming that mono- and dihydroxo species of Cd^{2+} are the only complexes formed in our experiments, the following two equilibria have to be considered

$$Cd^{2+} + OH^- \underset{K_1}{\rightleftharpoons} Cd(OH)^+ \qquad [A]$$

$$Cd(OH)^+ + OH^- \underset{K_2}{\rightleftharpoons} Cd(OH)_2^\circ \qquad [B]$$

Equilibrium constants for both reactions were written in the following way

$$K_1' = \frac{[Cd(OH)^+]}{[Cd^{2+}]\ a_{OH^-}} = K_1 \frac{f_{Cd^{2+}}}{f_{Cd(OH)^+}} \qquad [5.2a]$$

$$K_2' = \frac{[Cd(OH)_2]}{[Cd(OH)^+]\ a_{OH^-}} = K_2\ f_{Cd(OH)^+} \qquad [5.2b]$$

where f_X is the activity coefficient of species X, [X] denotes its concentration and K_1 and K_2 are the thermodynamic equilibrium constants of reaction [A] and [B], i.e. with all compositions expressed as activities.
From material balances for total cadmium (Cd_{tot}) and bound OH^- (OH_{compl}), by substitution of the equilibrium constants K_1' and K_2', the following expression is obtained

$$K_1' + K_1'\ K_2'\ X + Y = 0 \qquad [5.3]$$

in which

$$X = \left(\frac{[OH_{compl}] - 2[Cd_{tot}]}{[OH_{compl}] - [Cd_{tot}]}\right) a_{OH^-}$$

and

$$Y = \left(\frac{[OH_{compl}]}{[OH_{compl}] - [Cd_{tot}]}\right) \frac{1}{a_{OH^-}}$$

are experimentally accesible.
By plotting X as a function of Y, values for K_1' and K_2' can be derived from the slope and intercept of a Y(X) plot. All experimental curves could be fitted quite satisfactorily if K_2' is zero, implying that the formation of dihydroxo complexes may be neglected under the experimental circumstances.
To convert K_1' into the corresponding thermodynamic equilibrium constant K_1, activity coefficients for $Cd(OH)^+$ and Cd^{2+} at the composition of the test solutions are needed. The values of $f_{Cd(OH)^+}$ and $f_{Cd^{2+}}$ were calculated from the Debye-Hückel equation (cf. (3)).

$$-\log f_i = \frac{F^3 z_i^2 (2000\pi\omega)^{1/2}}{2.303N(4\pi\varepsilon\varepsilon_o RT)^{3/2}\left[1 + a_i\left(\frac{2000F^2\omega}{\varepsilon\varepsilon_o RT}\right)^{1/2}\right]} \qquad [5.4]$$

where f_i is the activity coefficient of component i, N is Avagadro's number, a_i is the distance of closest approach of the ions and ω is the total ionic strength of the solution. All other symbols have their usual meaning. The distance of closest approach, a_i, was in both cases, more or less arbitrarily, set at 0.5 nm. Values of K_1', K_1 and the activity coefficients needed in calculating the latter are given in Table 5.1. As Eq.[5.4] only provides crude predictions of activity coefficients in concentrated solutions, K_1 values computed for the experiments in 0.1 M $Cd_2(NO_3)$ are placed in brackets.

Table 5.1 Activity coefficients of Cd species according to the Debye-Hueckel theory and equilibrium constants for the formation of monohydroxo complexes in solutions of variable $KNO_3/Cd(NO_3)_2$ composition at 20 and 60 °C.

Exp	T °C	c_{KNO_3} M	$c_{Cd(NO_3)_2}$ M	$f_{Cd(OH)^+}$	$f_{Cd^{2+}}$	K_1' $1.mol^{-1}$ $*10^{-3}$	K_1 $1.mol^{-1}$ $*10^{-4}$
1	20	0.20	0.02	0.726	0.277	4.0	1.05
2	20	0.02	0.02	0.800	0.409	6.2	1.21
3	60	0.20	0.02	0.710	0.254	6.8	1.90
4	60	0.02	0.02	0.826	0.467	10.7	1.89
5	20	0.20	0.10	0.685	0.220	6.8	(2.11)
6	20	0.02	0.10	0.713	0.258	9.4	(2.60)
7	60	0.20	0.10	0.668	0.199	9.8	(3.30)
8	60	0.02	0.10	0.697	0.234	14.0	(4.16)

From the data in Table 5.1 it follows that - presumably within experimental error and within the systematic errors made in using the DH equation - K_1 is independent of the KNO_3 concentration. This is an indication of the negligible occurrence of Cd - NO_3 complexes under the conditions of our adsorption experiments (chapter 6). However, K_1 increases substantially on increasing the $Cd(NO_3)_2$ concentration from 0.02 to 0.1 M. From a thermodynamic point of view, the value of the (activity-based) equilibrium constant should be independent of the total electrolyte concentration. Given the consistency of our experimental curves it is expected that the variation in K_1 is due to inapplicability of Debye-Hückel theory to rather concentrated solutions of multivalent ions as used in our experiments. At the lowest Cd_{tot} level, therefore, the calculated values of K_1 will be most reliable, and in average amount to ca. $1.1 \cdot 10^4$ $l.mol^{-1}$ at 20 °C and $1.9 \cdot 10^4$ $l.mol^{-1}$ at 60 °C, respectively. These average values describe the experimental results at Cd_{tot} = 0.02 M quite well, as is illustrated in Fig. 5.3.

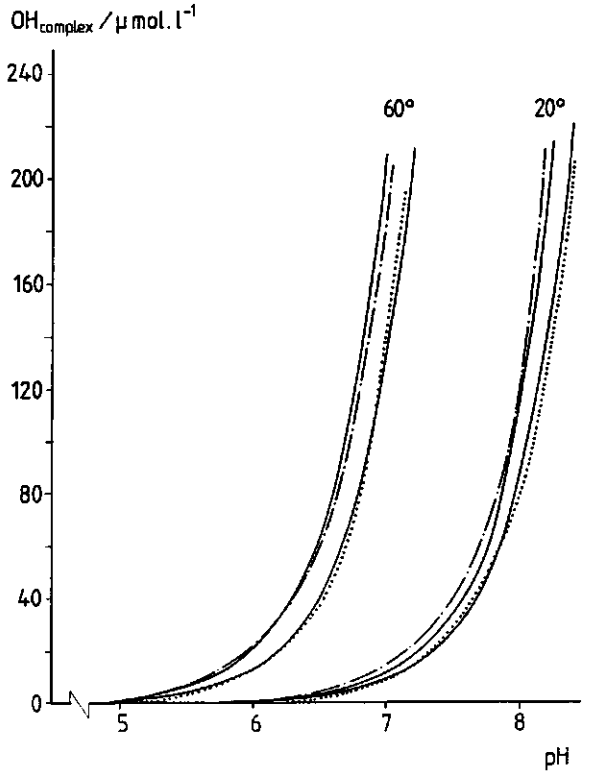

Fig.5.3 OH_{compl} as a function of pH in 0.02 M $Cd(NO_3)_2$ at 20 and 60 °C at two KNO_3 concentrations. Solid lines indicate theoretical relations calculated from the mean values for the equilibrium constant K_1.

Qualitative conclusions from the measurements are somewhat restricted by the uncertainty about the activity coefficients to be used in the calculations. However, our experiments provide valuable qualitative information on the speciation of cadmium as a function of temperature.

As has already been noticed, all experimental curves in fact show temperature congruence: they merge if shifted with respect to pH. However, if these curves would be replotted as a function of pOH, the temperature effect becomes very small. From the difference in pK_w, at a certain pOH, one can calculate a difference in pH between 20 and 60 oC of ca. 14.167 - 13.017 = 1.150 (4). The shift of our experimental results is for all electrolyte ratios of the same order of magnitude (1.1 - 1.2). From this it follows that the influence of temperature on reaction [A] is only very small and, due to its negligible contribution over the experimental pH range, the temperature dependence of reaction [B] may also be ignored.

The fact that corresponding (Cd_{tot}, pOH) curves merge within experimental error implies that reaction [A] is essentially athermic (ΔH is very small). This means that the formation of $Cd(OH)^+$ complexes in solutions containing cadmium ions, is primarily determined by the availability of OH^- ions from the dissociation of water. The conclusion that formation of the monohydroxo complex of cadmium is essentially an entropy-driven process, is confirmed by the data of Baes and Mesmer (5), who report a ΔH value of +55 $kJ.mol^{-1}$ for the reaction

$$Cd^{2+} + H_2O \rightleftharpoons Cd(OH)^+ + H^+ \qquad [C]$$

Taking into account the heat of dissociation of water (-56 $kJ.mol^{-1}$ at 20 °C, (6)), this would lead to a ΔH of -1 $kJ.mol^{-1}$ for reaction [A].

At 20 °C, from the average value of K_1 at the lowest cadmium concentration, for reaction [C] a pK value of 14.2 - 4.0 = 10.2 follows, in reasonable agreement with the literature value of 10 (7). From our data, a value for the Gibbs energy of complex formation of ca. -23 $kJ.mol^{-1}$ follows for reaction [A]. Using van 't Hoff's law

$$\left(\frac{\partial \ln K}{\partial T}\right) = -\frac{\Delta H}{RT^2} \qquad [5.5]$$

from the change in K_1 with temperature, an estimate of the enthalpy change

accompanying reaction [A] can be made. Assuming that ΔH is constant over the temperature interval considered, a value of ca. -9 $kJ.mol^{-1}$ follows for the heat of complex formation. We believe that our method overestimates the enthalpic contribution, because of the problems encountered in calculating proper activity coefficients in solutions of relatively high concentration.

Combining our thermodynamic data and those taken from literature, an estimate of the entropy change involved in the formation of $Cd(OH)^+$ complexes in aqueous solutions containing $Cd(NO_3)_2$ and KNO_3, can be obtained. Using a value of -1 $kJ.mol^{-1}$ for ΔH and -23 $kJ.mol^{-1}$ for ΔG^o, the standard entropy of complex formation is found to be +75 $J.mol^{-1}.K^{-1}$ (20 °C). The standard entropy of hydration of the Cd^{2+} ion in aqueous solution is ca. -210 $J.mol^{-1}.K^{-1}$ (8). Considering only changes in state of hydration of the Cd^{2+} ion, these entropy data indicate that reaction of Cd^{2+}_{aq} with OH^- liberates about 35 % of the hydration entropy. It is generally assumed that ca. ten molecules of water contribute to the hydration of Cd^{2+} in aqueous solution (8). This could indicate that the $Cd(OH)^+$ complex is hydrated by about 6 á 7 water molecules.

5.5 Conclusions

The exchange of a water molecule in the inner coordination sphere of a Cd^{2+} ion for a hydroxyl ion does not lead to the formation of new chemical bonds, but results in a randomization. Our conclusions that the formation of $Cd(OH)^+$ species is essentially athermal has important consequences for the interpretation of the cadmium adsorption onto insoluble oxides and related phenomena as will be discussed in the following chapters.

5.6 References

1. Sillén, L.G., and Martell, A.E., "Stability Constants of Metal - Ion Complexes", The Chemical Society, London, 1964.
2. Schindler, P.W., in "Adsorption of Inorganics at Solid - Liquid Interfaces" (M.A. Anderson and A.J. Rubin, Eds), Ann Arbor Science, Ann Arbor, 1981.
3. MacInnes, D.A., "The Principles of Electrochemistry", Dover Publications Inc., New York, 1961.

4. CRC Handbook of Chemistry and Physics, 62nd Edition (R.C. Weast and M.J. Astle, Eds), CRC Press, D-145, 1981.

5. Baes, C.F., and Mesmer, M.E., "The Hydrolysis of Cations", Wiley Interscience, New York, 1976.

6. Tyrell, H.J.V., and Beezer, A.E., "Thermometric Titrimetry", Chapman and Hall Ltd, London, 1986.

7. Hunt, J.P., "Metal Ions in Aqueous Solution", W.A. Benjamin Inc., New York - Amsterdam, 1963.

8. Monk, C.B., "Electrolytic Dissociation", Academic Press, London - New York, 1961.

6. TEMPERATURE DEPENDENCE OF CADMIUM ION ADSORPTION ON RUTILE AND HEMATITE

6.1 Introduction

In the past, only little attention has been paid to the temperature dependence of (heavy metal) ion adsorption onto insoluble oxides. Only very few studies dealing with the subject can be found in literature (1-3). Studying the influence of temperature on the adsorption process provides important information on the driving forces involved in adsorption.

In the preceding chapters we focussed our attention on a number of contributions to the adsorption process. In particular the influence of temperature on the surface properties of the adsorbents and on the adsorptive has been studied. From these temperature-dependent measurements we were able to obtain relevant information on the thermodynamics of processes involved in the overall cadmium adsorption to be discussed in the following chapters. Prior to looking at the experimental facts obtained for the adsorption of cadmium ions onto rutile and hematite, it is expedient to review the results obtained sofar.

For the adsorbents we concluded in chapter 3 that their surface charge is quite sensitive to changes in temperature. In adsorption studies it should therefore be realized that the interpretation of sets of experimental isotherms measured at constant pH over a range of temperatures is not straightforward because the electrical characteristics of the interface strongly change with temperature. The fact that in some experimental adsorption studies at constant temperature, pH has been taken as a leading parameter in the adsorption process, may have introduced the 'mistake' to study heavy metal ion adsorption onto inorganic oxides only as a function of temperature at fixed pH (as e.g. did Gray and Malati (1)). The conclusion that the adsorption is an entropically favorable process, was too easily drawn solely from the observation that adsorption increases with increasing temperature at fixed pH.

As in our case we deal with ion adsorption onto charged interfaces, electrostatic interactions will contribute to the total Gibbs energy of adsorption, $\Delta_{ads}G$. The magnitude of the electrical term depends on the electrical potential in the plane where adsorption of the species takes place. This potential, in turn, is related to the charge density of the surface. Using

the experimental surface charge(pH) relations of rutile and hematite as a function of temperature, it was found convenient to measure cadmium adsorption isotherms as a function of initial surface charge density, σ_o^*. In this way, at different temperatures isotherms are obtained that allow comparison on a phenomenological basis, without the direct need to invoke model assumptions.

From the analysis of the temperature dependence of the σ_o(pH) relation on both oxides, we concluded that chargeable groups at the oxide surfaces, as far as their chemical properties are concerned, strongly resemble bulk hydroxyl ions (chapter 3). It has been frequently suggested in literature (cf. (4)) that these surface groups are responsible for the adsorptive binding of heavy metal ions. Accepting this mechanism, our conclusion that Cd^{2+} - OH^- interactions in solution are almost exclusively entropic should be of great value in the interpretation of experimental adsorption isotherms. As stated before (chapter 5), specific adsorption of (heavy metal) cations onto oxides is always accompanied by a reduction of pH. This could be due either or both to uptake of hydroxyl ions from the bulk solution and release of protons from the interfacial region. This process is not of a simple 1:1 - stoichiometry, though.

In view of the above, we formulate the following working hypothesis. At a certain value of the surface charge, the adsorption of Cd species is expected to occur on ≡S-OH sites at the surface. As long as Cd^{2+} ions are concerned, the process is likely to be similar to bulk Cd^{2+} - OH^- association, and therefore expected to be mainly driven by a gain in hydration entropy. Changes in pH observed on adsorption, in this picture, must be ascribed to adjustment of the surface charge by expulsion of protons.

The fact that in bulk solutions only at high pH values $Cd(OH)_2$ complexes are formed, indicates that $Cd(OH)^+$ species do not show a pronounced affinity for OH^- ions in the pH range considered. The proposed analogy between cation adsorption and bulk reactions, would imply that it is not very favorable for $Cd(OH)^+$ species to adsorb as such onto oxides. In first instance, therefore, we will only have to deal with the adsorbability of Cd^{2+} ions onto the oxide substrates. This is only a prediction of general trends, however. Comparing results for different adsorbents (i.e. TiO_2 and Fe_2O_3) should eventually help to discriminate between general and specific (chemical) interactions in the overall adsorption.

6.2 Experimental

6.2.1 Adsorption experiments

For the measurement of the adsorption of cadmium onto rutile and hematite the experimental set-up as described in chapter 2 was used. All isotherms were obtained under pH-static conditions. For that purpose we used a micro computer (HP 86B) with data-acquisition system (HP 3488A), in the same configuration as previously described. The computer program was extended with a pH-stat routine for the adsorption experiments, such that after each addition of $Cd(NO_3)_2$ stock solution, after an equilibration of ca. 15 minutes, the pH-stat value was restored by the step-wise addition of 0.1 M KOH (Merck Titrisol) from an automatic buret (Metrohm 655 Dosimat). The procedure of back titration was as follows. Every one to two minutes the electromotive force (E) of the cell was measured. After addition of a first, fixed, volume of base (usually 0.1 ml) the suspension was equilibrated. When the drift in E became less than 0.1 mV/min., the volume of the next addition was calculated on the basis of the preceding ΔE (mV/ml) and the remaining traject up to the electromotive force corresponding with the pH-stat value, E_{work}. After E_{work} had been reached within ca. 10 %, a more strict equilibrium condition of 0.02 mV/min was used. By following this procedure it was possible in all experiments to reach the pH-stat value within ± 0.5 mV.

Adsorption measurements were performed as follows. After standardization of the cell with buffer solutions (Merck Titrisol) of pH 4.00, 7.00, 9.00 and 11.00 (values at 20 °C), 500 mls of the oxide suspension, containing ca. 10 grams of the oxide were brought into the titration vessel, dry KNO_3 was added and the suspension was equilibrated overnight at low pH at the desired temperature. Before the actual adsorption measurement was started, the oxide was titrated with 0.1 M KOH to pH ca. 10, subsequently with 0.1 M HNO_3 to pH 3.5, and finally with KOH to the actual working pH in the adsorption measurements. These preliminary titrations were performed in the same way as those used in the determination of the surface charge on these oxides (chapter 3). The pre-titrations were performed in order to ascertain that pH-induced alterations, if any, in the interfacial region could take place. Then a small volume of a $Cd(NO_3)_2$ solution (usually 1.0 M) was added from an automatic pipet (Gilson P1000). Meanwhile E of the cell was monitored. Once the electromotive force had stabilized, the pH-stat procedure was

started, and the suspension was automatically titrated back to its working pH. Usually the entire procedure from cadmium addition to sampling took about 60 to 90 minutes. In the pH-range studied, in all cases the rutile suspensions settled readily when stirring was stopped. Samples from the supernatant of such suspensions could be withdrawn without significant loss of oxide. Hematite suspensions, however, appeared to be more stable under the experimental conditions. In that case a homogeneous sub-sample of the stirred suspension was taken, filtered and the total weight of oxide in the remaining suspension was corrected for the amount of Fe_2O_3 withdrawn with the sample. The 10 ml sub-samples of the supernatant, respectively the suspension, were withdrawn from the vessel using a syringe. After sampling, a subsequent $Cd(NO_3)_2$ addition was made and the whole procedure was repeated. Cadmium concentrations in the samples were determined by means of atomic absorption spectrophotometry or differential pulse polarography. Adsorbed amounts of cadmium were calculated from mass balances for $Cd(NO_3)_2$ and oxide. After a few samples had been taken the volume of the suspension was corrected by the addition of KNO_3 solution of the same concentration as the suspension. In this way the total volume of the suspension was kept constant within ca. 5 %. From the volumes of base needed to maintain the pH-stat value, OH^- co-adsorption data were directly obtained.

6.2.2 Microelectrophoresis

Electrophoretic mobilities of the oxide particles were determined with a Malvern Zetasizer II microelectrophoresis apparatus. For our measurements the cell was equiped with a perspex capillary, in order to minimize problems concerning electro osmosis and 'electro precipition' of oxide particles onto the wall of the capillary. A rather dilute suspension of the oxide in KNO_3 (solid concentration ca. 200 mg/l) was titrated in the automatic titration cell as described before. At certain pH values, samples were withdrawn from the suspension with a syringe and injected immediately into the electrophoresis cell. This sampling procedure was used to minimize the contact of the sample with the atmosphere (prevention of CO_2 contamination). For the measurements in the presence of cadmium, volumes of $Cd(NO_3)_2$ stock solution needed to establish a certain degree of coverage of the oxide with Cd, were determined indirectly from obtained adsorption isotherms and the volume and sol concentration of the test solution. In these experiments, the pH of the samples was controlled by titration in the potentiometric set-up.

6.3 Results and discussion

Adsorption isotherms for cadmium onto rutile and hematite were measured as a function of temperature ((5),20, 40 and 60 °C) and initial surface charge density. Normally, experiments were performed in 0.02 M KNO_3. Results for rutile are given in Fig.6.1 for different values of the initial surface charge, σ_o^*.

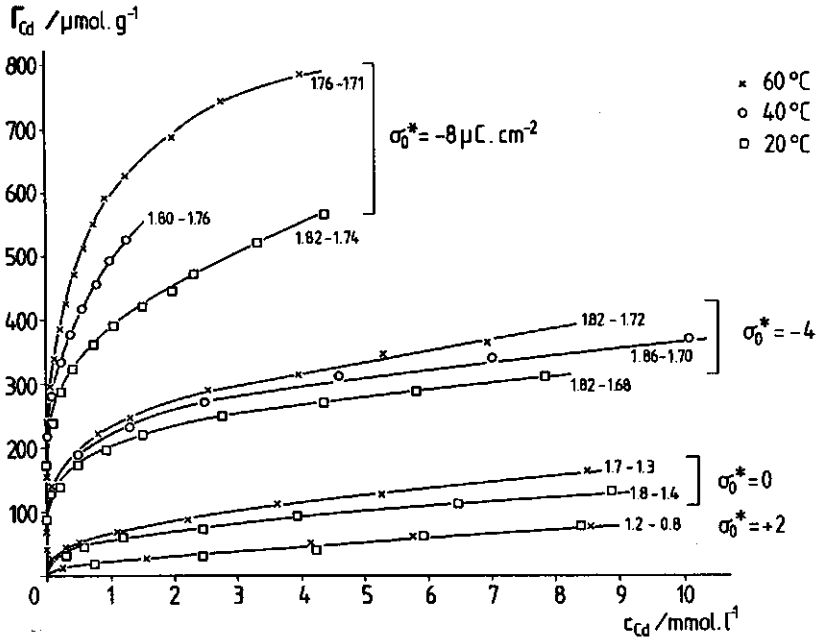

Fig.6.1 Adsorption of cadmium ions onto rutile as a function of temperature Initial surface charge density, σ_o^*, is indicated. Electrolyte: 0.02 M KNO_3. The numbers along the curves are the measured co-adsorption ratios.

In the case of hematite (Fig.6.2), only the region of positive surface charges is experimentally accessible in cadmium adsorption studies. At pH values around or above pH^o of the oxide, bulk precipitation of $Cd(OH)_2$ would occur, thus thwarting the interpretation of depletion data. In Figs 6.1 and 6.2, observed OH^- co-adsorptions are indicated as the molar ratio OH^- adsorbed/ Cd adsorbed. This ratio, r_{OH}, is fairly constant along each isotherm, albeit that for rutile the isotherms for neutral or slightly positive values of σ_o^* tend to show a more substantial decrease in r_{OH}, with

increasing equilibrium concentrations. In all cases the range of co-adsorption ratios, calculated from low to high Cd equilibrium concentration, is given in the figures. For hematite, experimental data tend to be less accurate than for rutile, presumably caused by the sampling routine: total sol concentrations are becoming more and more uncertain along the isotherm. Therefore, only mean values for r_{OH} and smoothed adsorption isotherms are presented in Fig.6.2.

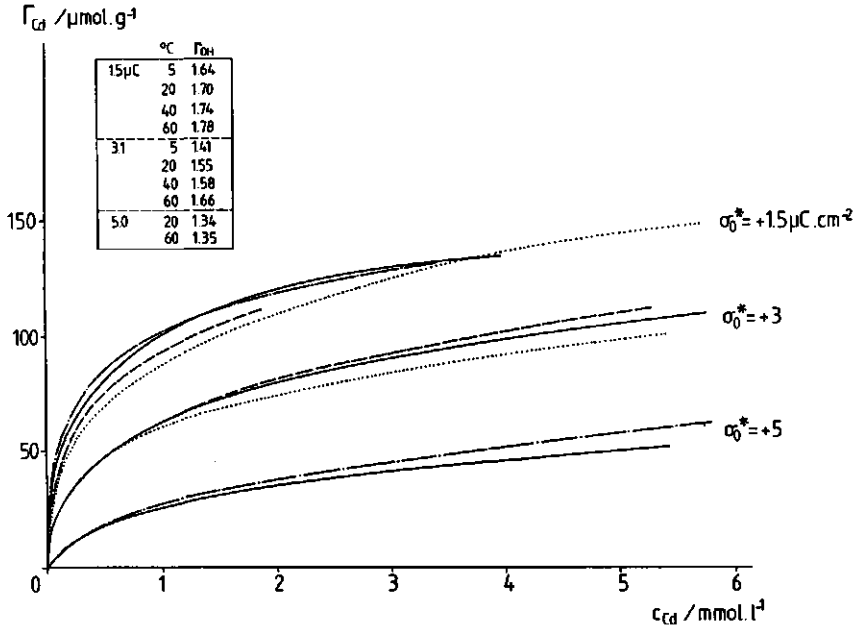

Fig.6.2 Adsorption of cadmium ions onto hematite as a function of temperature (····· 5 °C, —— 20 °C, - - - 40 °C, -·-·-· 60 °C). Initial surface charge density is indicated. Electrolyte: 0.02 M KNO_3.

Both for rutile and hematite r_{OH} is essentially independent of temperature. For these oxides the highest isotherms show a co-adsorption ratio of 1.75 ± 0.02. Apparently, under our experimental conditions r_{OH} = 1.75 is a kind of 'plateau value of co-adsorption'.

Superficial inspection of the adsorption results in both systems already provides valuable information on the driving forces in the process of Cd adsorption onto inorganic oxides. For rutile, at neutral or positive surface charges, adsorption is relatively weak. One must conclude that electrostatic contributions are of major importance in the process considered.

For hematite, σ_o^* plays also an important role, but here the chemical contribution obviously is much stronger than for rutile. Even at strongly positive charged interfaces, chemical forces are able to overcome electrostatic repulsion.

The observed temperature dependence of cadmium adsorption onto negatively charged rutile seems to indicate that this temperature effect has its basis in the electrostatics of adsorption. As hardly a significant temperature influence is observed on neutral or positively charged interfaces, it follows that the chemical contribution to $\Delta_{ads}G$ only modestly changes with temperature. The same has been found for proton adsorption onto these surfaces (chapter 3).

For rutile, the cadmium adsorption has also been measured in 0.2 M KNO_3. Isotherms at initial surface charge densities of -8 and -4 $\mu C/cm^2$ are given in Fig.6.3. Straightforward conclusions are not easily drawn from the comparison of adsorption isotherms in 0.02 M (Fig.6.1) and 0.2 M KNO_3. As the specifically adsorbed cadmium charge is only partly compensated by the co-adsorption of OH^- ions, a reversal of net charge will occur at higher degrees of surface coverage. In this case one would expect the adsorption to increase with increasing electrolyte concentration, due to a decreased electrostatic repulsion at higher electrolyte levels. Experimentally, the opposite is observed, however. We have to consider that increasing the electrolyte concentration results in a lower co-adsorption ratio. Furthermore, the adsorption potential at constant σ_o^* depends on the salt concentration. Therefore, treating the electrolyte concentration dependence of cadmium adsorption onto oxides requires the elaboration of these effects (for a discussion see section 6.4).

Electrophoretic mobilities of a rutile suspension in 0.02 M KNO_3 have been measured as a function of pH at 20 ^oC. Results are given in Fig.6.4. From this figure a value for the i.e.p. of roughly 5.9 follows. The p.z.c. of rutile under the same conditions is located at pH ~ 5.6. The small difference between p.z.c. and i.e.p. indicates that -at least around the p.z.c.- no strong specific adsorption of K^+ or NO_3^- onto rutile occurs.

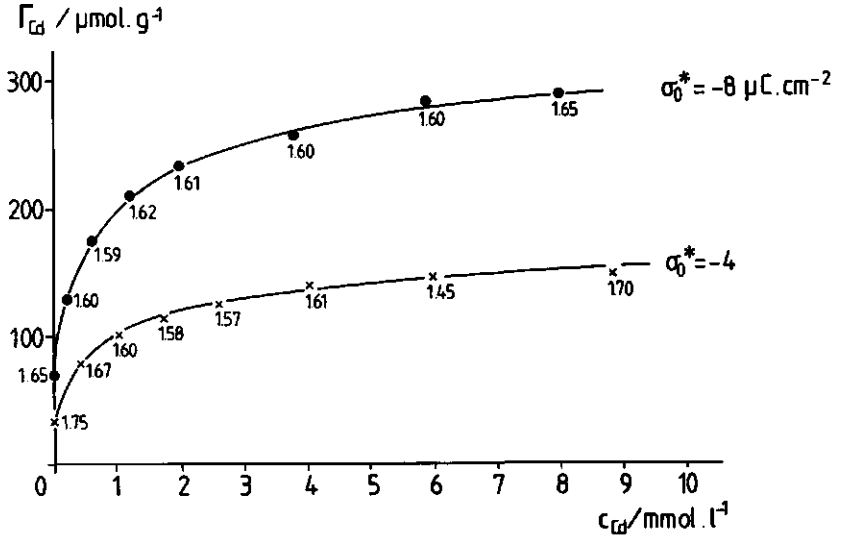

Fig.6.3 Adsorption of cadmium ions onto rutile at 20 °C in 0.2 M KNO_3. Initial surface charge -8.0 and -4.0 µC/cm^2.
Measured r_{OH} values are indicated.

In Fig.6.5 the influence of adsorbed cadmium on the electrophoretic mobility of rutile particles is given. The curve is recorded at an initial surface charge density of -8.0 µC/cm^2 (at 20 °C in 0.02 M KNO_3 corresponding to pH 7.83). A first conclusion is that a reversal of electrokinetic charge takes place on adsorption of cadmium ions, already at low $Cd(NO_3)_2$ concentrations. Combination of our electrophoretic results with the corresponding adsorption isotherm (Fig.6.1), enables us to draw qualitative conclusions on the co-adsorption of supporting electrolyte ions under these conditions. The i.e.p. in the presence of $Cd(NO_3)_2$ is situated around pCd = 5.6. At this concentration, about 135 µmoles Cd^{2+}/g and ca. 230 µmoles OH^-/g are adsorbed on the rutile. Taking for the specific surface area of rutile a value of 51 m^2/g), this corresponds to a net adsorbed Cd/OH charge of about +7.3 µC/cm^2. From this result it is clear that at least the major part of the initial surface charge, in the i.e.p. is compensated by adsorbed Cd/OH charge. From both electrophoresis results it seems that, within experimental uncertainty, around the i.e.p., neither significant adsorption of K^+ nor of NO_3^- ions occurs.

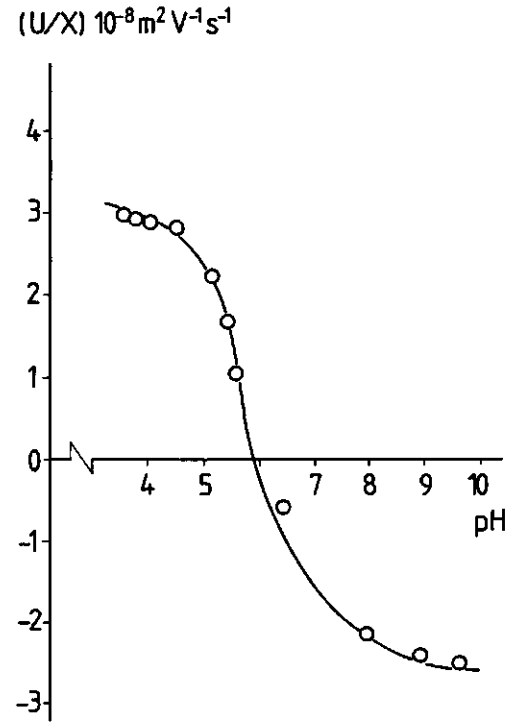

Fig.6.4 Electrophoretic mobility of rutile sol as a function of pH. Electrolyte: 0.02 M KNO_3. Temperature 20 °C. Sol concentration 150 mg/l.

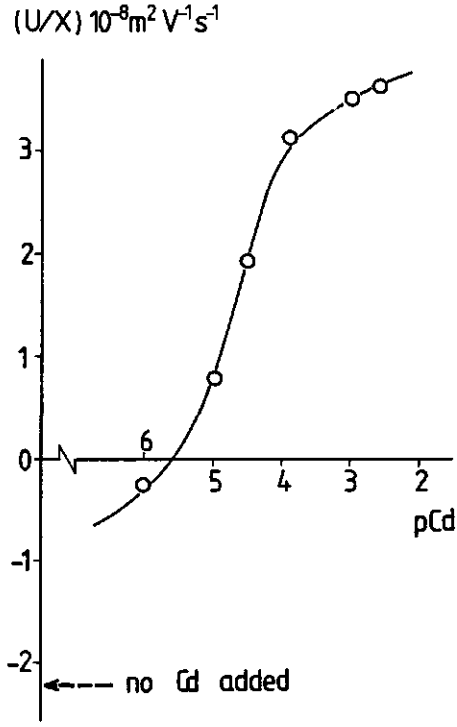

Fig.6.5 Electrophoretic mobility of rutile sol in the presence of $Cd(NO_3)_2$. Electrolyte 0.02 M KNO_3. Temperature 20 °C. Sol concentration 150 mg/l.

6.4 Model analysis

For the analysis of the experimental cadmium adsorption results we used a Langmuir type isotherm equation

$$\frac{\Theta}{1-\Theta} = \frac{c_A}{55.5} \exp\left(-\frac{\Delta_{ads}G}{RT}\right) \qquad [6.1]$$

where θ is the degree of surface coverage, c_A the equilibrium concentration of the adsorptive A, and $\Delta_{ads}G$ is the total Gibbs energy of adsorption. In general, the Gibbs energy of adsorption depends on θ. In the case of electrosorption, the electrostatic contribution also depends on the adsor-

bed charge and thus on θ. Furthermore, non-electrostatic lateral interactions may figure in the adsorbed phase (e.g. of a hydrational origin). This last mentioned type of interaction will also be θ-dependent. A linear dependence of ΔG_{lat} on θ is assumed in the following analysis. According to these considerations, the total Gibbs energy of adsorption can be thought as being composed of the following constituents

$$\Delta_{ads}G = \Delta G^{o}_{chem} + \theta\Delta G_{lat} + \Delta G_{el} \qquad [6.2]$$

Here ΔG^{o}_{chem} is the Gibbs energy of chemical interactions between adsorbent and adsorbate, ΔG_{lat} contains all lateral interactions of non-electrical nature and ΔG_{el} is the electrostatic contribution to the overall adsorption Gibbs energy. Substitution of Eq.[6.2] in Eq.[6.1] yields a Frumkin-Fowler-Guggenheim (FFG) - type equation

$$\frac{\theta}{1-\theta} = \frac{c_A}{55.5} \exp\left([-\Delta G^{o}_{chem} - \theta\Delta G_{lat} - zF\psi_{ads}]/RT\right) \qquad [6.3]$$

where ψ_{ads} is the electrical potential at the locus of adsorption.

Application of Eq.[6.3] to our experimental results requires model assumptions for the adsorption process studied. For the calculations of ψ_{ads}, a 'plane of adsorption' has to be identified. Furthermore, a double layer model is needed to establish the actual electrical potential in this plane.

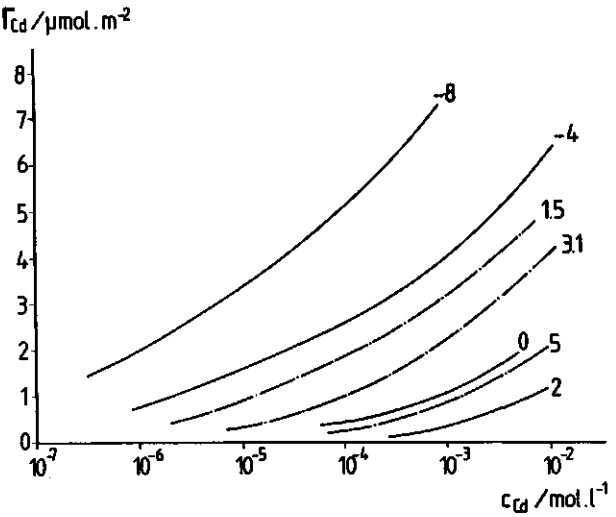

Fig.6.6 Adsorption of cadmium ions onto rutile (———) and hematite (-- · -- · --) at 20 °C. Initial surface charge densities are indicated. Electrolyte: 0.02 M KNO_3.

In Fig.6.6 adsorption isotherms of cadmium onto both rutile and hematite in 0.02 M KNO_3 at 20 °C are given as a semi-logarithmic plot. Adsorbed amounts of cadmium are normalized with respect to the BET surface area of the oxides. On first inspection of this figure, a uniformity in the shape of all isotherms is observed. The shift of the individual curves with changing initial surface charge, σ_o^* sheds light on the electrical properties of the systems under consideration. From Eq.[6.2] it follows for low degrees of surface coverage (where lateral interactions vanish) and assuming that chemical interactions are independent of the surface charge density, that

$$\left(\frac{\partial \ln c_A}{\partial \sigma_o}\right)_{\theta \to 0} = \left(\frac{\partial \Delta G_{el}}{\partial \sigma_o}\right)_{\theta \to 0} \qquad [6.4]$$

In the low θ limit, where only the adsorption of the first Cd entity has to be considered, for ΔG_{el} the following relation holds

$$\Delta G_{el} = zF\psi_{ads,o} \qquad [6.5]$$

with $\psi_{ads,o}$ being the electrical potential in the adsorption plane of the uncovered interface.

In chapter 3 it was already concluded that, whatever the physical basis may be, the Gouy-Stern double layer model is able to describe all observations hitherto made on rutile and hematite, as far as their σ_o(pH) behavior is concerned. An inner layer capacitance of ca. 440 $\mu F/cm^2$ follows from GS fits, corresponding to a relatively thin layer with high dielectric permittivity. As the crystal ionic radius of a Cd^{2+} ion (0.1 nm (5)) is of the same order of magnitude as the Stern layer thickness, it is consistent to use the same double layer model, with the outer Helmholtz plane (OHP) as the plane of specific cadmium adsorption. Then Eqs [6.4] and [6.5] can be combined to yield

$$\left(\frac{\partial \ln c_A}{\partial \sigma_o}\right)_{\theta \to 0} = \frac{zF}{RT}\left(\frac{\partial \psi_s}{\partial \sigma_o}\right)_{\theta \to 0} \qquad [6.6]$$

where $\psi_s = \psi_{ads}$ is the potential at the OHP.
The LHS of Eq.[6.6] follows from the horizontal shift in the semi-logarithmic adsorption isotherms of Fig.6.6 for low degrees of surface coverage,

whereas the RHS term was calculated using the Poisson-Boltzmann equation for a flat double layer, extended with a charge-free Stern layer with a capacitance of 440 μF/cm2. In Fig.6.7 the experimentally determined horizontal shifts of the isotherms with initial surface charge are plotted together with the theoretically expected ones on the basis of the GS model. From this figure we concluded that a simple Gouy-Stern approach is able to predict satisfactorily the relative position of adsorption isotherms of cadmium onto both rutile and hematite over a range of charge densities, varying from -8 to +5 $\mu C/cm^2$.

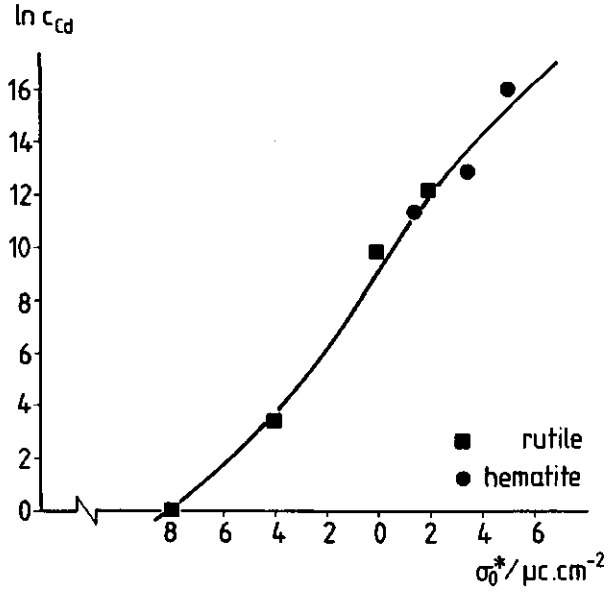

Fig.6.7 Experimental shifts of cadmium adsorption isotherms on rutile and hematite at low degrees of surface coverage, compared to theoretical shifts on the basis of GS theory (solid curve). Temperature: 20 °C.

For the analysis of the experimental isotherms according to the FFG model, electrical contributions have to be taken into account. As the Gouy-Stern model describes the double layers on rutile and hematite in the absence of specific adsorption satisfactorily, this concept is also used to calculate adsorption potentials in the presence of specifically adsorbed cadmium. The FFG equation (Eq.[6.3]) was linearized as follows

$$\ln\left\{\frac{\theta}{1-\theta}\,\frac{55.5}{c_A}\exp\left(\frac{zF\Delta\psi_{ads}}{RT}\right)\right\} + \theta\,\frac{\Delta G_{lat}}{RT} = -\frac{\Delta G^{o}_{chem}}{RT} - \frac{zF\psi_{ads,o}}{RT} \qquad [6.7]$$

where $\Delta\psi_{ads} = \psi_{ads} - \psi_{ads,o}$ is the normalized adsorption potential, ψ_{ads} is

the potential in the plane of adsorption at surface coverage θ and $\psi_{ads,o}$ is the adsorption potential of the uncovered surface. The chemical interaction parameter ΔG^{o}_{chem}, follows from the intercept minus the $\psi_{ads,o}$ term of a plot of the logarithmic term in Eq.[6.7] as a function of θ, whereas ΔG_{lat} is obtained from the slope of such a line.

The magnitude of electrical potentials was determined as follows. As was stated before, the adsorption plane was identified with the OHP. The potential $\psi_{ads,o}$, in our opinion simply is the Stern potential of the uncovered interface as calculated from the value of σ_0^* using GS theory.
In the next chapter (7), the co-adsorption of OH^- ions will be discussed in detail. Anticipating the conclusions to be reported, Cd^{2+} ions are supposed to adsorb in the OHP, whereas depletion of OH^- ions from solution is considered as an adjustment of the surface charge initiated by the specifically adsorbed Cd^{2+} ions. The potential of the oxide-solution interface is assumed to maintain its Nernst value on adsorption of Cd^{2+} ions. Adsorption of cadmium hydroxo complexes as such is supposed to be absent.

The adsorption potential $\psi_{ads} = \psi_s$ is a function of the surface potential (~pH) and the specifically adsorbed Cd^{2+} charge in the OHP, σ_s. For all experimental situations, ψ_{ads} could be computed as a function of $\Gamma_{Cd^{2+}}$ (σ_s), from the non-linear Poisson-Boltzmann equation. Solutions of that equation were obtained by numerical integration according to the Runge-Kutta method, using IMSL subroutines (6).

As an example, in Fig.6.8 ψ_{ads} is plotted as a function of the surface potential ψ_o at 20 °C in 0.02 M (1-1) electrolyte, for different values of σ_s. At given pH and $\Gamma_{Cd^{2+}}$, from such a plot the corresponding value for the adsorption potential can be obtained by interpolation.

An attendant problem in using Eq.[6.7] in our analysis, is that degrees of surface coverage are needed instead of the experimentally determined Γ's. Therefore a value for the plateau adsorption has to be estimated in some way. As it is not at all obvious from our experimental isotherms (Figs 6.1 and 6.2) whether a well-defined plateau develops, we have only a first (rough) guess for Γ_{max}. For the highest adsorbed amount available (rutile, 60 °C, -8 $\mu C/cm^2$), Γ seemingly approaches a plateau at ca. 18 $\mu moles/m^2$. This would correspond with an extremely close-packed monolayer of Cd species, with a 'molecular cross section' of about 0.1 nm^2. Using this value

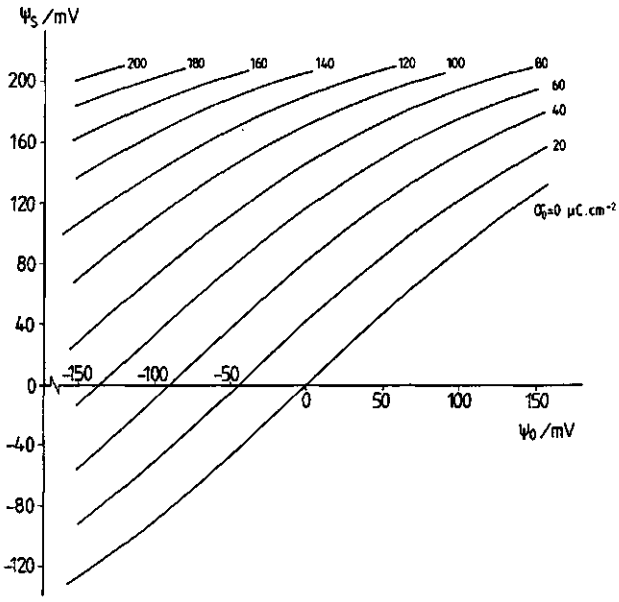

Fig.6.8 Potential at the outer Helmholtz plane as a function of the surface potential at different amounts of specifically adsorbed charge, according to the Gouy-Stern model. Inner layer capacitance 440 μF/cm². Electrolyte: 0.02 M (1-1). Temperature: 20 °C.

for Γ_{max}, the linearization procedure according to Eq.[6.7] yields straight lines that show a kink around $\theta \sim 0.4$ (Fig.6.9). A more reasonable estimate for the cross section of a, partly hydrated, adsorbed cadmium ion would be of the order of 0.2-0.3 nm², corresponding to $\Gamma_{max} \approx 7$ μmol/m². Lines calculated with this value of Γ_{max} are also given in Fig.6.9. From the examples given in the figure it follows that ΔG_{1at} (~slope) is quite sensitive towards the choice of Γ_{max}, whereas ΔG^{o}_{chem} (~intercept) is only slightly

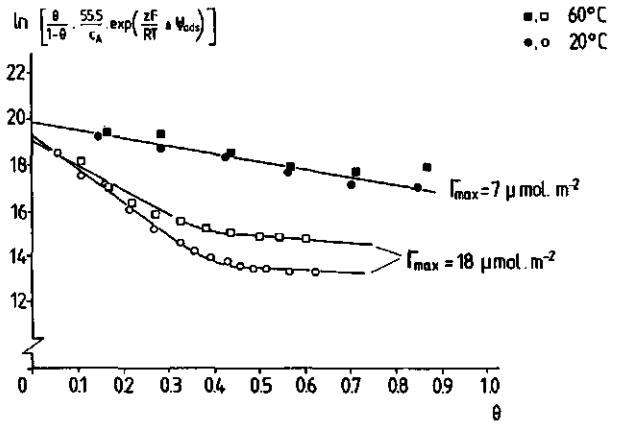

Fig.6.9 Linearized FFG relation (Eq.[6.7]) for the adsorption of cadmium ions onto rutile at 20 and 60 °C for two different values of Γ_{max}. Electrolyte: 0.02 M KNO_3. Initial surface charge: -8 μC/cm².

affected by the actual choice of that parameter. Large values for ΔG_{lat} are not to be expected in our case, because lateral interactions of an electrostatic nature have already been accounted for in ΔG_{el}. This suggests that $\Gamma_{max} \sim 7$ μmol/m^2 is a reasonable estimate for Cd monolayer coverage on oxides. Therefore, our experimental results were analyzed using this value of Γ_{max} for both rutile and hematite. Values for ΔG^{o}_{chem} and ΔG_{lat} are compiled in Table 6.1.

Table 6.1 Chemical and lateral contributions to the overall Gibbs energy of adsorption of cadmium ions onto rutile and hematite as a function of temperature, initial surface charge density and salt concentration. θ*'s calculated with* Γ_{max} *= 7* μmoles/m^2. ψ_{ads} *calculated from GS theory.*

OXIDE	c_{KNO_3} mol/l	T °C	σ_o μC/cm2	ΔG^{o}_{chem} kJ/mol	ΔG_{lat}
RUTILE	0.02	20	-8.0	-24	+7
			-4.0	-24	+5
			0.0	-27	+7
			+2.0	-28	~0
		60	-8.0	-30	+8
			-4.0	-27	+7
			0.0	-30	-1
			+2.0	-33	-5
	0.2	20	-8.0	-25	+8
			-4.0	-22	+9
HEMATITE	0.02	20	+1.5	-42	+6
			+3.1	-41	+2
			+5.0	-42	~0
	0.02	60	+1.5	-46	+5
			+3.1	-46	+2
			+5.0	-47	-1

Some trends are inferred from Table 6.1. The chemical contribution to the Gibbs energy of adsorption is not strongly influenced by the initial surface charge on the oxides. Furthermore, in the case of rutile, an increase in salt concentration from 0.02 to 0.2 M KNO_3, essentially leaves the chemical term unaffected. In fact, it is surprising that the model accounts so well for the influence of the electrolyte concentration. At corresponding initial surface charge densities, the pH-stat values and thus the surface potentials differ remarkably at the two salt concentrations. Also the (ψ_o, ψ_s) relations are different. Within the model, the electrical contribution to the Gibbs energy of adsorption calculated according to the GS double layer model, however, fully accounts for the largely different adsorption isotherms at both electrolyte levels. The important observation, made before, that ΔG^o_{chem} is only slightly dependent on the temperature, is now confirmed. The lateral interaction term is found to depend on the initial surface charge, temperature and electrolyte concentration. As has been previously shown, the absolute value of ΔG_{lat} is very sensitive to the actual choice of Γ_{max}. Interpretation of this contribution is virtually impossible, because all kinds of uncertainties are compounded in this term. The fact that in most situations small positive (i.e. repulsive) values for ΔG_{lat} are obtained is in line with our expectations.

Chemical Gibbs energies for the adsorption of protons (chapter 3) and cadmium ions are compared in Table 6.2.

Table 6.2 Standard chemical Gibbs energies for the adsorption of H^+ and Cd^{2+} onto insoluble oxides at 20 °C.

OXIDE	$\Delta G^o_{chem,H+}$ kJ/mol	$\Delta G^o_{chem,Cd2+}$	$r_{H/Cd}$
Rutile	-31	-26	1.2
Hematite	-49	-42	1.2
$r_{hem/rut}$	1.6	1.6	

From this table it can be concluded that for each of the two oxides the same ratio between the chemical affinities for protons and cadmium ions is found. The fact that also a constant affinity ratio between rutile and hematite is obtained for both the adsorption of H^+ and Cd^{2+}, directly follows from the previous observation. That for both oxides the chemical affininity for protons is only a factor 1.2 higher than for cadmium ions, clearly illustrates the ambuigity of the distinction between 'surface ion' and 'specifically adsorbed ion', solely on the basis of chemical affinities. It may be concluded that the binding mechanism for both ionic species at the oxide interface must be very similar. As we already showed for proton adsorption onto oxides in chapter 3, it is most likely that adsorption of Cd^{2+} ions involves chemical interaction of the species with 'surface hydroxyls' (i.e. $\equiv S\text{-}O^-$, $\equiv S\text{-}OH$ or $\equiv S\text{-}OH_2^+$ groups). Chemical affinity data indicate that forces determining the position of pH^o of an oxide ('electronegativity' of surface hydroxyls), are responsible for the chemical affinity for cadmium ions, too. For both oxides the difference in ΔG^o_{chem} for Cd^{2+} adsorption is reflected by the difference in pH^o of rutile and hematite. This might be a good reason to only consider monodentate binding of Cd^{2+} to the surface, and not, as is frequently suggested in literature (e.g. (7)), association of one metal species with two surface hydroxyls.

6.5 Conclusions

On the basis of experimental results on the adsorption of ions onto rutile and hematite, we could hypothesize as follows. For oxides, with the characteristics of rutile and hematite, i.e. showing mastercurves in their (σ_o, $pH-pH^o$) behavior and temperature congruence of these curves, a similar Cd adsorption behavior is expected. The collected evidence suggests that for these oxides, from the position of pH^o, a reliable prediction of their Cd adsorption isotherms can be made, by calculating ΔG^o_{chem} from our $r_{H/Cd}$ factor and ΔG_{el} from Gouy-Stern theory.

6.6 References

1. Gray, M.J., and Malati, M.A., J. Chem. Tech. Biotechnol. 29, 135, 1979
2. Blaakmeer, J., M.Sci thesis, Wageningen, 1983.

3. Lyklema. J., in "Interactions Solide - Liquide dans les Milieux Poreux" (J.M. Cases, Ed.), Editions Technip, Paris, 1985.
4. Schindler, P.W., in "Adsorption of Inorganics at Solid - Liquid Interfaces" (M.A. Anderson and A.J. Rubin, Eds), Ann Arbor Science, Ann Arbor, 1981.
5. CRC Handbook of Physics and Chemistry, 6nd Edition (R.C. Weast and M.J. Astle, Eds), CRC Press, F-175, 1981.
6. IMSL Library, Houston (TX), 1984.
7. Hohl, H., and Stumm, W., J. Colloid Interface Sci. 55, 281, 1976.

7. SPECIFIC ION ADSORPTION ON OXIDES. SURFACE CHARGE ADJUSTMENT AND PROTON STOICHIOMETRY

7.1 Introduction

Electrical double layers on oxides have a number of common characteristics that are not found on other model systems like silver halides and mercury. One of them is the relatively high charge that can be obtained and another one is that the shapes of surface charge (σ_o) - pH curves at least qualitatively resemble surface charge - surface potential curves as predicted by diffuse double layer theory. Notwithstanding these high surface charges neither are colloidal oxides particularly stable nor do they exhibit particularly high electrokinetic potentials ζ. These two observations suggest, if not prove, that a large fraction of σ_o is compensated by countercharge that is very close to the surface. Various pictures and models developed for the double layer on oxides recognize these features, at least qualitatively. For a quantitative interpretation models are needed. Some double layer properties are easily accounted for, such as the shapes of the σ_o(pH) curves. Others are more difficult, like the computation of ζ as a function of pH and ionic strength.

In the present paper attention is paid to the so-called co-adsorption ratio r_{OH}, that is the ratio between the amount of OH^- ions that co-adsorb with each specifically adsorbing cation if this adsorption takes place at constant pH. For specific adsorption of anions the corresponding factor could be called r_H. This r_{OH} factor has been measured for a number of systems to which we add data for cadmium adsorption on rutile and hematite (1). The r_{OH} factor is an important double layer parameter because it reflects charge compensation processes in the inner part of the double layer, hence its behavior is a suitable criterion for the applicability of various models. Below we shall show that r_{OH} is mainly electrostatically determined and on the basis of a simple double layer model predict values that agree well with experiment (2).

7.1.1 General observations with respect to r_{OH}

In literature, the following trends with respect to r_{OH} are commonly observed:

1) The majority of available r_{OH} values are in the range $1.0 < r_{OH} < 2.0$.

2) Usually, r_{OH} changes with pH for a given metal ion - oxide combination.
3) At fixed pH, for a given oxide, r_{OH} hardly depends on the nature of the adsorbing M^{2+} cation.

Recently, attempts have been made to interpret this OH^- co-adsorption on oxides, essentially following two different approaches. Perona and Leckie (3) derived a relationship, based on interfacial thermodynamics, in which r_{OH} is related to changes in bulk activities upon adsoption of the adsorptive and protons or hydroxyl ions at fixed metal adsorption. Although this approach leads to a promising description of their experimental results, it is -by its very principle- incapable to explain why OH^- co-adsorption is omnipresent in the systems under consideration.

An alternative stems from the field of 'surface complexation'. This school of thought considers observed base consumptions in pH-static adsorption studies as a resultant of the formation of surface complexes in a particular ratio. For example, Schindler (2) explains the proton stoichiometry of an adsorption reaction as resulting form a certain ratio between two surface reactions:

$$\equiv S\text{-}OH + M^{2+} \rightleftharpoons \equiv S\text{-}O\text{-}M^{+} + H^{+}$$

and

$$\begin{matrix} \equiv S\text{-}OH \\ \equiv S\text{-}OH \end{matrix} + M^{2+} \rightleftharpoons \begin{matrix} \equiv S\text{-}O \\ \equiv S\text{-}O \end{matrix}\!\!\diagdown\!\!\diagup M + 2H^{+}$$

The symbol $\equiv S\text{-}OH$ is used to indicate a titratable group in the surface.
This approach, in fact, accepts a certain proton stoichiometry as an experimental fact, but does not offer a reliable prediction for the magnitude of, or trends in, r_{OH}.

For sake of completeness, studies in which the preferential adsorption of metal hydroxo complexes of specified composition is considered as the cause of net OH^- co-adsorption should also be mentioned. In some cases this reasoning works well, although when the nature of the metal ion or the solution pH are such that hydroxo species are virtually absent, this approach is unable to explain observed co-adsorptions.

In the present paper, a new interpretation is presented that accounts for most trends observed so far. The backbone of our approach is that the high inner layer capacitances imply almost complete charge neutralization in that layer, which in turn, sets definite laws to the extent to which specific cation adsorption is accompanied by co-adsorption of hydroxyls or expulsion of protons. Considering the fact that the inner layer capacitances are very high, it does not matter all that much which model is chosen for the distribution of ions in that layer and therefore we choose for the relatively simple Gouy - Stern theory with all specifically adsorbed metal ions in the Stern plane, of which the potential is identified as the diffuse double layer potential ψ_d. In other words, the outer Helmholtz layer is considered part of the diffuse layer and the inner layer is charge-free; it has a high capacitance C_s.

7.2 Surface charge adjustment

7.2.1 Theoretical considerations

In one of our previous studies on the surface charge - pH relation for rutile and hematite as a function of temperature, we concluded that these oxides most likely exhibit (pseudo-) Nernstian characteristics (1). In fact, for a strongly related oxide, RuO_2 (4), Nernst response has been independently proven (5).
Accepting Nernst behavior as a fact for these oxides, it follows that

$$\psi_o = \frac{RT}{F} (pH^o - pH) = - \frac{RT}{F} \Delta pH \qquad [7.1]$$

where ψ_o is the potential of the interior of the solid with respect to the bulk of the solution, pH^o is the point of zero charge of the particular oxide and R,T and F have their usual meaning.

The potential decay around a particle with distance r is given by the Poisson equation

$$\nabla^2 \psi(r) = - \frac{\rho}{\varepsilon \varepsilon_o} \qquad [7.2]$$

where $\psi(r)$ is the potential at distance r from the surface, ρ is the space charge density and $\varepsilon\varepsilon_o$ is the dielectric permittivity.

The charge on the oxides surface is defined by

$$\sigma_o = F(\Gamma_{H^+} - \Gamma_{OH^-}) \qquad [7.3]$$

According to our interpretation, the surface charge is located at the solid phase boundary where the potential assumes its Nernst value.
In the charge free layer near the surface, where $\rho = 0$, the potential drop simply follows from

$$\nabla^2\psi(r) = 0, \qquad 0<r<\delta \qquad [7.4]$$

where δ is the thickness of this layer. We shall call the capacitance of this inner layer C_s.
In the diffuse part of the double layer ($r>\delta$), the potential decay is found by substituting in Eq.[7.2] Boltzmann terms for all ionic species present, yielding the Poisson - Boltzmann equation

$$\nabla^2\psi(r) = -\frac{e}{\varepsilon\varepsilon_o}\sum_i z_i n_i \exp(z_i e\ \psi(r)/kT), \qquad \delta<r<\infty \qquad [7.5]$$

where n_i and z_i are the number and valency of ion i, respectively, e is the unit of charge and k is the Boltzmann constant.
In Eq.[7.5], ε in the diffuse region is assumed to be constant and equal to its bulk value.
Eqs [7.4] and [7.5] can be solved under the constraint that both $\psi(r)$ and $d\psi(r)/dr$ vanish in the bulk solution ($r\to\infty$), and the charge density at the Stern plane, σ_s, is known, according to

$$\sigma_s = zF\Gamma_{M^{z+}} \qquad [7.6]$$

with $\Gamma_{M^{z+}}$ being the amount of specifically adsorbed multivalent metal ions.
In the computations two approximations are usually taken into account:

1) All metal ions are assumed to be adsorbed as M^{z+}; adsorption of hydroxo complexes, if any, has been ignored.
2) Contributions of metal ions to the diffuse part of counter charge is not taken into account.

Point 2) is motivated by the fact that the concentration of carrier (1-1) electrolyte is relatively high, and M^{z+} adsorption is of the high-affinity

type taking place almost exclusively in the Stern plane. However, in comparison of experimental Cd adsorption results with model calculations, a more precise analysis can be presented because $\Gamma_{Cd}2+$ is known in our experiments.

The applicability of Eq.[7.1] to oxides implies that specific adsorption of ions at fixed pH, must result in adjustment of the surface charge, σ_o, in such a way as to largely compensate the specifically adsorbed charge, in order to maintain a Nernstian surface potential.

Values for r_{OH} can then be calculated from the difference in surface charge densities, with ($\sigma_{o,M}z+$) and without (σ_o) specific adsorption, at a certain pH

$$\Delta\sigma_{ads} = \sigma_{o,M^{z+}} - \sigma_o \qquad [7.7]$$

When the charge compensation $\Delta\sigma_{ads}$ is expressed in terms of co-adsorption of OH^-, a theoretical value for r_{OH} is found according to

$$r_{OH} = z \frac{\Delta\sigma_{ads}}{\sigma_s} = z \frac{\Delta\sigma_s}{F\Gamma_M z+} \qquad [7.8]$$

where z is the valency of the cation.
For specific adsorption of anions (valency z-) the corresponding equation reads

$$r_H = z \frac{\Delta\sigma_{ads}}{F\Gamma_A z-} \qquad [7.8a]$$

These relations are restricted to the case of strong specific adsorption. The opposite case of purely non-specific, diffuse layer adsorption will be briefly addressed at the end of the following section.

7.2.2 Model calculations

Calculations were performed using a FORTRAN '77 computer program based on Eqs [7.1] to [7.8] for the case of specific adsorption of bivalent cations. Solutions of the differential equations [7.4] and [7.5] were obtained by numerical integration according to the Runge-Kutta method, using IMSL subroutines (6). In the following calculations, the supporting electrolyte was taken to be an indifferent (1-1) salt (say: KNO_3). The inner layer capaci-

tance C_s was usually, more or less arbitrarily, set at the value of 440 $\mu F/cm^2$, typically high for oxides. However, later we shall give some examples for low C_s.

In Fig.7.1 the consequences of the choice of C_s on r_{OH} are illustrated. Values for r_{OH} were calculated in the point of zero charge for low levels of M^{2+} adsorption. In 0.02 M indifferent (1-1) electrolyte, r_{OH} first strongly increases with increasing C_s. At high values for C_s, r_{OH} approaches a value of 2.0. Physically this can be understood as follows. When C_s becomes so high that the distinction between the surface- and Stern plane charge vanishes, all charge is located at the surface and the charge may rise to infinitely high values and each adsorbed cation is compensated by two OH^-'s. This figure clearly illustrates that for our purpose, the actual choice of C_s only slightly influences the extent of surface charge adjustment, provided it is high.

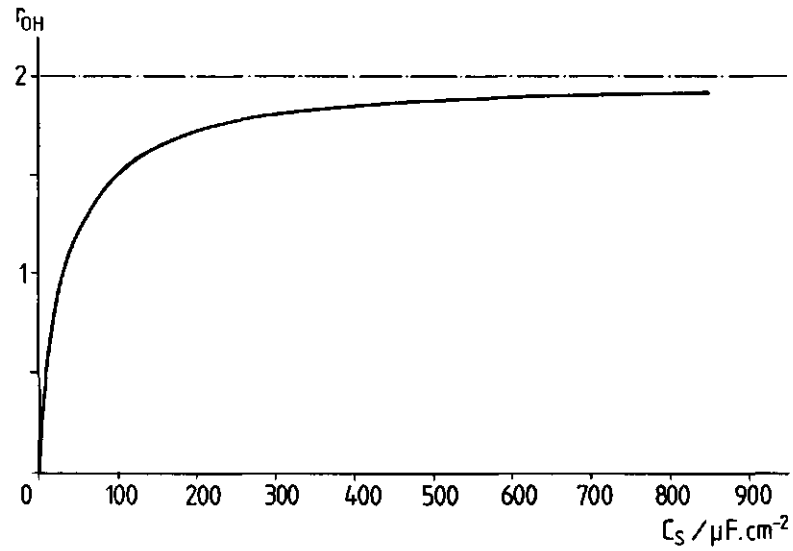

Fig.7.1 Influence of the inner layer capacitance on r_{OH}. Values for r_{OH} calculated in the point of zero charge (ΔpH=0), for low specific adsorption levels. Electrolyte: 0.02 M (1-1). Temperature: 20 °C.

In Fig.7.2 the influence of the Stern charge (Γ_{M2+}) on r_{OH} is given for a moderately high indifferent electrolyte concentration (0.02 M) at room temperature. From this figure it follows that $r_{OH}(\Delta pH)$ is symmetrical around its maximum. For low Stern charges, r_{OH} reaches its maximum around the point of zero charge. For the case of low Γ_{M2+} it can be easily shown

that in the point of zero charge (ΔpH=0), r_{OH} is given by

$$r_{OH} = \frac{2}{\varepsilon\kappa\delta/\varepsilon_s + 1} \qquad [7.9]$$

where κ is the reciprocal double layer thickness.

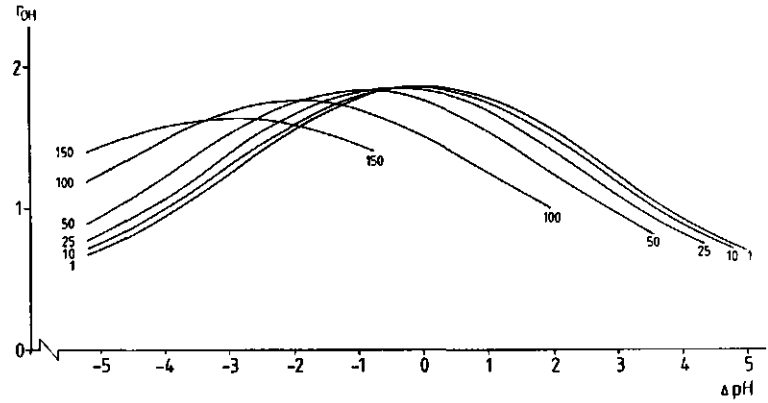

Fig.7.2 OH^- co-adsorption ratio, r_{OH}, as a function of ΔpH for varying amounts of specifically adsorbed charge. σ_s ($\mu C/cm^2$) is indicated. Inner layer capacitance 440 $\mu F/cm^2$. Electrolyte: 0.02 M (1-1). Temperature: 20 °C.

Two interesting limiting values for r_{OH} follow from Eq.[7.9]: at sufficiently low supporting electrolyte concentration (κ→0), r_{OH} reaches its maximum at a value of 2, and when the C_s becomes very low ($\delta/\varepsilon_s \to \infty$), r_{OH} approximates zero. The physical meaning of the former observations is that if there is no indifferent electrolyte to participate at the screening of the specifically adsorbed charge, the latter must be entirely compensated for by adjustment of σ_o. The fast decrease of r_{OH} with vanishing C_s follows from the fact that now the potential drop mainly takes place in the inner layer and therefore specific adsorption does not substantially influence the surface charge.

With increasing cation adsorption a shift of the curves in Fig.7.2 towards lower values of pH is observed. Under the conditions of Fig.7.2, r_{OH} maximally attains a value of about 1.8. At high Stern charges the position of this maximum is found to shift to the acid region, and its value to decrease to about 1.6. The figure shows that, for a given oxide, r_{OH} is a function of both pH and $\Gamma_M{}^{2+}$, as has already been stated before (7) on the basis of experimental results. It is interesting to note that adsorption of M^{2+} onto an oxide results in a charge adjustment that depends on ($pH-pH^o$).

Therefore, r_{OH} varies in magnitude with ΔpH. As far as we are aware, this is the first time that it is noted that ΔpH, rather than pH, is the leading parameter controlling the 'proton stoichiometry'.

The influence of the indifferent electrolyte concentration is illustrated in Fig.7.3. The main trend is that, under otherwise identical circumstances, r_{OH} approaches the limiting value of 2.0, whereas this maximum decreases to 1.6 in 0.2 M 1-1 electrolyte, in accordance with the trends predicted by Eq.[7.9]. Physically this implies that at low electrolyte levels the compensation of σ_S is due to H^+/OH^- mainly, whereas at higher electrolyte concentrations the adsorbed charge is more effectively screened by indifferent ions which can do part of the screening. One should note that in comparison of experimental results with model calculations at low supporting electrolyte concentrations, the actual M^{2+} isotherm substantially influences the shape of the curve. In this case, already at low $c_{M^{2+}}$, there is a contribution of M^{2+} ions to the diffuse counter charge.

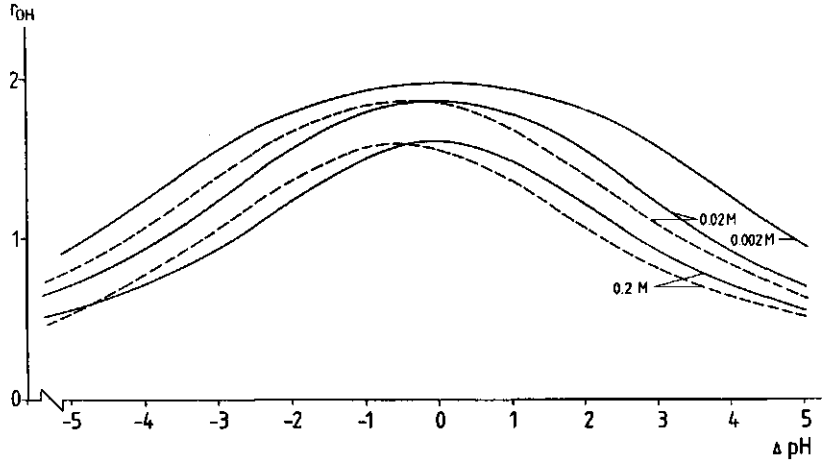

Fig.7.3 Influence of the concentration 1-1 electrolyte on r_{OH} as a function of ΔpH. C_s = 440 μF/cm². Temperature: 20 °C. ——— : σ_s = 1 μC/cm², - - - - - : σ_s = 25 μC/cm².

In Fig.7.4 attention is paid to the influence of temperature on the charge adjustment. It is seen that in the temperature range studied, hardly detectable changes in r_{OH} with T occur. This finding supports our conclusion that the screening, which determines r_{OH} is primarily of an electrostatic nature.

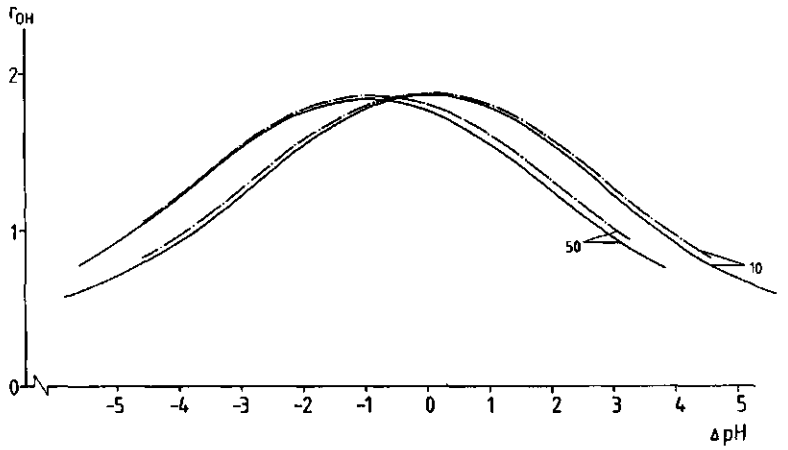

Fig.7.4 Temperature influence on the theoretical $r_{OH}(\Delta pH)$ relation at σ_{ads} = 10 and 50 $\mu C/cm^2$. C_s = 440 $\mu F/cm^2$.
Electrolyte: 0.02 M (1-1). ——— : 20 °C, - - - - - : 60 °C.

Reduction of the value of the inner layer capacitance, e.g. to values that are found to be more representative for AgI or Hg (ca. 30 $\mu F/cm^2$; (8)), dramatically changes the picture (Fig.7.5). In this case, already at relatively low specific adsorption levels, the maximum in $r_{OH}(\Delta pH)$ would strongly shift towards lower pH, whereas absolute values of r_{OH} are small (< 1.0) as compared to the high capacitance case. This result is in agree-

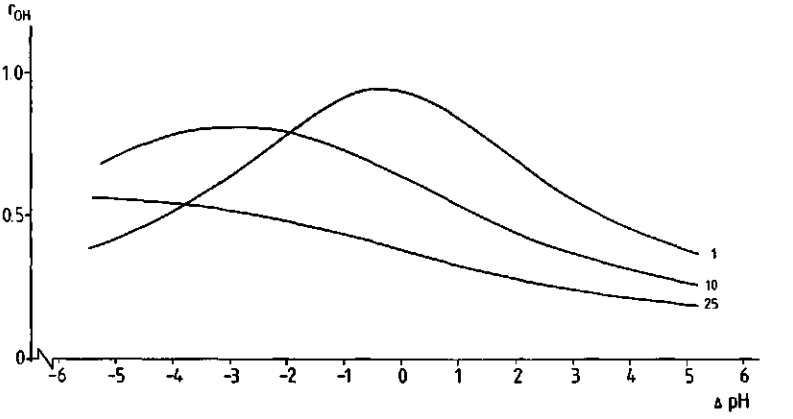

Fig.7.5 $r_{OH}(\Delta pH)$ for σ_s = 1, 10 or 25 $\mu C/cm^2$ at an inner layer capacitance of 30 $\mu F/cm^2$. Electrolyte: 0.02 M (1-1). Temperature : 20 °C.

ment with Eq.[7.9]: the lower C_s, the lower the maximum in $r_{OH}(\Delta pH)$. The experimental observation that co-adsorption ratios for the adsorption of M^{2+} ions onto oxides usually are in the range $1.5<r_{OH}<2.0$, is in our picture consistent with the fact that oxide surfaces should be considered as being 'high capacitance'.

All numerical results obtained so far, have been calculated for flat double layers. Calculations for other particle geometries, have also been performed. However, for spherical and cylindrical particles, using size parameters corresponding to a surface area of approximately 50 m^2/g, hardly any influence on $r_{OH}(\Delta pH)$ could be observed.

For the extreme situation where the M^{2+} ion does not show any specific interaction with the interface, $r_{OH}(\Delta pH)$ as a function of the concentration of both (1-1) and (2-1) electrolytes at 20 °C is given in Fig.7.6. Here only at $pH>pH^o$ a co-adsorption of OH^- is observed. This situation is typical for a purely diffuse double layer in which r_{OH} is expected to increase along an individual 'isotherm' and where r_{OH} is very sensitive to the indifferent electrolyte concentration. As expected, the difference between curves at different $c_{M}2+$ diminishes with increasing (1-1) electrolyte content.

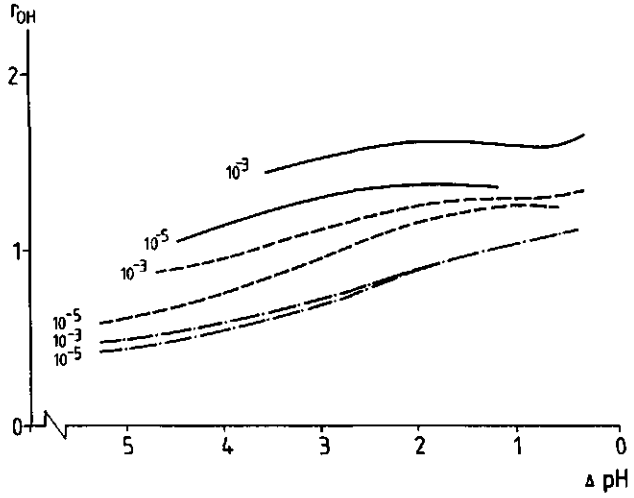

Fig.7.6 OH^- co-adsorption for purely diffuse M^{2+} adsorption at differente concentrations (1-1) electrolyte. $c_{M}2+ = 10^{-5}$ and 10^{-3} M. C_s = 440 μF/cm².
——— : 0.002 M (1-1)
- - - - : 0.02 M (1-1)
-·-·-·- : 0.2 M (1-1).

7.3. Comparison with experimental observations

In literature only a limited number of studies can be found in which 'proton stoichiometries' of metal ion adsorption onto oxides have been explicitely determined. A critical collection of these data has been given by Schindler (2). The applicability of our theory to experimental data depends on the characteristics of the oxides. Nernst response of the surface potential on pH is one of the main prerequisites. For most of the (oxihydr)oxides described in literature, Nernst behavior has not (yet) been verified. Therefore, the comparison of experimental proton stoichiometries with theory remains somewhat limited. In fact, for α-Fe_2O_3, TiO_2 (,Al_2O_3) and RuO_2 evidence for a Nernstian $\psi_o(\Delta pH)$ relation is available (4).

As has been illustrated in a preceding section, in our theory ΔpH is one of the main parameters for the OH^- co-adsorption process. Therefore, in Table 7.1 points of zero charge of the oxides of interest are also included, together with concentration and nature of the supporting electrolyte.

From Fig.7.7, support for our theory is gained from the fact that the majority of literature data is in rather close agreement with theoretical predictions, thus suggesting that for most of the (oxihydr)oxides a Nernstian surface charge - pH relation is to be expected.

As the theory presented, is only based on characteristics of the adsorbent, it should mutatis mutandis be applicable to anion adsorption onto insoluble oxides as well. In this case, a co-adsorption of protons is expected, as was indeed observed a.o. by Van Riemsdijk and Lyklema (14) for the adsorption of phosphate onto gibbsite ($Al(OH)_3$). Depending on the total P concentration, they report a proton co-adsorption ratio of 0.8 to 1.0 H^+ adsorbed/P adsorbed at pH 5.0. Assuming that HPO_4^{2-} is the adsorbing species and realizing that at pH 5, $H_2PO_4^-$ is by far the most abundant P species in solution whereas pH^o for gibbsite is $\sim$ 9, this result does not fit too well into the general picture. Given the uncertainties about the phosphate adsorption process, verification of the surface charge adjustment theory for anions must await more detailed measurements of the co-adsorption factor.

Fig.7.7 demonstrates that the main trends in literature values for co-adsorption phenomena on insoluble inorganic oxides are well described by the charge adjustment theory. As far as we know, this is the first attempt to quantify and explain co-adsorption phenomena within the basis of a general framework.

Table 7.1. Proton stoichiometry of specific ion adsorption.

'oxide'	pH^o	M^{z+}	electrolyte	pH	r_{OH}	Ref.
α-Al_2O_3	8.3	Pb^{2+}	0.1 M $NaClO_4$	4	1.0	9*)
				5	1.3	
				6	1.5	
				7	1.7	
δ-MnO_2	~2**)	Co^{2+}	-	4	2.1	10
		Zn^{2+}	-	4	2.1	
'FeOOH	8.5	Pb^{2+}	-	6	1.6	11
			-	5	1.2	
'MnOOH'	~3	Pb^{2+}	0.02 M $NaNO_3$	6	1.4	12
		Cd^{2+}		6	1.3	
		Zn^{2+}		6	1.1	
SiO_2	~2.5**)	Zn^{2+}	?	6	1.2	13
		Co^{2+}		6.3	1.3	
		Co^{2+}		7.3	1.2	
		Ni^{2+}		6.3-6.8	1.4	
		Mn^{2+}		6.4-7.7	1.2	
α-Fe_2O_3	8.7	Cd^{2+}	0.02 M KNO_3	8.1	1.7	1
				7.6	1.55	
				6.9	1.3	
TiO_2	5.6	Cd^{2+}	0.02 M KNO_3	7.8	1.8	1
				7.0	1.75	
				5.6	1.7	
$Al(OH)_3$	~9**)	$HPO_4^=$	0.1 M KCl	5	~ -1.9	14

*) The dependence of r_{OH} on pH has been determined from the original data in ref. 9

**) pH^o value not reported in original paper.

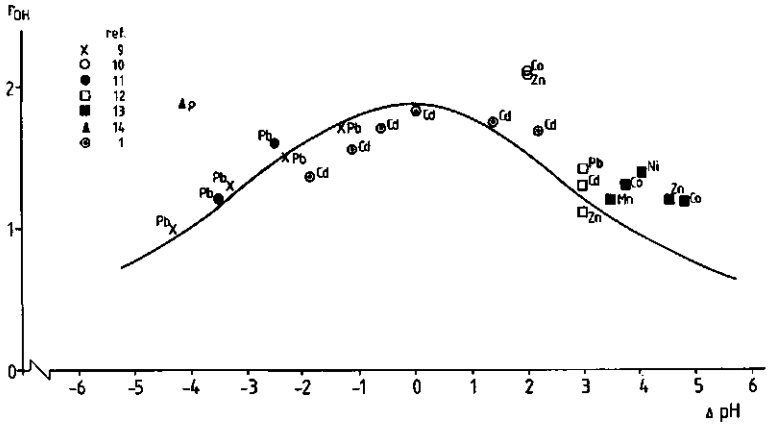

Fig.7.7 OH^- co-adsorption for the specific ion adsorption of bivalent metal ions onto insoluble inorganic oxides. ——— : theoretical curve for C_s = 440 $\mu F/cm^2$, 0.02 M (1-1) electrolyte, T = 20 °C and σ_s = 10 $\mu C/cm^2$.

A case study: adsorption of Cd onto rutile and hematite

Detailed information is now available on the adsorption of cadmium ions onto rutile and hematite, including concomitant OH^- adsorption, which we measured as a function of pH, temperature, salt concentration and some other variables. The procedure was based on a potentiometric pH-stat technique. Experimental details can be found in ref.(1).

In Fig.7.8 experimentally observed OH^- co-adsorption ratios for the adsorption of cadmium ions onto rutile and hematite are compared with the theoretical values as a function of ΔpH. Although the amounts of cadmium adsorbed differ considerable for both substrates in the pH range under consideration, it is seen that r_{OH} closely follows the general characteristics predicted by the charge adjustment theory.

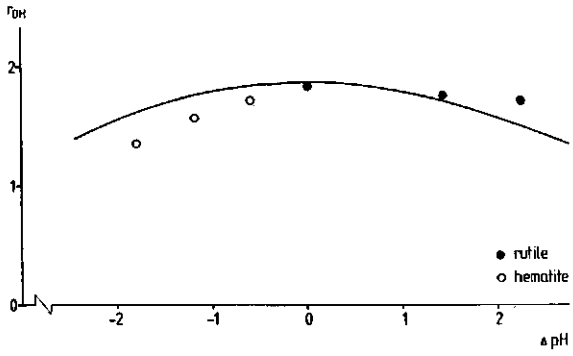

Fig.7.8 Co-adsorption of OH^- for the adsorption of Cd^{2+} ions onto rutile and hematite as a function of ΔpH. Electrolyte : 0.02 M KNO_3. Temperature : 20 °C.

The influence of indifferent electrolyte concentration on r_{OH} has been experimentally determined for the adsorption of Cd^{2+} onto rutile. For two values of pH, 7.83 and 7.00, corresponding to $\Delta pH = 2.26$ and 1.43 respectively, experimental proton stoichiometries are compared with the theoretically expected ones in Fig.7.9. For both pH values the trend in r_{OH} is well described by the theoretical relation: r_{OH} decreases modestly with increasing salt concentration. For low ΔpH, the agreement between theory and experiment is satisfactory. The theory seems to slightly underestimate the dependence of r_{OH} on ΔpH at both electrolyte levels, however.

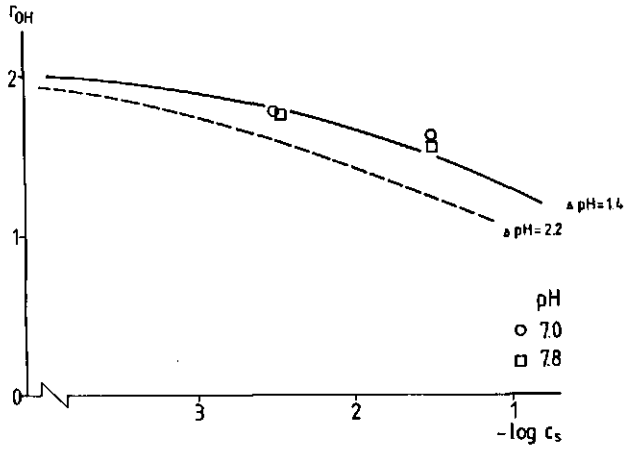

Fig.7.9 Influence of KNO_3 concentration on the OH^- co-adsorption ratio for Cd^{2+} ions onto rutile at 20 °C.

As concluded before, there was no significant influence of the temperature ($5<T<60$ °C) (1).

In Fig.7.10 the influence of Γ_{Cd} on r_{OH} is given for the adsorption onto rutile at several pH values. In the calculations the actual adsorption isotherms, given in chapter 6, were used to determine the total ionic strength and double layer composition. On negatively charged surfaces, good agreement between experiment and theory is obtained. At lower values of pH, the experimentally observed dependence of Γ_{Cd} is somewhat underestimated. Whether this effect is real is hard to say: at these pH values Cd adsorption levels are relatively low, and therefore, especially at higher c_{Cd} errors in Γ_{Cd} strongly increase with decreasing pH.

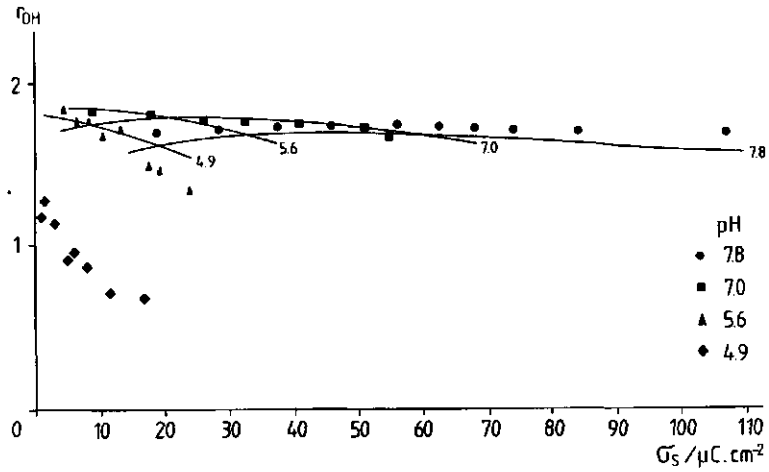

Fig.7.10 Co-adsorption of OH^- onto rutile, for the adsorption of Cd^{2+} ions, as a function of σ_{Cd} for some pH values. Electrolyte: 0.02 M KNO_3. C_s = 440 μF/cm^2. Temperature : 20 °C.

7.4 Conclusions

The proposed theory on co-adsorption phenomena accompanying specific (cat)ion adsorption onto inorganic oxides, is essentially non-specific, based on generally observed characteristics of the oxide-solution interface only. The major premises for the applicability of the theory are:

1) Strong charge accumulation near the surface of the oxide.
2) The main material property governing the charge dependence of r_{OH} is the difference between the working pH and the point of zero charge.
3) The surface potential(pH) relation obeys Nernst's law.

Within this theoretical framework, the magnitudes of co-adsorption for a variety of cations on a series of insoluble inorganic oxides are satisfactorily predicted. Moreover, trends observed in OH^- co-adsorption ratios for the specific adsorption of cadmium ions onto rutile and hematite as a fuction of salt concentraton, temperature and pH are reasonably well described by the theory. In general, the experimentally observed dependence of r_{OH} on the adsorbed amount of cadmium is somewhat underestimated by the theory. Nevertheless, our theory provides a useful tool in predicting co-adsorption phenomena.

From a physical point of view our approach offers new insights into the matter of 'proton stoichiometry', in the sense that there is no need to invoke chemical complexation to account for the experimentally observed trends in r_{OH}. Rather, the purely electrostatic nature of the charge compensation around the inner layer resembles ion condensation, as observed with polyelectrolytes (15).

7.5 References

1. Fokkink, L.G.J., de Keizer, A. and Lyklema, J., in preparation./this thesis, chapter 6.
2. Schindler, P.W., in "Adsorption of Inorganics at Solid-Liquid Interfaces", (M.A. Anderson and A.J. Rubin, Eds), Ann Arbor Science, Ann Arbor, 1981.
3. Perona, M.J. and Leckie, J.O., J. Colloid Interface Sci. 106, 64, 1985.
4. Fokkink, L.G.J., de Keizer, A., Kleijn, J.M., and Lyklema, J., J. Electroanal. Chem. 208, 401, 1986.
5. Siviglia, P., Daghetti, A., and Trasatti, S., Colloids Surf. 7, 15, 1983.
6. IMSL Library, Houston (TX), 1984.
7. Hayes, K.F., and Leckie, J.O., submitted to J. Colloid Interface Sci.
8. Bijsterbosch, B.H., and Lyklema, J., Adv. Colloid Interface Sci. 9, 147, 1978.
9. Hohl, H., and Stumm, W., J. Colloid Interface Sci. 55, 281, 1976.
10. Loganathan, P., and Burau, R.G., Geochim. Cosmochim. Acta 37, 1277, 1973.
11. Gadde, R.R., and Laitinen, H.A., Environ. Lett. 5, 223, 1973.
12. Gadde, R.R., and Laitinen, H.A., Anal. Chem. 46, 2022, 1974.
13. Vydra, F., and Galba, J., Coll. Czech. Chem. 34, 3471, 1969.
14. Van Riemsdijk, W.H., and Lyklema, J., J. Colloid Interface Sci. 76, 55, 1980.
15. Manning, G.S., Quart. Rev. Biophys. 11, 179, 1978.

8. MICROCALORIMETRY OF ION ADSORPTION. ADSORPTION ENTHALPY OF CADMIUM IN THE RUTILE-KNO_3 SYSTEM

8.1 Introduction

In our study on the adsorption of cadmium ions onto insoluble oxides, thermodynamic parameters for the adsorptive processes could be obtained (1). It has already been shown in chapter 4 that microcalorimetry can contribute to the understanding of the double layer formation on oxides (2). It is the main aim of this chapter to measure and discuss the enthalpy of cadmium adsorption in these systems.

If in an equilibrated oxide suspension, containing cadmium ions, the pH is changed by - say - the addition of base, the following processes will take place:

1) The surface charge density on the oxide becomes more negative (through dissociation of surface groups).
2) More cadmium ions will adsorb.
3) Concomitant proton release/OH^- co-adsorption results.

Provided all processes are reversible on the time scale of observation, exactly the opposite happens if acid is added to the suspension.

In measuring the heat effect of the abovementioned base addition, the sum of the enthalpies of the three processes is obtained (apart from dilution and neutralization contributions which can be readily accounted for). Therefore, interpretation of calorimetric measurements in the oxide - cadmium system requires a (model - based) picture of the three contributing processes. From microcalorimetric acid/base titrations on rutile and hematite in the absence of specific adsorption, heats of surface charge formation are already available (2). Using these data, the enthalpic contributions associated with the change in surface charge density can be accounted for. At issue is now the sole effect of cadmium adsorption together with induced co-adsorption.

From a phenomenological point of view it is impossible to decide whether OH^- co-adsorption is due to changes in surface charge or to co-adsorption of hydroxyl ions accompanying cadmium adsorption. The matter of OH^- co-adsorption has already been discussed in some detail (3). From this study

we concluded that the measured OH^- co-adsorptions can be totally ascribed to the adjustment of the surface charge to the specifically adsorbed charge of the Cd^{2+} ions. Keeping this result in mind, it is concluded that points 1) and 3) above virtually describe the same physical process, i.e. association/dissociation of surface groups. Therefore it is our opinion that experimentally observed base consumptions in Cd^{2+} adsorption experiments (again apart from bulk neutralization), must be ascribed to association of protons with, or dissociation of protons from the surface groups. Accordingly, the heat of adsorption of the Cd^{2+} ions as such follows from the total heats measured in a titration experiment by 'correcting' them for the total change in surface charge. Carrying out this correction is simple, as we found the adsorption enthalpy of protons onto insoluble oxides to be independent of the surface charge density (2).

In this chapter the experimental determination of enthalpies of adsorption of Cd^{2+} ions onto rutile and their interpretation will be discussed in some detail.

8.2 Experimental

All chemicals used were reagent grade or better. Titrants were 0.2 M HNO_3 and KOH, prepared from Merck Titrisol standard solutions. Water was prepurified as described in chapter 2. The rutile was taken from the same batch as used in the preceding chapters. The experimental procedure and the equipment used in the calorimetric measurements were the same as previously described (2). In all experiments the supporting electrolyte was 0.2 M KNO_3. Measurements were performed on batches of ca. 2 grams of the oxide, suspended in 50 mls of electrolyte solution. In principle, the calorimetric measurements were performed as follows. A certain volume of $Cd(NO_3)_2$ stock solution was added to the oxide suspension (final cadmium concentration in the suspension, Cd_{tot} = 5.10^{-3}, 2.10^{-2}, 4.10^{-2} or 8.10^{-2} M, respectively) at low pH, and the suspension was equilibrated overnight while being stirred. After equilibration, the pH was between 4 and 4.5, depending on Cd_{tot}. Then the pH was raised by the stepwise addition of small aliquots of 0.2 M KOH from an automatic buret (Metrohm 655 Dosimat), and the concomitant heat production was measured in the calorimeter. After each addition, the pH of the suspension was determined using the procedure described in ref.(2). When the pH of the suspension had reached a value of ca. 7.3, the titration

was stopped and the suspension was stirred overnight. High pH values, with the concomitant risk of bulk precipitation of cadmium and CO_2 contamination of the solutions were thus avoided. The next day a microcalorimetric acid titration was done. The pH was lowered by the stepwise addition of 0.2 M HNO_3.

In all cases, a separate experiment was performed to obtain the (pH,Γ_{Cd}) relation under exactly the same conditions as in the calorimetric titrations. These experiments were performed batchwise: in 100 ml Schott Duran bottles, 2 grams of rutile were suspended in 50 mls 0.2 KNO_3 solution of pH~4, containing $Cd(NO_3)_2$ in the same concentration as used in the corresponding calorimetric experiment. After equilibration of a series of these suspensions by shaking them overnight, to each of the bottles a variable volume of 0.2 M KOH was added, in such a way as to cover the whole range of volumes added in the corresponding thermometric titration. After 16 hours of shaking the pH of the suspensions was measured and a small aliquot of the supernatant was withdrawn for the determination of c_{Cd} (differential pulse polarography). From the equilibrium values of pH and c_{Cd}, the amount of Cd^{2+} and OH^- adsorbed were calculated (2).

8.3 Results

The experimental cadmium adsorption is given in Fig.8.1 for different values of Cd_{tot}. For all but the lowest total cadmium concentration, Γ_{Cd} increases steeply and continuously with increasing pH. The sigmoid shape of the (Γ_{Cd},c_{Cd}) relation at Cd_{tot} = 5.10-3 M is due to depletion of the solution at pH $\gtrsim$ 6. Even though at the higher Cd_{tot} values the total electrolyte concentration changes drastically with pH through adsorption, the amount of Cd^{2+} ions adsorbed in the diffuse layer in all cases is negligible. Due to co-adsorption of OH^- ions (ca. 1.7 OH^-/Cd^{2+} adsorbed (3)), only at high values of pH the overall surface charge becomes slightly negative in some cases. In this situation most of the Cd^{2+} present in the system is specifically adsorbed, and therefore the electrolyte level and the diffuse double layer composition are mainly determined by the KNO_3.

In order to check the reversibility of the cadmium adsorption, an analogous batchwise experiment was performed by adding small volumes of nitric acid to cadmium containing rutile suspensions, initially equilibrated at pH = 7.3. In this case, too, Γ_{Cd} and Γ_{OH} were measured after 16 hours of

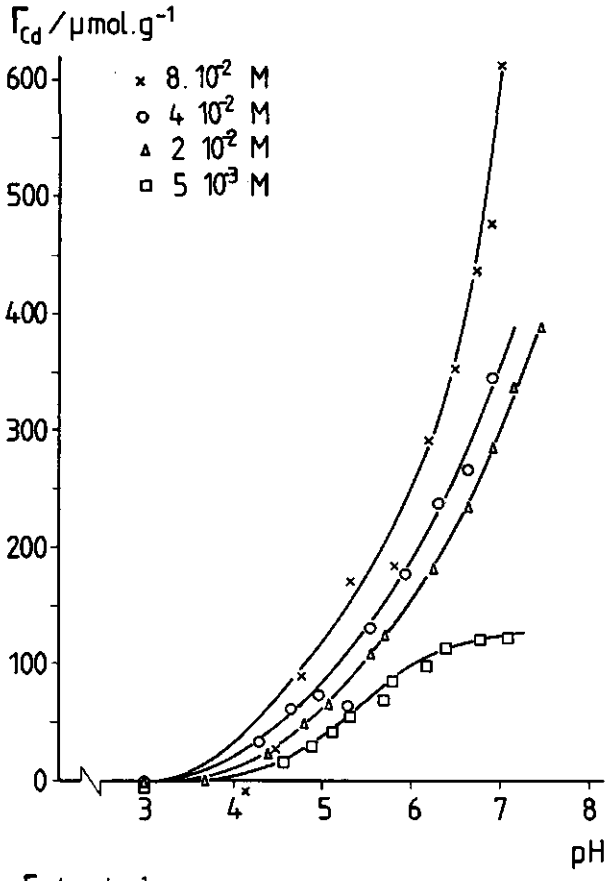

Fig.8.1 Amount of cadmium adsorbed on rutile as a function of pH at several total cadmium concentrations.
Electrolyte: 0.2 M KNO_3. Temperature: 20 °C. Suspension concentration: 2.0 g TiO_2 in 50 mls solution.

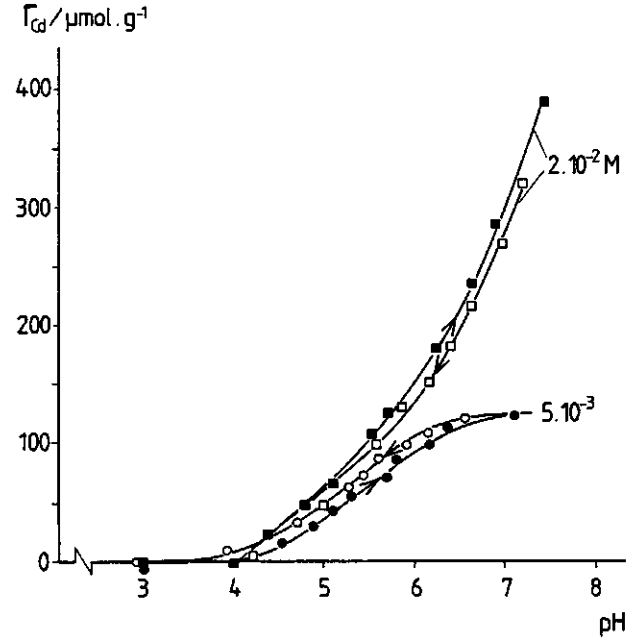

Fig.8.2 Adsorption-desorption of cadmium in rutile suspensions for two indicated concentrations of Cd_{tot}. Solid symbols refer to adsorption, open symbols to desorption. Carrier electrolyte: 0.2 M KNO_3. Temperature: 20 °C. Suspension concentration: 2.0 g TiO_2 per 50 mls solution.

equilibration. Results of the desorption experiments are compared to the corresponding adsorption curves in Fig.8.2. From these results we concluded that under the experimental circumstances only insignificant adsorption/desorption hysteresis occurs.

In our calorimetric cadmium adsorption experiments, the measurable heat production was found to be complete within one minute, whereas during the following ten minutes no additional heats of reaction could be observed. This suggests that cadmium adsorption onto rutile is a quite fast process. Recent observations on the Cd^{2+}-hydrous ferric oxide system (4), however, indicate that adsorption of cadmium ions onto that oxide still increases after contact times of 20 hours and more. If this were the case in our system, microcalorimetric measurements would not be very conclusive. In order to verify our microcalorimetric conclusion that cadmium adsorption onto rutile is much faster than on hydrous ferric oxide, the rate of Cd adsorption on rutile was studied in a batch-wise experiment by the stepwise addition of KOH to a well-equilibrated $Cd(NO_3)_2$-rutile-KNO_3 system and monitoring the Cd concentration. The equilibration period between two successive additions was chosen as ten minutes, 90 minutes and 24 hours, respectively. The concomitant change in surface charge density was determined from the measured pH and theoretical blank corrections (5), and appeared to become constant within ten minutes. A similar experiment was performed in order to assess the rate of desorption: in a suspension equilibrated at high pH, now the pH was lowered by titration with HNO_3. Results of both experiments are given in Fig.8.3. It is clear that in both the adsorption and desorption experiment, Γ_{Cd} only slightly changes after ten minutes. Combined with the fact that the measurable heat production in the calorimetric experiments is complete within one minute, this observation strongly suggests that Cd^{2+} adsorption onto rutile is a fast process. The fact that Dzombak and Morel (4) observed so much longer adsorption times could possibly be ascribed either or both to the following two points.

i) Slow adsorption might be more characteristic for poorly crystalline oxihydroxides than for well-crystallized samples.

ii) The perturbation from equilibrium in their experiments is much larger than in our case, where the pH is only slightly adjusted.

The above rate- and hysteresis experiments encouraged us to measure and interpret microcalorimetric data, using a relatively fast thermometric acid/base titration procedure.

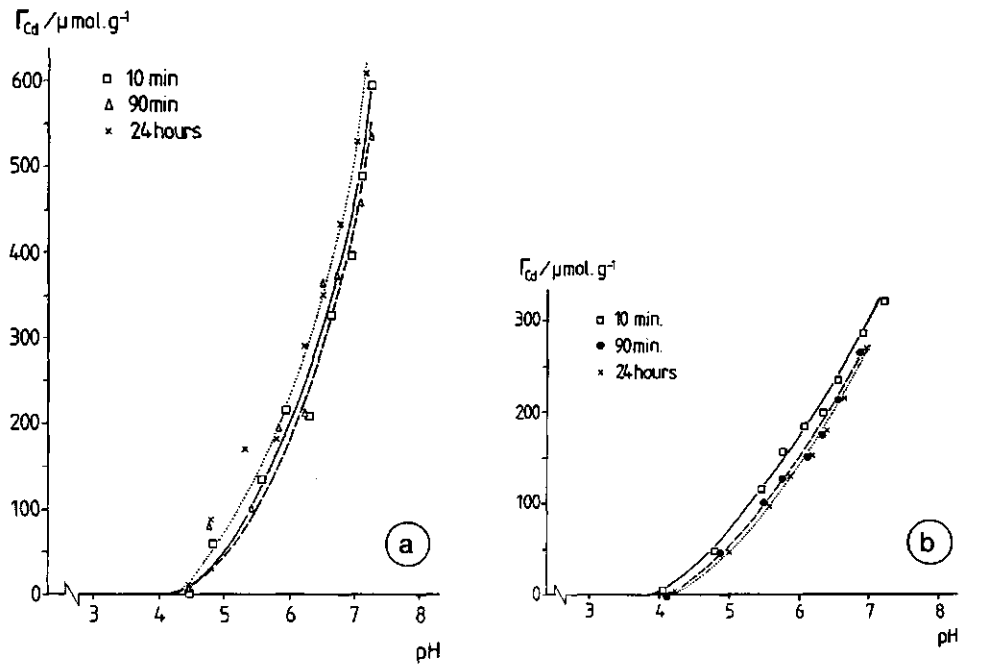

Fig.8.3 Influence of equilibration time between two succesive titrant additions on the adsorption-desorption behavior in the rutile-KNO_3 system in a simulated 'thermometric' acid/base titration. Cd_{tot} concentration is indicated.
Electrolyte: 0.2 M KNO_3. Temperature: 20 °C.
Solids concentration: 2.0 g TiO_2/50 mls.
a. Adsorption. b. Desorption.

Experimentally observed total reaction enthalpies for the adsorption of cadmium ions onto rutile are given as a function of pH for four different total-Cd concentrations in Fig.8.4. Analogous data for the desorption experiments are also presented in the figure. As indicated above, the enthalpies reported in Fig.8.4 are the sums of three (dependent) contributions. The overall heat is almost constant with pH, but depends on the total cadmium concentration in the system and hence on Γ_{Cd}. The slopes of the lines depend on the direction of the titration. On titration of the suspension with base (Cd^{2+} adsorption), OH^- ions are depleted from the solution, whereas acid titration results in desorption of cadmium and depletion of protons. Phenomenologically, depletion of OH^- gives rise to a larger heat effect than does H^+ depletion (2).

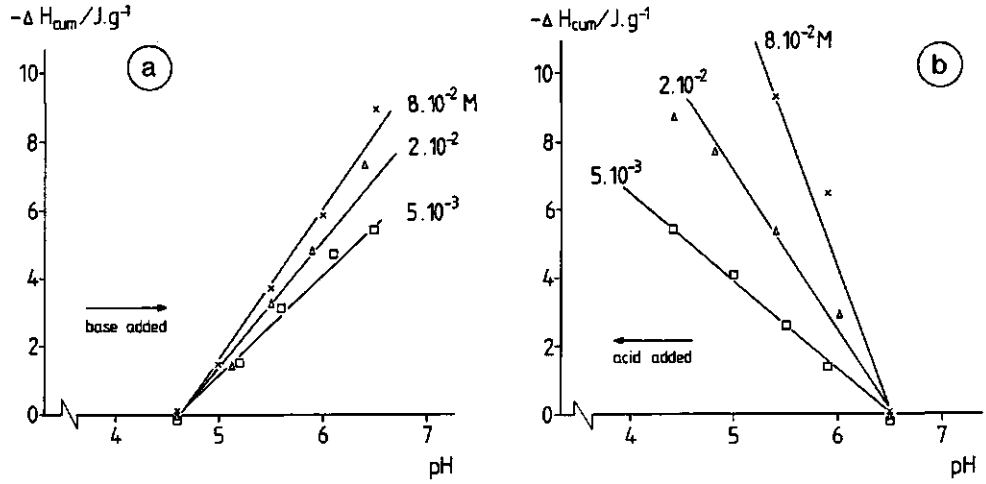

Fig.8.4 Cumulative overall heat of adsorption-desorption of cadmium in the rutile-KNO_3 system as a function of pH for different concentrations of Cd_{tot}. Total cadmium concentration as indicated. Electrolyte: 0.2 M KNO_3. Temperature: 20 °C. Solids concentration: 2.0 g TiO_2/50 mls.
a. Adsorption. b. Desorption.

8.4 Discussion

As stated before, the measured heat effects given in Fig.8.4 apply to the overall cadmium adsorption process. In order to obtain adsorption enthalpies for the cadmium ions as such, the enthalpic contributions due to surface charge adjustment has to be corrected for. In the following elaboration, protons will be considered the only charge determining species for oxides, i.e. it is assumed that on addition of base to an oxide suspension protons desorb (dissociate) from surface groups. The corresponding heats of ad- or desorption of protons have been determined experimentally for rutile in 0.2 M KNO_3 (2). An important conclusion from this study was that the actual heat effects associated with charge formation are independent of the surface charge density and salt concentration. The experimental enthalpy of proton adsorption onto rutile amounts to -20 ± 2 kJ/mol. The mean value (-20 kJ/mol) was used in the following calculations of $\Delta_{ads}H_{Cd}$.

The measured heats were corrected for the total heat of proton desorption in order to yield the net Cd^{2+} adsorption enthalpy. Cumulative enthalpies, ΔH_{cum}, for the adsorption of Cd^{2+} ions onto rutile are plotted in Fig.8.5 as a function of Γ_{Cd}. It follows from the figure that the total cadmium

concentration does not markedly affect the curves, implying that the solution side, i.e. the amount of cadmium species in solution, does not realy influence the energetics of adsorption. Furthermore, $\Delta_{ads}H$ is hardly a function of the adsorbed amount, indicating that lateral interactions (of an enthalpic nature) in the adsorbed phase are small. As the electrolyte

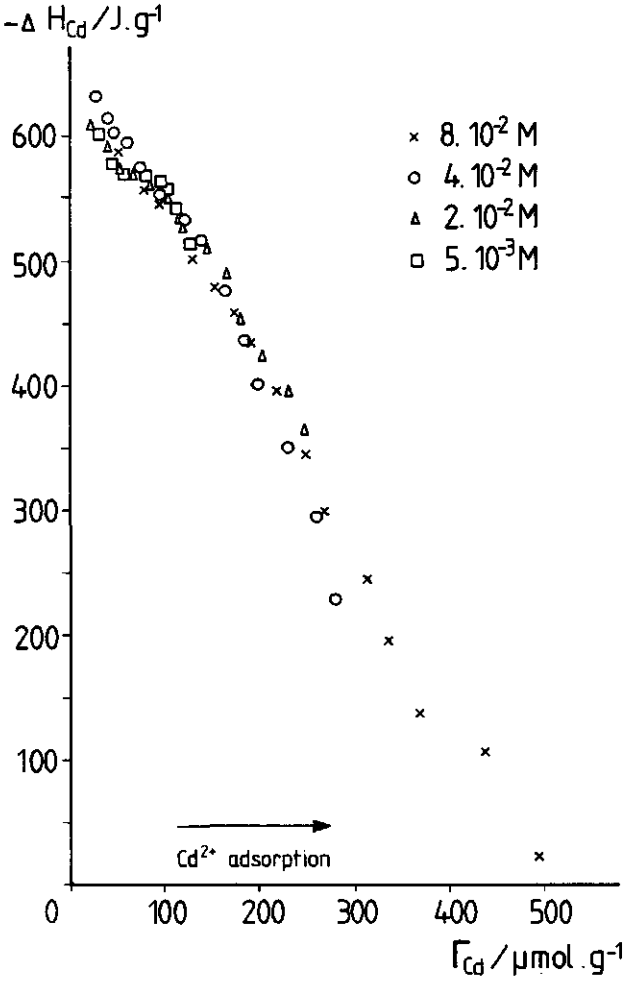

Fig.8.5 Cumulative heat of Cd^{2+} adsorption on rutile as a function of the amount adsorbed at different values of Cd_{tot}. Electrolyte: 0.2 M KNO_3. Temperature: 20 °C. Solids concentration: 2.0 g TiO_2/50 mls.

level in our experiments is rather high, lateral coulombic interactions will be screened. Hence it must be expected that the influence of σ_0 (and thus of pH) on $\Delta_{ads}H$ is small.

The experimental heat of adsorption amounts to ca. +10 ± 4 kJ/mol Cd^{2+} adsorbed. As all experimental uncertainties in the individual contributions

(ΔH_{H+}, $\Delta H_{Cd(OH)x}$) are compounded in this value the experimental error is substantial. For the desorption similar results were obtained ($\Delta_{des}H \sim -10$ kJ/mol).

Notwithstanding the experimental uncertainty of the data, important conclusions may be drawn from this study. It follows that even though Cd^{2+} ions show a pronounced affinity for inorganic oxides in general (cf. (6)), the adsorption of Cd^{2+} onto rutile is endothermic, i.e. from an energetic point of view is unfavorable. This directly implies that the adsorption must be entropy-driven. For the system under consideration here, both the chemical (non-electrostatic) contribution to the Gibbs energy of adsorption ΔG^{o}_{ads} (-26 kJ/mol (chapter 6) and $\Delta_{ads}H$ are now available. From these data it follows that the standard entropy change of Cd^{2+} adsorption onto rutile, ΔS^{o} is of the order of +120 J/mol.K at 20 °C. Comparison of these data with the thermodynamic parameters for the formation of $Cd(OH)^{+}$ complexes in aqueous solutions ($\Delta H \sim -1$ kJ/mol, $\Delta S^{o} \sim 89$ J/mol.K; (1,7)), suggests that the bulk and surface reaction are closely related: both reactions are driven by a gain in entropy. There is a strong indication that in both processes association of Cd^{2+} ions with OH species is involved, leading to a pronounced change in state of hydration of the reactants. The relatively small Cd^{2+} ion is highly hydrated in aqueous solutions. The standard entropy of hydration of cadmium ions amounts to -210 J/mol.K (8). If for sake of simplicity, it is assumed the only changes in hydration are concerned with the Cd^{2+} ion, we can explain our results by assuming that the Cd^{2+} ion on adsorption roughly looses half its hydration shell.

From the above reasoning, one would expect the adsorption of multivalent cations on a particular oxide to increase with increasing entropy of hydration, in the sequence (8)

$$Ba^{2+} \sim Pb^{2+} < Ca^{2+} < Cd^{2+} \sim Mn^{2+} < Cu^{2+} \sim Zn^{2+} \sim Mg^{2+} < Fe^{3+} \sim Al^{3+}$$

Apart from some interesting exceptions (Pb^{2+},Mg^{2+}) that usually adsorb much stronger than expected according to their entropy of hydration, this sequence is roughly confirmed by a variety of adsorption studies (6).

A pronounced analogy between the reaction of Cd^{2+} ions with bulk hydroxyls and the adsorption process of these cations onto rutile is apparent. Energetically Cd-OH bonding in both processes has proven to be an unfavorable

process. Most likely it is the less tightly bound 'outer sphere' water molecules that are liberated in both bulk complex formation and in adsorption, and thus provide the entropical driving force of adsorption. The strongly bound water molecules in the inner coordination sphere of the Cd^{2+} ion may be partly replaced by surface hydroxyls in the adsorption process. The enthalpy of dehydration is largely compensated for by the enthalpy of 'surface complex' formation.

8.5 Conclusions

The fast thermometric titration technique can be successfully applied to determine the enthalpy of adsorption of cadmium ions onto rutile. Additional measurements and thorough insight into the adsorption processes are needed to enable interpretation of the microcalorimetric data in terms of adsorption enthalpies. Adsorption of cadmium ions onto rutile in 0.2 M KNO_3 solutions is an endothermic process, $\Delta_{ads}H$ amounting to ca. +10 kJ/mol. A substantial change in hydration entropy of the Cd^{2+} ion is considered the main driving force in the adsorption process. A pronounced similarity between the formation of $Cd(OH)^{+}$ complexes in aqueous solutions and the adsorption of Cd^{2+} ions at the rutile-solution interface, strongly suggests that on adsorption Cd^{2+} ions associate with 'surface hydroxyls'.

8.6 Acknowledgements

This chapter was written in co-authorship with Miss Ineke Rhebergen, who also did most of the experiments. We wish to express our gratitude for her kind co-operation.
Thanks are also due to Mr. Anton Korteweg for his technical assistance.

8.7 References

1. This thesis, chapters 3,4,6.
2. Fokkink, L.G.J., de Keizer, A., and Lyklema, J., in preparation/this thesis, chapter 4.
3. Fokkink, L.G.J., de Keizer, A., and Lyklema, J., submitted to J. Colloid Interface Sci./this thesis, chapter 7.

4. Dzombak, D.A., and Morel, F.M.M., J. Colloid Interface Sci. 112, 588, 1986.

5. Davies, C.W., "Ion Association", Butterworths, London, 1962.

6. Schindler, P.W., in "Adsorption of Inorganics at Solid-Liquid Interfaces", (M.A. Anderson and A.J. Rubin), Ann Arbor Science, Ann Arbor, 1981.

7. Hunt, J.P., "Metal Ions in Aqueous Solution", W.A. Benjamin, Inc., New York, Amsterdam, 1963.

8. Monk, C.B., "Electrolytic Dissociation", Academic Press, London, New York, 1961.

9. CONCLUDING REMARKS AND SUGGESTIONS FOR FURTHER RESEARCH

9.1 General picture of surface properties of insoluble oxides

The present study added new insights into the properties of insoluble oxide - solution interfaces.

As far as the surface charge characteristics are concerned, we found that - notwithstanding the chemical and crystallographic differences of the oxide lattices - rutile and hematite suspensions show interesting common features. Stated generally, the interfacial region of insoluble oxides could be considered as a densely packed two dimensional array of OH-like species (as has already been noted before by Bolt and van Riemsdijk (1)), effectively shielding most of the properties of the underlying oxide matrix. However, the surface phase on oxides must be 'transparant' for at least one of the lattice characteristics, because it is an experimental fact - confirmed by this study - that the point of zero charge depends on the nature of the oxide. It is logical to presume that electronic properties of the lattice cation, determining the M-O bond strength in the oxide crystal, are also 'felt' by the surface oxygens. From this point of view it is not surprising that the surface groups associated with small, highly charged titanium ions in the rutile lattice are more reactive towards protons than are the surface groups on hematite. Both the position of the point of zero charge and the calorimetrically determined heats of proton adsorption on TiO_2 and α-Fe_2O_3 support this reasoning. Once the system has reached its point of zero charge, the only remaining lattice property of the interface has been 'neutralized' and looked at it from the solution side, the surface phases of the oxides will have become very similar. As expected from the above, surface charge - pH relations for rutile and hematite, provided they are normalized with respect to their p.z.c., are identical within experimental error (2).

Investigations on the influence of temperature revealed another interesting congruence phenomenon with the two oxides. The (σ_o,pH) curves are shifted to the acid region with increasing temperature, but their shapes remain essentially unchanged (3). It has been shown that this behavior is to be expected for mainly diffuse countercharges on Nernstian surfaces. Therefore, two points had to be clarified

i) Why is the counter charge on oxides mainly diffuse?

ii) Why is the surface potential dependent on solution pH according to Nernst's law?

Point i) could possibly be explained as follows: because 'surface hydroxyls' are water-like species (cf. their properties in H^+ and Cd^{2+} adsorption), they can substitute a molecule of hydration water of an 'indifferent' -say- K^+ ion, without real chemical interaction. This would imply an extremely effective screening of the surface charge by counter ions. The ion, however, would still be classified as 'indifferent'.

Point (ii) is more difficult to handle. The crucial question is whether or not non-lattice ions can give rise to a Nernstian potential-pH relation. For regular inorganic oxides as RuO_2, α-Fe_2O_3, Al_2O_3 (4,5), there is experimental evidence for Nernst behavior. The fact that these oxides are electrical conductors might be important for their surface potential - pH characteristics. The site-binding approach has given the constraints for (pseudo-) Nernst characteristics of non-conducting oxidic materials (6). Most of the currently investigated oxides are ionic or metallic conductors, however.

Apart from the fact that the reason why Nernstian response of oxides should apply for the moment remains somewhat obscure, all experimental observations made in this study could be reasonably well explained by assuming this type of ψ_o-pH relation.

From an experimental point of view, the fact that the surface charge is substantially influenced by temperature has not always been recognized in literature. Thermodynamic analyses of pH-static adsorption results as a function of temperature on oxides as if they were obtained at constant surface charge density, must lead to erroneous conclusions.

9.2 Cadmium adsorption on oxides

The cadmium adsorption characteristics obtained in this study are in agreement with the general picture of the oxide-solution interface given above. Cadmium adsorption is a complex process: in all situations, on adsorption of cadmium ions a depletion of OH^- ions from the bulk solution is observed. As has been shown in this thesis (7), OH^- depletion is due to an adjustment of the surface charge to the specifically adsorbed charged entities.

If the process of cadmium adsorption is studied calorimetrically by chang-

ing pH in an oxide-$Cd(NO_3)_2$-KNO_3 system, both on addition of acid and base heat is liberated (8). Even if the heat of neutralization, accompanying the pH change in solution is accounted for, measured reaction enthalpies are exothermic. Two sub-processes contribute to the overall reaction:

i) change in the surface charge density

ii) adsorption or desorption of Cd^{2+} ions.

As we showed in chapter 4, increasing or decreasing of the surface charge density by depletion of H^+ or OH^- ions from solution is always an exothermic process. Corrected for the sub-process of surface charge adjustment by adsorption or desorption of protons, the cadmium adsorption enthalpy is endothermic. At high (indifferent) electrolyte levels, as used in our calorimetric study, electrostatic contributions to the adsorption enthalpy will be practically negligible. It is not surprising, therefore, that we obtained a $\Delta_{ads}H$ for cadmium on rutile that is essentially independent of the degree of surface coverage.

From the above mentioned case-study it should be clear that correct interpretation of overall heat effects requires thorough study of all sub-processes involved, in order to be able to arive at the valid conclusions on the driving force: though heat is liberated in the calorimetric study of cadmium adsorption on rutile, the Cd^{2+} adsorption itself is an endothermic process.

The processes of hydroxo complex formation in the bulk solution and adsorption onto an oxide surface of cadmium ions are schematically depicted in Fig. 9.1.

From the simplified general scheme it can be noted that our picture of the cadmium adsorption onto inorganic oxides is strongly based on entropical considerations concerning the Cd^{2+} ion. The hydration numbers, h, indicated in the scheme are generally accepted in a sense that for M^{2+} ions in literature hydration numbers of the order of ten are frequently mentioned (cf. (9)). From our investigations on complex formation in solution, for the $Cd(OH)^+$ complex we derived that it is presumably hydrated by 6-7 water molecules. For the adsorbed Cd^{2+} ion, part of the hydration water molecules could be substituted by surface hydroxyls, without substantially changing the hydration enthalpy (10). From this point of view one would expect the Cd^{2+} ion to loose more than half its hydration shell on adsorption. This reasoning is roughly justified by our experimental data on entropy changes in both processes.

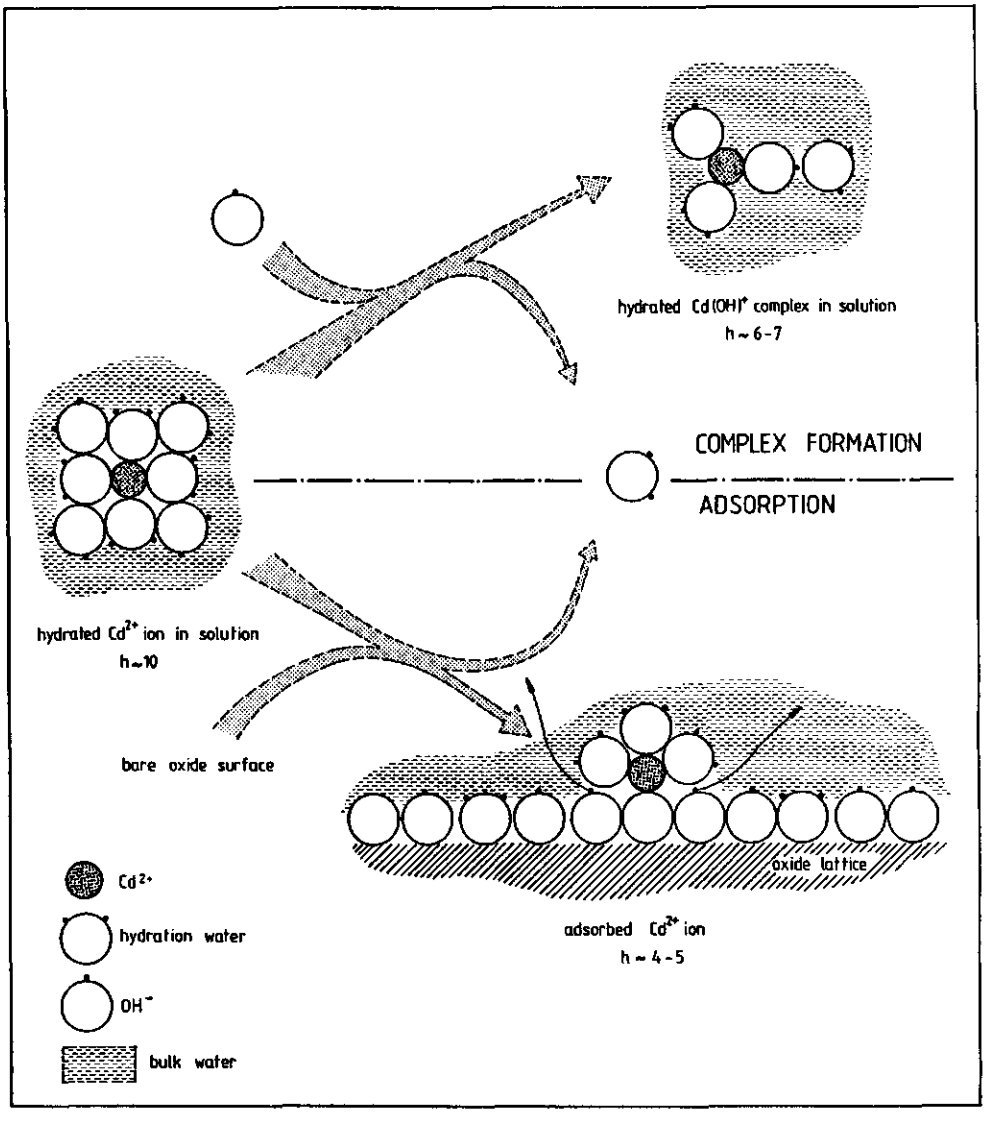

Fig. 9.1 Schematic representation of $Cd(OH)^+$ complex formation in aqueous solution and adsorption of hydrated Cd^{2+} ions at the insoluble oxide-solution interface. Estimated hydration numbers (h) are indicated in the figure. For further details see text.

A consequence of our model is that the adsorption of (hydrated) Cd^{2+} ions does not substantially change the structure of the solution side of the

interfacial region. The electron distribution on oxygens directly surrounding the adsorbed Cd^{2+} ion will usually differ from those on the original surface groups, affecting their chemical affinity for (cat)ions. Still they provide a very similar adsorption site for subsequently adsorbing Cd^{2+} species. From this point of view it is not surprising that adsorption isotherms of heavy metal ions on oxides generally do not exhibit real plateau-values. Therefore we restricted the model analyses to the low surface coverage (sub-monolayer) range.

Our approach helps to provide a mechanistical backbone for the mathematical 'surface precipitation model', recently put forward by Farley et al. (11). The term 'precipitation' in our opinion is questionable for the processes considered. Precipitation suggests an over-saturation of the solution with respect to the species to be precipitated from it. In our picture this does not necessarily need to be the case for the adsorption of heavy metal ions onto oxides.

By thermodynamic analyses of charge formation and cadmium adsorption on rutile and hematite, the processes could be quite well characterized. In Table 9.1, the thermodynamic parameters for the adsorption processes are given. In fact, this table is a combination of Tables 3.1 and 6.2, supplied by information obtained by direct microcalorimetry of cadmium adsorption (chapter 8).

The thermodynamic framework for the adsorption processes depicted in Fig. 9.1 is more or less completed. The data in the table 9.1 can be shortly discussed in scope of the proposed processes.

On rutile, for both protons and Cd^{2+} ions the entropy of adsorption roughly is half the dehydration entropy of the ions. The same applies to the adsorption of H^{+} on hematite. It is most likely, therefore, that this is also the case for cadmium adsorption on hematite. These data seem to indicate that Cd^{2+} ions and protons loose about half their hydration shell on adsorption onto oxides. The entropical contributions to the Gibbs energy of adsorption is largely independent of the type of oxide. Differences in chemical adsorption affinity of rutile and hematite are thus of an enthalpic nature.

The difference in $\Delta_{ads}H$ for cadmium ions and protons on rutile is -18 kJ/mol and for hematite this value amounts to -16 kJ/mol. This near constant adsorption enthalpy difference must have its basis in the chemical

Table 9.1 Thermodynamic parameters for the adsorption of H^+ and Cd^{2+} ions onto insoluble oxides. Data in brackets are estimated values.

	H^+ adsorption			Cd^{2+} adsorption		
	ΔG^o_{H+}	$\Delta_{ads}H_{H+}$ kJ/mol	$T\Delta_{ads}S^o_{H+}$	$\Delta_{ads}G^o_{Cd2+}$	$\Delta_{ads}H_{Cd2+}$ kJ/mol	$T\Delta_{ads}S^o_{Cd2+}$
Rutile	-31	-18	+13	-26	+10	+36
Hematite	-49	-36	+13	-42	(-6)	(+36)

adsorbent-adsorbate interaction, as enthalpic dehydration contributions are supposed to be rather aspecific and mainly concerned with the adsorbing ion. It is a well-known feature that e.g. covalent bond enthalpies are additive, i.e. that two species involved in the bond formation contribute with an almost constant number to the total bond formation enthalpy in different compounds (cf. (12)). In this respect it is not surprising that for the difference in $\Delta_{ads}H$ for Cd^{2+} and H^+ on rutile and on hematite, an almost constant value of about -17 kJ/mol is obtained. This result has important consequences for the generalization of our results, as will be shown in the following section.

9.3 Applications

It may be clear from this study that proton adsorption characteristics of inorganic oxides, which are relatively easy to assess and well-studied, provide valuable information on the adsorption behavior of heavy metal ions onto these substrates. Within the mechanistical framework developed, it seems quite straightforward to predict the adsorbability of cadmium ions onto other oxides. From the position of the point of zero charge of an oxide it must be possible to obtain a quite accurate indication of the cadmium adsorption enthalpy using the data from Table 9.1.

For other metal ions, some supplementary information is required. However, we believe that a few accurate experimental data on the adsorption of -say- Zn^{2+} ions onto RuO_2, suffice to provide reasonable estimates of the adsorption behavior of that ion onto other related oxides, using tabulated values for the hydration entropy and the additivity of the chemical interaction enthalpy, previously noted.

In applied sciences where adsorption of heavy metal ions is an important topic, e.g. in soil- and aquatic chemistry, this study offers the possibility to account, in a relatively easy and accurate way, for the adsorption onto the oxidic fraction of the adsorption complex, with a minimum of experimental effort.

9.4 Suggestions for further research

From the work presented in this thesis, one of the most crucial characteristics of the oxide-solution interface proved to be the high inner layer capacitance of the double layer. Both our elaboration of microcalorimetric and OH^- co-adsorption data lean to a large extent on this high capacitance. In order to verify our conclusions, it would be helpful to return to the classical AgI model system for which the inner layer capacitance is much lower. Performing pH- and pAg-static cadmium adsorption experiments on AgI could yield insight into the role of the inner layers in surface charge formation ($\Delta_{ads}H$ of charge determining ions as a function of σ_o). Such experiments also would provide a valuable check on our surface charge adjustment theory: actual adsorption of hydrolyzed cadmium species and changes in surface charge on adsorption in this system can be experimentally distinguished. Both processes can be measured independently as the depletion of H^+ and Ag^+ ions from solution, respectively.

Furthermore it is necessary, of course, to validate our conclusion on general oxide double layer properties by carefully studying an as broad as possible variety of inorganic oxides. The role of the electrical properties of the lattice on the interfacial behavior of oxides, in particular the exceptional properties of the SiO_2-solution interface (13), could possibly be investigated on more or less strongly doped silica's. The constraint of final conductivity of lattices as a prerequisite for Nernstian (pH, ψ_o) response could thus be verified.

9.5 References

1. Bolt, G.H., and van Riemsdijk, W.H., in "Soil Chemistry, part B" (G.H. Bolt, Ed.), Elsevier Scientific Publishing Company, Amsterdam-Oxford-New York, 1982.
2. Fokkink, L.G.J., de Keizer, A., Kleijn, J.M., and Lyklema, J., J. Electroanal. Chem. 208, 401, 1986.
3. This thesis, chapter 3.
4. Siviglia, P., Daghetti, A,, and Trasatti, S., Colloids Surf. 7, 15, 1983.
5. Penners, N.H.G., thesis Wageningen, 1985.
6. Healy, T.W., and White, L.R., Adv. Colloid Interface Sci. 9, 303, 1978.
7. This thesis, chapter 7.
8. This thesis, chapter 8.
9. Monk, C.B., "Electrolytic Dissociation", Academic Press, London-New York, 1961.
10. This thesis, chapters 5 and 8.
11. Farley, K.J., Dzombak, D.A., and Morel, F.M.M., J. Colloid Interface Sci. 106, 226, 1985.
12. Morisson, R.T., and Boyd, R.N., "Organic Chemistry", Allyn and Bacon Inc., Boston, 1973.
13. Tadros, Th.F., and Lyklema, J., J. Electroanal. Chem. 9, 303, 1978.

SUMMARY

The adsorption of charge-determining (H^+ and OH^-) and cadmium ions on rutile (TiO_2) and hematite (α-Fe_2O_3) has been studied in different concentrations KNO_3 as a function of temperature and pH.

Rutile and hematite show identical surface charge - pH behavior, except for the position of the point of zero charge (pH^o): normalized with respect to pH^o, (σ_o,pH) curves of both oxides are experimentally indistinguishable.

Measurement of the surface charge density on these oxides at temperatures other than room temperature is well possible with the potentiometric titration technique, provided certain precautions are taken. The surface charge - pH relations of rutile and hematite have been studied as a function of temperature in the range $5<T<70$ °C. Temperature changes affect the relative position of these curves but do not significantly change their shapes. This phenomenon has been called 'temperature congruence of surface charge'. It is shown that temperature congruence is to be expected for high capacitance double layers on Nernstian surfaces. This high capacitance value is related to the specific structure of oxide surfaces in aqueous solutions.

A thermodynamic treatment has been put forward, that relates the observed shifting of (σ_o,pH) curves with temperature to the enthalpy of proton adsorption/desorption in the interfacial region. We showed that pH^o is determined by the enthalpy of proton association with the surface rather than by the entropy. Entropy changes accompanying charge formation are aspecific in the sense that for hematite and rutile identical values for ΔS^o are obtained. The adsorbing proton loses about half of its hydration water on adsorption.

Enthalpies obtained by the thermodynamic analysis could be verified by direct microcalorimetric titrations of rutile and hematite suspensions. Calorimetric heats of charge formation are independent of the surface charge density on the oxides. This behavior is shown to be typical for high capacitance interfaces, because in this case electrical and countercharge contributions to the enthalpy of charge formation practically compensate each other.

The adsorption of cadmium ions on rutile and hematite has been measured using a potentiometric pH-stat technique. The influence of temperature on the adsorption is relatively small. The surface charge density of the ox-

ide, however, is a major factor determining the adsorbability of Cd^{2+} ions.

On adsorption of cadmium ions, hydroxyl ions are depleted from the solution. This OH^- co-adsorption could be explained in terms of 'surface charge adjustment'. Our surface charge adjustment theory is based on the constant potential principle: on specific adsorption of (cat)ions, the surface potential is assumed to maintain a constant (Nernst) value. Considering the specific characteristics of oxide - solution interfaces, our OH^- co-adsorption data for the adsorption of cadmium onto rutile and hematite at different temperatures, and those taken from literature for other heavy metal ions onto inorganic oxides, could be explained satisfactorily within the framework of the theory.

Experimental adsorption isotherms of Cd^{2+} were analysed according to the Frumkin - Fowler - Guggenheim model, where chemical, electristatic and lateral interactions are taken into account. The chemical contribution to the Gibbs energy of adsorption was shown to be insensitive towards changes in surface charge density and electrolyte concentration, which is an indication of the correctness of the model.

The enthalpy of cadmium adsorption in the rutile-$Cd(NO_3)_2$-KNO_3 system could be obtained from calorimetric acid/base titrations. The adsorption of Cd^{2+} ions on rutile was shown to be slightly endothermic, even though calorimetric measurements always showed exothermic overall heat effects. It was inferred that Cd^{2+} adsorption on rutile is driven by a gain in hydration entropy.

A strong correlation between Cd^{2+} adsorption and the formation of $Cd(OH)^+$ complexes in aqueous solutions is observed. Both reactions are mainly driven by a gain in hydration entropy. This finding supports the idea that surface groups on oxides resemble bulk OH^- ions.

The fact that the adsorpion of protons and cadmium ions on oxides in this study were shown to be strongly related processes, has important practical implications. With a minimum of experimentation it is now possible to predict the adsorption of heavy metal ions on oxides, using essentially easily obtainable and accurate potentiometric acid/base titration data.

SAMENVATTING

Onder adsorptie verstaan we het zich ophopen van stoffen in een grensvlak. Grensvlakken zijn de overgangsgebieden tussen twee verschillende fasen, bijvoorbeeld tussen een gas en een vloeistof, tussen twee niet mengbare vloeistoffen of tussen een vaste stof en een vloeistof.

Aan grensvlakken vinden interessante natuurkundige en scheikundige processen plaats. Eigenschappen van de ene fase gaan min of meer geleidelijk over in die van de ander. Ophoping van een stof in zo'n grensvlak kan om vele redenen plaatsvinden.

Adsorptieverschijnselen spelen in ons dagelijks leven een grote rol. Tijdens de afwas adsorberen zeepmolekulen op kleine vetdeeltjes en brengen en houden die door hun speciale eigenschappen in oplossing. Voor de landbouw zijn adsorptieprocessen van levensbelang. Meststoffen die aan de grond worden toegevoegd, adsorberen aan de gronddeeltjes en worden op die manier voor planten als het ware in voorraad gehouden. Zou geen adsorptie optreden, dan zouden deze stoffen met het regenwater in de grond wegzakken en zo voor de plant onbereikbaar worden.

Voor ongewenste verbindingen in de bodem, zoals bestrijdingsmiddelen, zware metalen, fosfaten in hoge koncentraties, geldt ook dat - als ze onverhoopt in de bodem aanwezig zijn - hun lot onder andere wordt bepaald door de wisselwerkingen die optreden met de bodemdeeltjes. Ook hier speelt adsorptie vaak een belangrijke rol. Zo is het in bepaalde delen van ons land aan adsorptie te danken dat er (nog) geen fosfaathoudend water uit de kraan komt.

In dit onderzoek is de adsorptie van een 'berucht' zwaar metaal, cadmium, bestudeerd. Het gebruik van dit metaal in allerlei produkten, zoals bijvoorbeeld motorolie, autobanden, kleurstoffen en batterijen, maakt dat er van deze stof flinke hoeveelheden in het milieu terecht zijn gekomen en nog komen. Cadmium is reeds in zeer lage koncentraties schadelijk gebleken voor de gezondheid van mens en dier. Het is daarom van belang te kunnen schatten hoe zo'n stof zich in de bodem zal gedragen: wordt ze stevig gebonden, bestaat het gevaar van uitspoeling naar het grondwater, wordt de stof gemakkelijk door planten opgenomen? Om dit soort vragen te kunnen beantwoorden is onder andere inzicht nodig in de wisselwerking van de stof met bodemdeeltjes.

Wij hebben er voor gekozen de wisselwerking tussen cadmium en oxiden nader te bekijken. Oxiden, meestal slecht oplosbare verbindingen opgebouwd uit zuurstof en een metaal, zijn vaak bouwstenen van grond. Naast klei en humus, maken oxiden dikwijls een belangrijk deel uit van de vaste stof in een bodem. Uit zeer veel onderzoek in het verleden is bekend dat oxiden van allerlei elementen gemeenschappelijke oppervlaktekenmerken vertonen. Zo is gebleken dat fijn verdeelde oxidekorreltjes in water (kolloidale dispersies, suspensies) een oppervlaktelading bezitten die afhangt van de zuurgraad (de pH) van het water. Het oppervlak kan, afhankelijk van de pH, positief, neutraal of negatief geladen zijn. Het ligt voor de hand dat de lading van de oxidedeeltjes een rol speelt in de adsorptie van cadmiumionen (dat wil zeggen: positief geladen cadmiumatomen). Immers: tegengestelde ladingen trekken elkaar aan, gelijksoortige ladingen stoten elkaar af.

De lading op oxiden in water wordt veroorzaakt door de adsorptie van, of het tekort aan, positieve waterstofionen en is daarom afhankelijk van de pH. Het proces van ladingsvorming is in dit onderzoek bestudeerd voor twee oxiden. Rutiel (een bepaalde kristalvorm van titaniumoxide, TiO_2) en hematiet (een kristallijn ijzeroxide, α-Fe_2O_3) werden gekozen als representatieve oxiden. Het blijkt dat de pH waarbij het oxide geen (netto) lading draagt afhangt van de soort oxide. Hematiet blijkt waterstofionen veel sterker aan zich te binden dan rutiel. Zelfs zo sterk dat het oppervlak van hematiet nog positief geladen is in basische oplossingen. Het gemak waarmee waterstofionen aan het oxide worden gebonden (geadsorbeerd) heeft te maken met de krachten die het oxidekristal zelf bij elkaar houden en die hangen op hun beurt weer af van de eigenschappen van het metaalion in het oxide.

De pH waarbij netto lading op het oxide-oppervlak ontbreekt, wordt het ladingsnulpunt, pH^o, van dat oxide genoemd. Als de pH van de suspensie lager is dan pH^o (de oplossing is dan dus zuurder, bevat meer waterstofionen), is het oppervlak positief geladen. Aan de andere kant van het ladingsnulpunt is de lading negatief. Het blijkt nu dat, als we de ladingsdichtheid op rutiel en hematiet bekijken als funktie van de pH uitgedrukt ten opzichte van het ladingsnulpunt, de beide oxiden zich experimenteel identiek gedragen. Vanuit het ladingsnulpunt bouwen ze op gelijke wijze hun lading op bij veranderende pH. Dit is een waardevolle waarneming omdat zij aangeeft dat, vanuit de oplossing bekeken, het niet te 'zien' is of zich achter het netto ongeladen grensvlak een rutiel- of een hematietkristal bevindt. Het vermoeden bestaat dat dit ook voor andere, soortgelijke, oxi-

den geldt. Voor rutheniumoxide (RuO_2; een oxide van belang voor de zonneënergieomzetting, althans in laboratoriumexperimenten), is in het laboratorium voor Fysische en Kolloidchemie in Wageningen hetzelfde gedrag waargenomen.

Individuele oxiden onderscheiden zich door de neiging die zij bezitten om waterstofionen te binden. Uit een, experimenteel zeer lastige, bepaling van de temperatuursinvloed op de ladingsvorming op rutiel en hematiet, konden we met behulp van een thermodynamische analyse de reaktiewarmte afleiden die vrijkomt bij de adsorptie van een waterstofion op het oxide. Zoals verwacht blijkt bij hematiet veel meer - bijna twee keer zoveel - warmte vrij te komen dan bij rutiel. Deze warmte werd ook rechtstreeks gemeten. Het blijkt dat gemeten en berekende waarden uitstekend met elkaar overeenstemmen, hetgeen wijst op de juistheid van de thermodynamische analysemethode en van de experimenten.

Omdat het belangrijk was te weten waarom precies en hoe cadmiumionen op oxiden adsorberen, zelfs als de wandlading op het oxide positief is, werd in dit onderzoek de temperatuursinvloed op het adsorptieproces bestudeerd. De invloed van de temperatuur op een bepaald proces geeft inzicht in de krachten die dat proces doen verlopen. Er bestaan in de natuur twee elkaar tegenwerkende tendensen

i) Ordening ten gevolge van krachten tussen molekulen.

ii) 'Wanordening' onder invoed van de warmtebeweging.

De eerste heeft te maken met veranderingen in de energie. Zoals bekend streeft de natuur (of beter: een systeem) naar zo laag mogelijke energie: een steen valt altijd naar beneden, een kompasnaald wijst altijd naar het noorden. De tweede drijfveer wordt entropie genoemd. Entropie is een maat voor de wanordelijkheid van een systeem. De natuur streeft naar maximale entropie, dus een zo groot mogelijke wanorde.

Normaal verlopende processen zijn altijd een compromis tussen minimale energie en maximale entropie. Zoals elk natuurlijk proces kan adsorptie plaatsvinden doordat adsorptie de energie van het systeem verlaagt, of juist de entropie er van doet toenemen. Dit laatste nu blijkt het geval te zijn voor de adsorptie van cadmium ionen op oxiden. Dat bij adsorptie - bij het zich netjes ordenen van molekulen in een grensvlak - de wanorde van een

systeem kan toenemen is bijvoorbeeld als volgt in te zien. We hebben een oplossing waarin zich onder andere oxidedeeltjes en cadmium ionen bevinden. De positief geladen cadmiumionen in de oplossing zijn alle omringd door watermolekulen. Watermolekulen bezitten een bijzondere eigenschap. Hoewel ze als geheel ongeladen zijn, is de ene kant van het molekuul enigzins negatief geladen en de andere kant net zo veel positief; ze zijn polair. Watermolekulen zijn dipolen. Het relatief hooggeladen cadmiumion wordt in oplossing omringd door zo'n tien watermolekulen die met hun negatieve kant proberen de lading er van af te schermen (verlaging van de elektrische energie). Als nu een grensvlak aanwezig is waaraan het cadmium ion zijn energie anderszins kan minimaliseren, is een gedeelte van het omringende, gestruktureerde, water overbodig geworden en kan zich weer 'vrij' in de oplossing bewegen. Terwijl het cadmiumion verloor aan entropie, het werd vastgeplakt op het oxide-oppervlak, won het water aan entropie. De balans blijkt nu zo uit te slaan dat de entropiewinst van het water ruimschoots het entropieverlies van het cadmiumion kompenseert.
Het blijkt dat de struktuur van het grensvlak tussen oxide en oplossing zodanig is dat cadmiumionen er goed 'passen'. Het hydratatiewater dat het cadmiumion in de oplossing omringde wordt gedeeltelijk vervangen door op water gelijkende groepen op het oxide oppervlak. Omdat oxiden in water alle een soortgelijke oppervlaktestruktuur bezitten, verwachten we dat de entropiewinst slechts weinig afhangt van het soort oxide. Dit vermoeden konden we voor rutiel en hematiet experimenteel bevestigen.

Vergelijking van de onderzoeksresultaten voor waterstofionen (de ladingsvorming) en cadmiumionen voor beide oxiden leerde dat het adsorptiegedrag van beide ionen sterk gerelateerd is. Hematiet, dat waterstofionen zoveel sterker bindt dan rutiel, laat ook een veel sterkere cadmiumadsorptie zien. Voor de praktijk van - bijvoorbeeld - het bodemkundig onderzoek betekent dit dat grondig onderzoek van de adsorptie van waterstofionen aan een bepaald bodemoxide informatie oplevert over de interakties die zware metaalionen met dat oxide zullen vertonen. Het grote voordeel hiervan is dat de ladingsvorming op oxiden veel gemakkelijker en nauwkeuriger - mits aan bepaalde experimentele voorwaarden wordt voldaan - te meten is dan de adsorptie van zware metalen.

We kunnen stellen dat de anorganische oxiden in dit onderzoek naar hun oppervlaktegedrag in oplossing een aantal van hun geheimen hebben prijsgegeven. De generalisaties die volgen uit dit werk zijn belangrijk voor

zowel de fundamentele kolloidchemie als voor de meer toegepaste landbouwwetenschappen. Het is wellicht overbodig op te merken dat het nog veel experimententeel en theoretisch onderzoek zal vergen voor we kunnen zeggen dat we echt begrijpen wat zich in het oxide-oplossingsgrensvlak afspeelt.

LEVENSLOOP

Lambertus Gerrit Jan Fokkink werd op 25 juni 1957 in Doetinchem geboren. Na zijn middelbare schoolopleiding bezocht hij vanaf 1976 de Hogere Technische School te Hengelo (Ov). Na het behalen van het HTS diploma Chemie in 1979, begon hij in augustus van dat jaar de studie Milieuhygiëne aan de Landbouwhogeschool te Wageningen. Het doktoraalexamen, met Kennis van de Bodemverontreiniging als hoofdvak en Fysische en Kolloidchemie en Waterzuivering als bijvakken, werd in maart 1984 afgelegd. Van april 1984 tot april 1987 werkte hij als assistent onderzoeker op de vakgroep Fysische en Kolloidchemie van de Landbouwhogeschool/Landbouwuniversiteit. In die periode werd het in dit proefschrift beschreven onderzoek uitgevoerd.

NAWOORD

Nu na drie jaar werken op de vakgroep dit boekje 'klaar' is, is het moment aangebroken om te overdenken wat deze periode tot zo'n boeiende heeft gemaakt.

De inspirerende atmosfeer op het lab, de grote kollegialiteit en de vele niet-wetenschappelijke aktiviteiten die er worden ontplooid zorgen ervoor dat het wetenschappelijke werk met een hoog rendement kan plaatsvinden.

Waar het de vak-specifieke problemen betreft heb ik kunnen putten uit het grote inzicht en de ruime ervaring van mijn promotor en co-promotor. Zij waren in staat de beginner die ik ben te doordringen van de ernst van de zaak en de gevaren die een oppervlakkige benadering van grensvlakverschijnselen met zich meebrengt.

In de meetfase van het onderzoek kon ik rekenen op de steun van Anton Korteweg. Ik ben me er nu meer dan ooit van bewust dat zonder vakkundige analytische vakgroepsgenoten goed onderzoek praktisch onmogelijk is.

De doktoraalstudenten die aan het onderzoek meewerkten gaven het werk een extra dimensie. Hun aktief meedenken en -werken heeft (hopelijk niet alléén) voor mij veel opgeleverd.

De vele geanimeerde gesprekken die ik de afgelopen jaren mocht voeren met 'oxidemensen' van binnen en buiten de landbouwuniversiteit hebben de indruk versterkt dat de waarheid in het midden ligt. Hun meningen en ideeën hebben het verloop van dit onderzoek stellig gunstig beïnvloed.

Bovenal is het te danken aan ons gezin dat ik altijd prettige herinneringen aan de Fysko-periode zal bewaren. Het moet gezegd: ondanks alles zaten er heel wat 'rotterige' dagen in die drie jaar. Na een fietstochtje met de kinderen of een paar bladzijden 'Pinkeltje' was de zaak meestal weer voldoende gerelativeerd om de werkzaamheden met frisse moed te hervatten. Anneke, Lotte, Tesse, ik ben me ervan bewust dat we dit samen hebben gedaan.

Ik ben er zeker van dat de ervaringen die ik in deze periode mocht opdoen ook elders en later hun nut zullen bewijzen.